

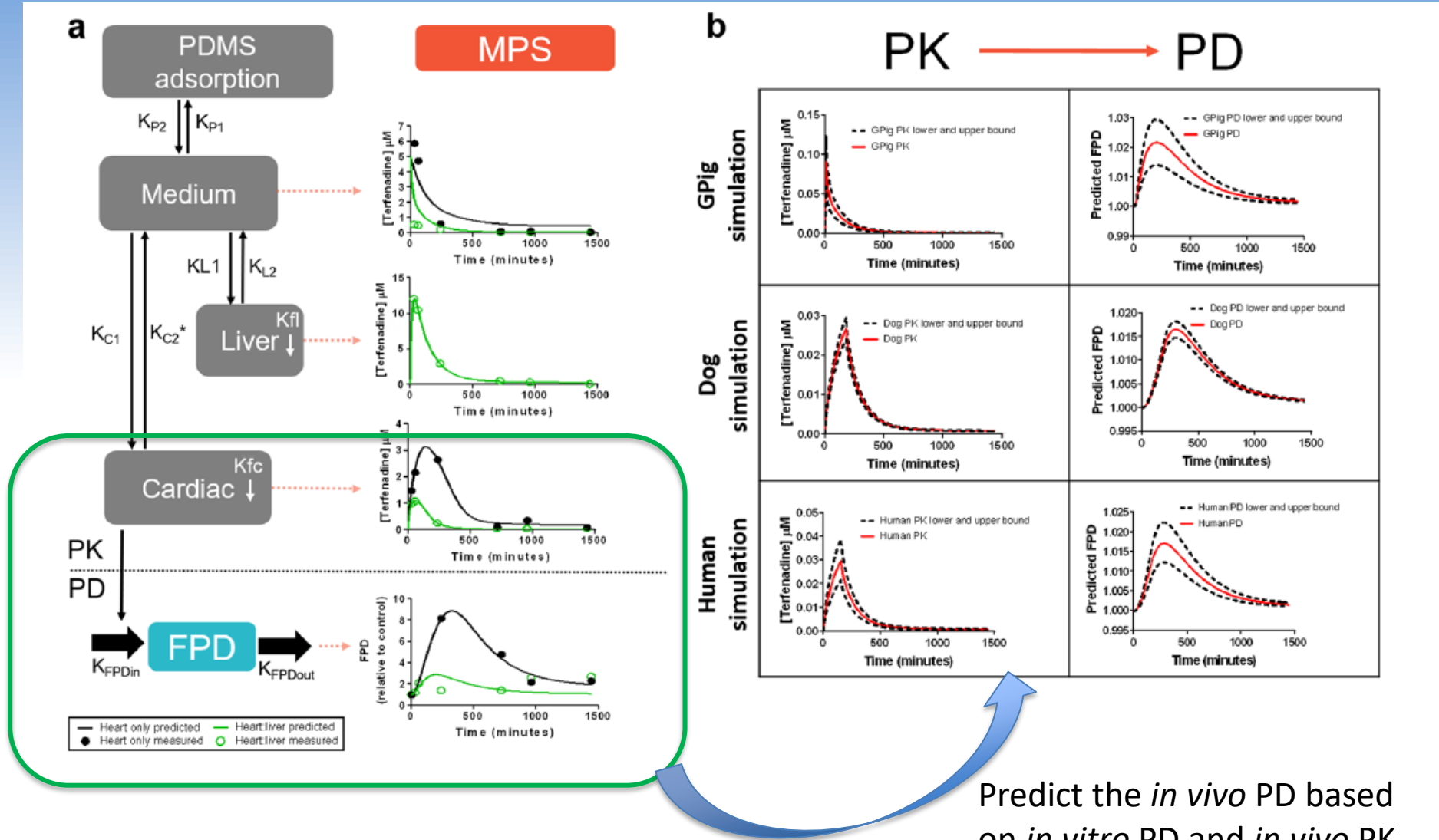
Human-on-a-Chip combined with PBPK modeling for *in vitro/in vivo* PK/PD extrapolation Part II: PBPK model

Viera Lukacova

Simulations Plus, Inc.

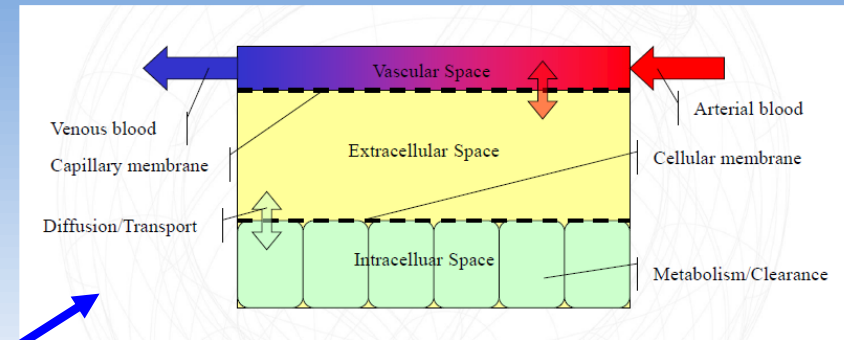
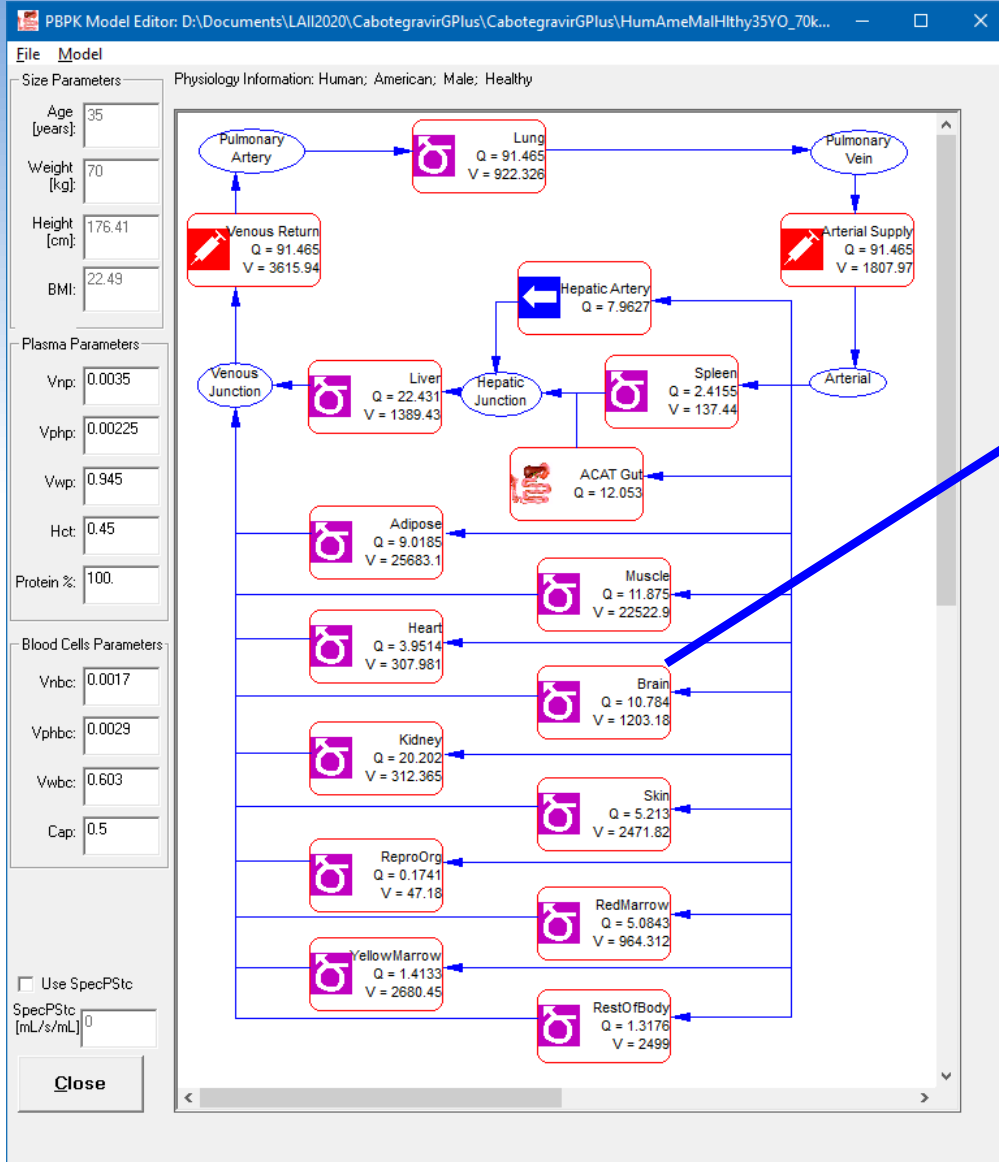
viera@simulations-plus.com

Compartmental HoacC Model



McAleer et al – Scientific Reports 2019, 9:9619

What is defined in a PBPK Model?



$$V_t \frac{dC_t}{dt} = \left(Q \times C_{bi} - \frac{Q \times C_t \times R_{bp}}{K_p} - CL_{int,u} \left(\frac{C_t \times f_{u,p}}{K_p} \right) \right)$$

- Each compartment represents a tissue:
 - Specific volume(s) *
 - Blood perfusion rate *
 - Enzyme/transporter expression levels *
 - Volume fractions of lipids & proteins *
 - Tissue: plasma partition coefficient (Kp)
 - Estimated from drug properties:
 - logD vs. pH
 - pKa(s)
 - Plasma protein binding
 - Blood: plasma concentration ratio

Perfusion-Limited Tissues

$$V_T \frac{dC_T}{dt} = Q_T \left(C_{b_i} - \frac{C_T R_{bp}}{K_p} \right) - CL_{int,u} \frac{C_T f_{up}}{K_p} - v_{metab}(C_{Tu})$$

V_T : Tissue volume

C_T : Drug concentration in tissue

Q_T : Tissue blood perfusion rate

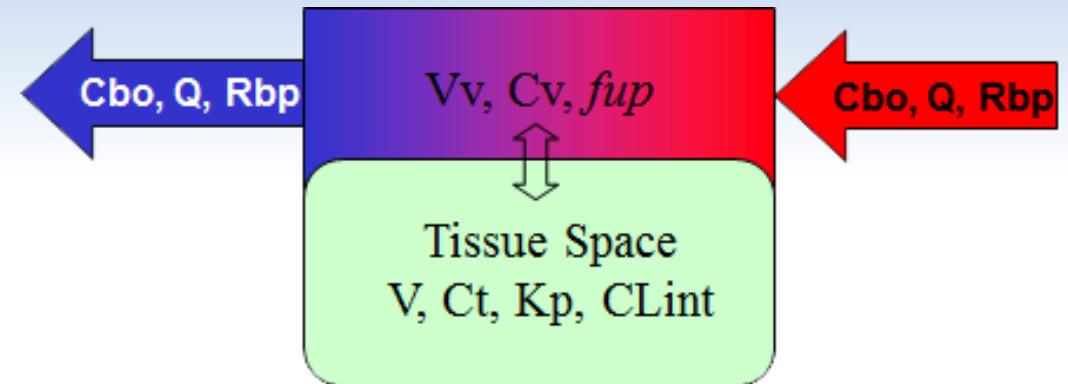
R_{bp} : Blood to plasma concentration ratio

K_p : Tissue to plasma partition coefficient

$CL_{int,u}$: Unbound intrinsic clearance in tissue

v_{metab} : Metabolism rate in tissue - based on unbound intracell conc

f_{up} : Fraction unbound in plasma



Permeability-Limited Tissues

$$\left(V_{ect} + V_{vasc} \frac{R_{bp}}{K_p} \right) \frac{dC_{ect}}{dt} = Q_T \left(Cb_i - \frac{C_{ect} R_{bp}}{K_p} \right) - perm$$

$$perm = PS_{TC} (C_{ect,u} - C_{ict,u}) + v_{influx} (C_{ect,u}) - v_{efflux} (C_{ict,u})$$

$$V_{ict} \frac{dC_{ict}}{dt} = perm - v_{metab} (C_{ict,u}) - CL_{int,u} C_{ict,u}$$

V_T : Tissue Volume

C_{ect} : Drug Concentration in extracellular space

C_{ict} : Drug Concentration in intracellular space

Cb_i : Drug Concentration in entering blood

Q_T : Tissue Perfusion

R_{bp} : Blood to Plasma Ratio

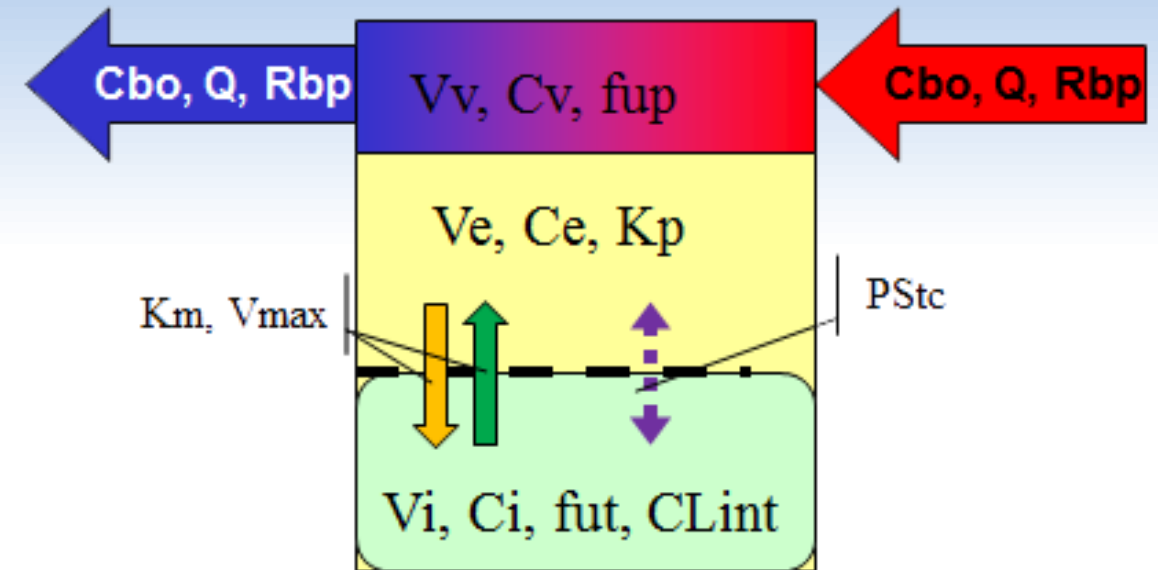
K_p : Tissue to Plasma Partition Coefficient

CL_{int} : Intrinsic Clearance in Tissue

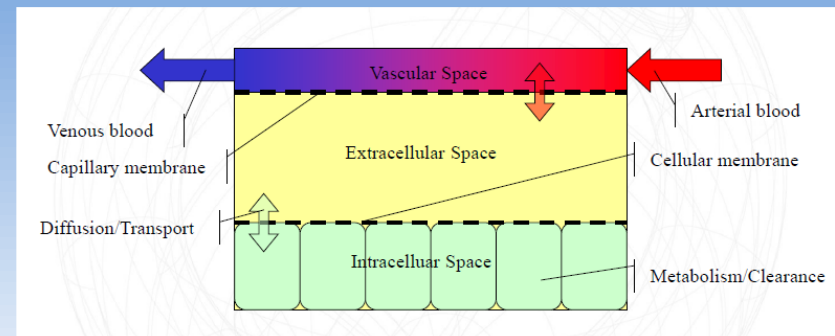
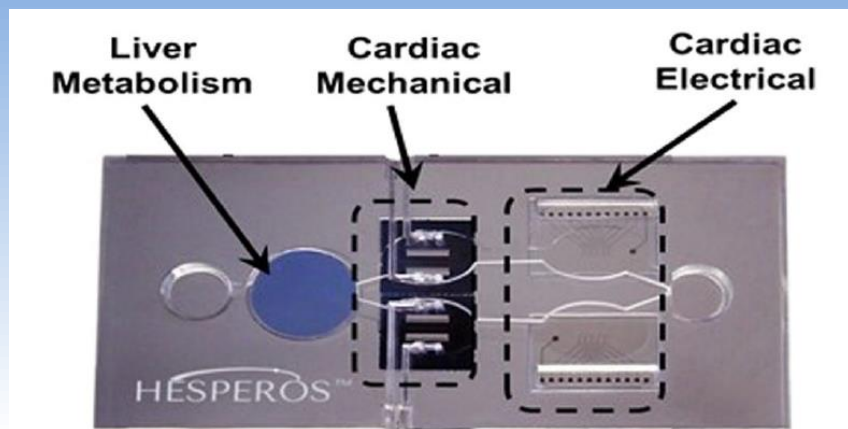
v_{metab} : Metabolism Rate in Tissue - based on unbound concentration

v_{trans} : Transport Rate - based on unbound concentration

PS_{TC} : Permeability-Surface Area Product

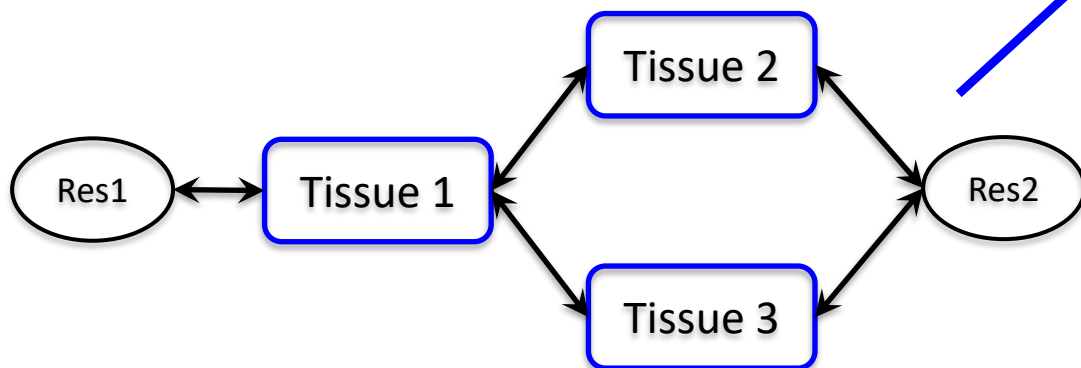


Mechanistic Hoac Model



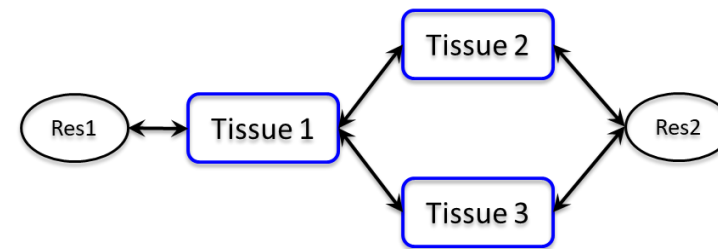
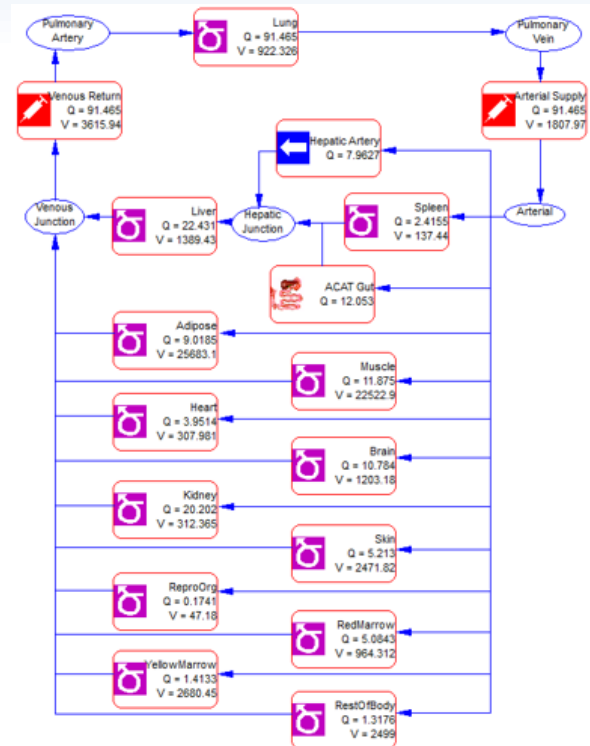
$$V_t \frac{dC_t}{dt} = \left(Q \times C_{bi} - \frac{Q \times C_t \times R_{bp}}{K_p} - CL_{int,u} \left(\frac{C_t \times f_{u,p}}{K_p} \right) \right)$$

- Each compartment represents a tissue:
 - Specific volume(s)
 - Media Flow rate
 - Enzyme/transporter expression levels
(*same as in vivo* – needs verification with standard substrate)
 - Volume fractions of lipids & proteins
(*same as in vivo* – needs verification by predicting distribution of known compound)
 - Tissue: media partition coefficient ($K_{p_{media}}$)
 - Dependent on drug properties:
 - logD vs. pH
 - pKa(s)
 - Plasma protein binding
 - Blood: plasma concentration ratio



Mechanistic Hoac vs. PBPK Model

- Possible differences in flow of media vs. plasma flow (depends on the HoacC setup)
- Tissue distribution and metabolism mechanisms – expected to be similar
- Possible binding to materials in HoacC system need to be considered



Translating parameters from *in vitro* to *in vivo*

- K_{pu} – account for differences between plasma *in vivo* and media *in vitro*
- PS_{TC} - initial assumption of constant Specific PS_{TC} (PS_{TC} per mL of tissue volume) - needs to be verified against test compounds
- Metabolism and/or carrier-mediated influx/efflux - initial assumption of *in vitro* expression = *in vivo* expression - needs to be verified against standard compounds

$$K_{pu} = V_{ew} + \frac{1/X_{[D],iw}}{1/X_{[D],p}} V_{iw} + \left(\frac{P \cdot V_{nl} + (0.3 \cdot P + 0.7) \cdot V_{phl}}{1/X_{[D],p}} \right) +$$

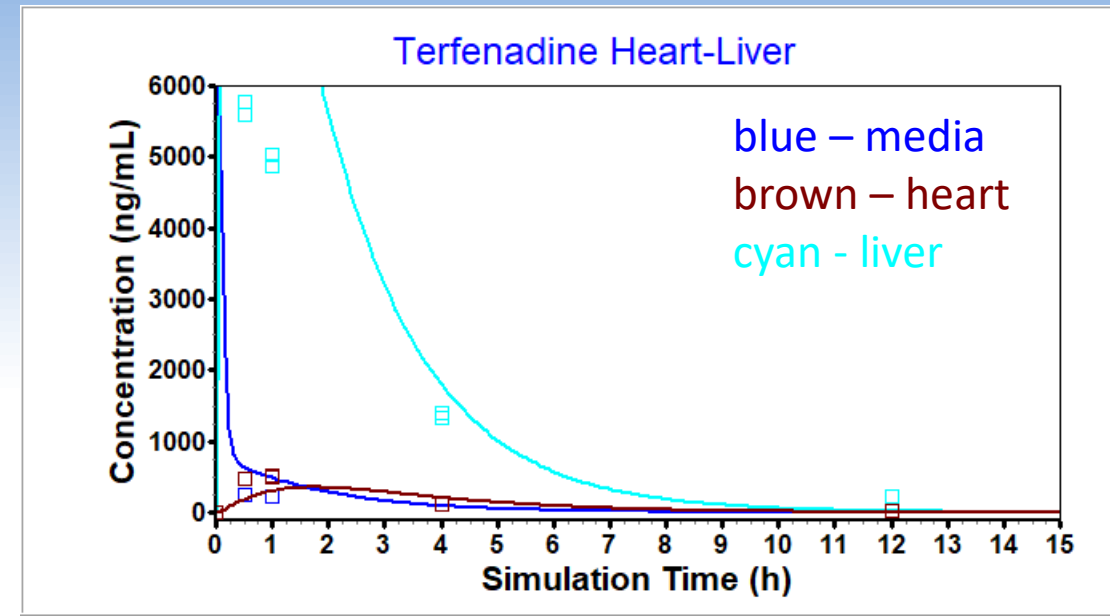
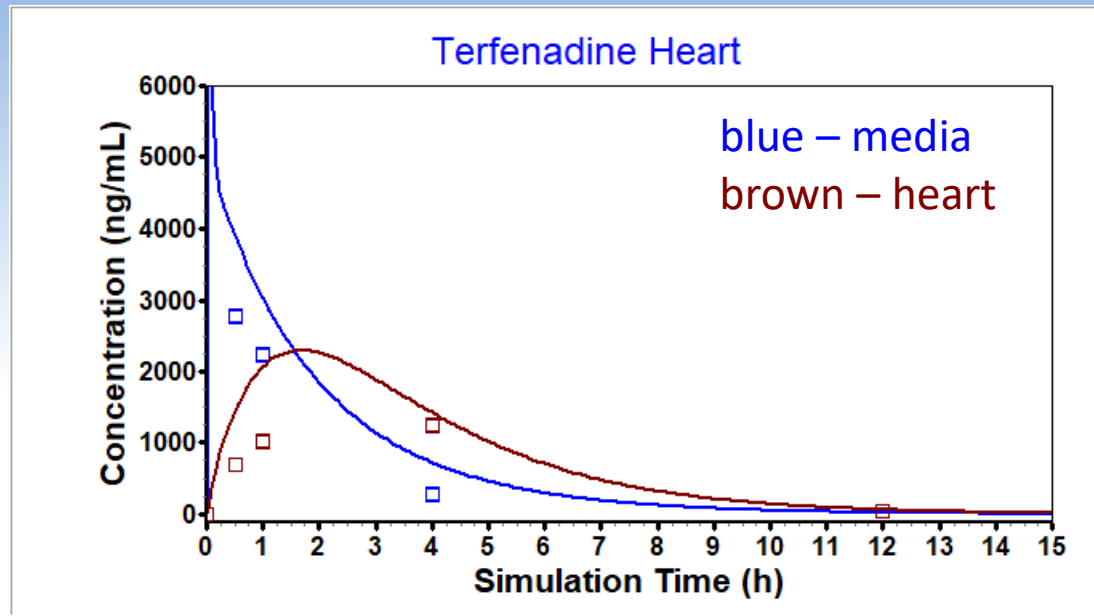
$$(Fn + Fa) \cdot \left[\frac{1}{fup} - 1 - \left(\frac{P \cdot V_{nlp} + (0.3 \cdot P + 0.7) \cdot V_{php}}{1/X_{[D],p}} \right) \right] \cdot RAtp +$$

$$(Fc) \cdot \left(\frac{Ka \cdot [AP]_T ((1/X_{[D],iw}) - 1)}{(1/X_{[D],p})} \right)$$

$$PassiveDiffusion = PS_{TC} (C_{ect,u} - C_{ict,u})$$

Mechanistic Hoac Model

(approximate results – preliminary model)



Fitted parameters:

- Distribution to Heart tissue
 - Fitted P_{stc} for permeability-limited tissue
- Non-specific binding

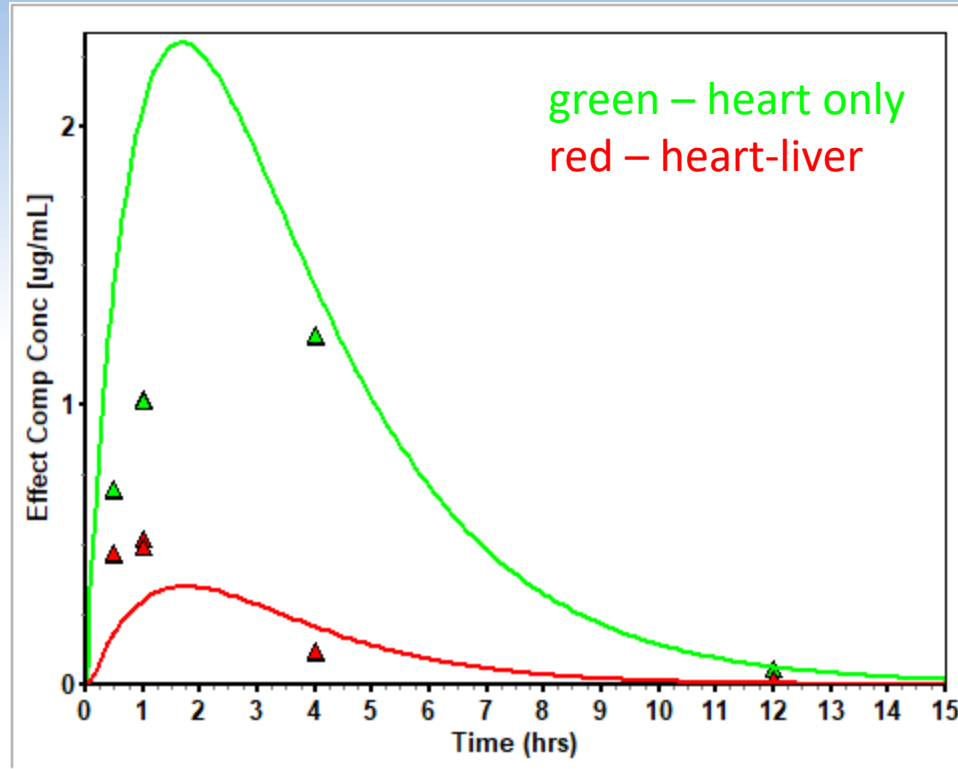
- Distribution to Liver tissue
 - Fitted K_p
- Elimination by CYP3A4
 - K_m predicted by ADMET Predictor®, V_{max} fitted

Observed data:
McAlear – Sci Reports 2019, 9:9619

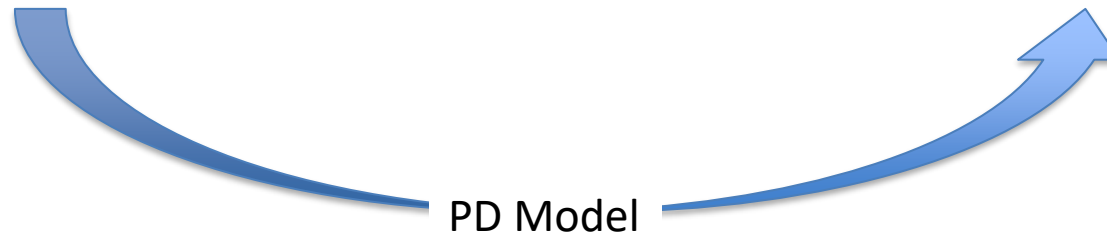
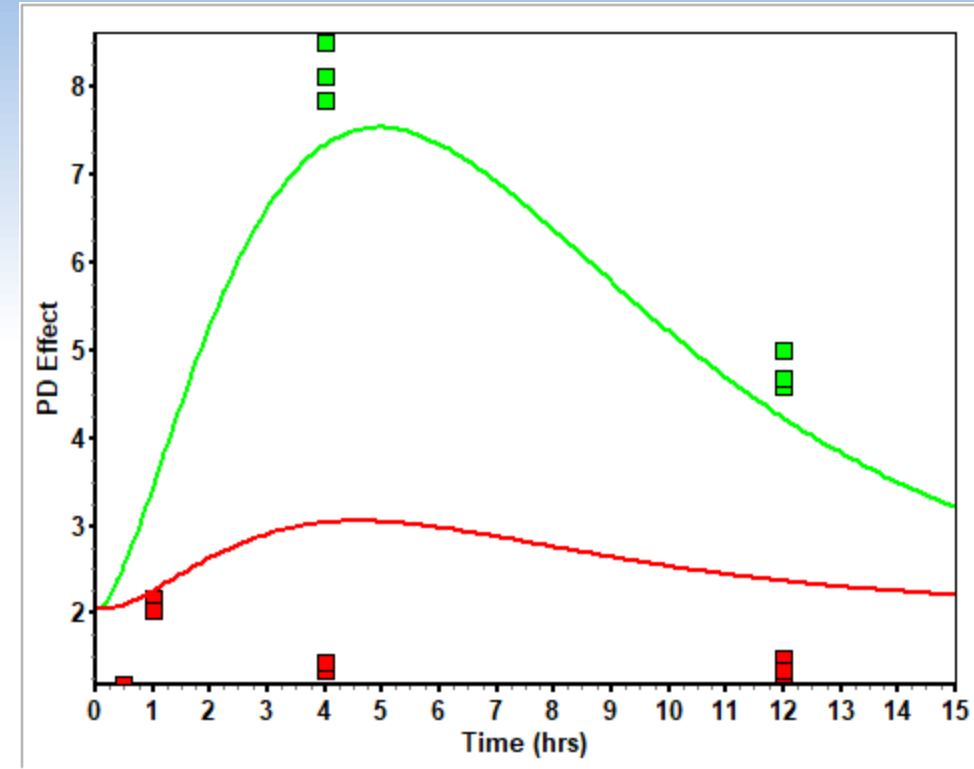
PD Modeling

(approximate results – preliminary model)

Heart concentrations

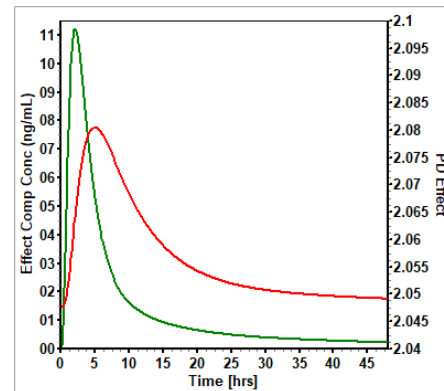
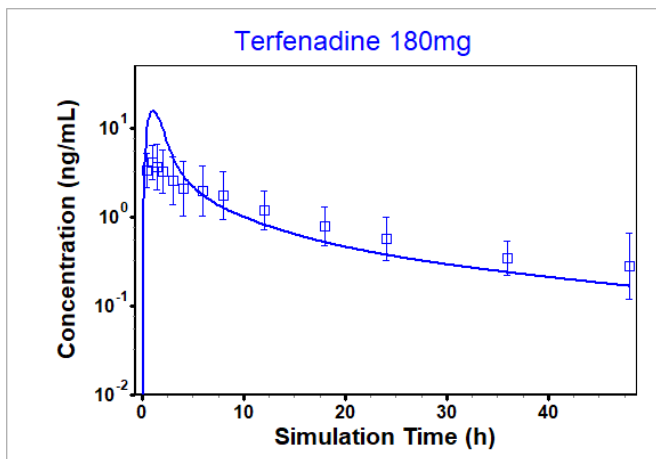
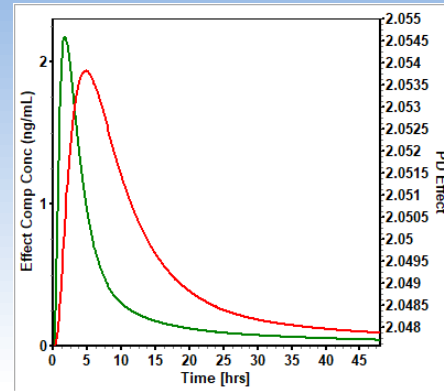
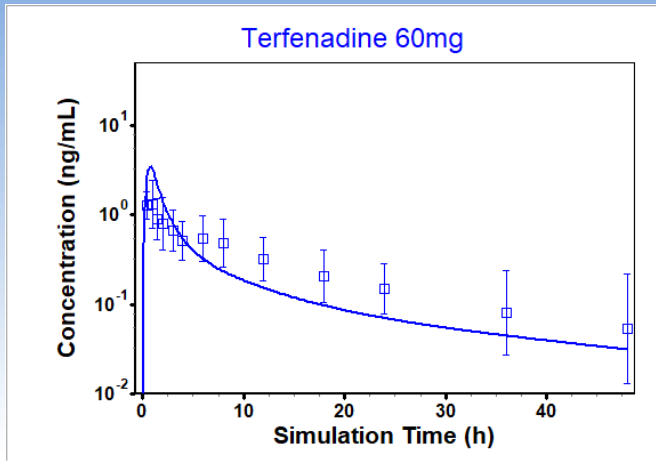


PD Effect



Observed data:
McAlear – Sci Reports 2019, 9:9619

Simulate PK/PD *in vivo*



Parameter scaling:

- Kps estimated based on *in vitro* Kp fitted for Liver compartment
 - The *in vitro* Kp,u was scaled to *in vivo* Kp
 - Found the method that most closely predicted the *in vivo* liver Kp
- Distribution into the Heart scaled from *in vitro* distribution (PStc) fitted for Heart compartment
 - Assumed Pstc per mL tissue is constant
- Fraction unbound in enterocytes predicted in MembranePlus™
- Remaining properties predicted by ADMET Predictor®
- Clearance had to be scaled – the results are shown with *in vivo* Vmax increased 100x from the fitted *in vitro* Vmax
 - Enzyme activity different than *in vivo*?
 - Different rate limiting process *in vitro*?
 - Impact of significant binding to plates?
 - Caused by approximate media flow?

Observed data:
Okerholm – Biopharm Drug Dispos 1981, 2, 185-190

Summary

- A mechanistic simulation of Hoac system has a potential for full PK/PD extrapolation with a PBPK model.
- The use of a PBPK model allows linking the PD effect to the specific tissue concentration.
- The preliminary simulations showed potential for adequate prediction of tissue distribution.
- A mechanistic model for Hoac system could be linked with other *in vitro* assays (i.e. HLM clearance measurements) to identify and predict impact of individual processes.

Questions?



For further information visit:

<https://hesperosinc.com/>

<https://www.simulations-plus.com/>

Hesperos Overview

- Over 20 US patents have been licensed by Hesperos thereby documenting the innovation and novelty of this platform. This also provides full freedom to operate in this space & a strong defensible IP position.
- Winner of the 2015 London-based *Lush Prize* for creating an alternative to animal testing for industry.
- Have won multiple SBIR grants including a \$2M Phase II and recently a \$4M phase IIB award to Bridge the “valley of death”.
- Established R&D contracts with multiple national and international Pharma companies.
- Moved into a new 14,100 sq. ft. state of the art facility in August 2019.
- Have recruited excellent staff for company, 32 at present.
- No products will be offered at this time, only services based on compounds sent to our Orlando facility.

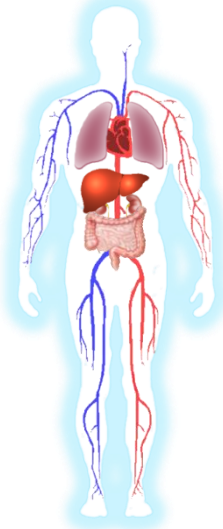


Clinically Relevant Functional Readouts

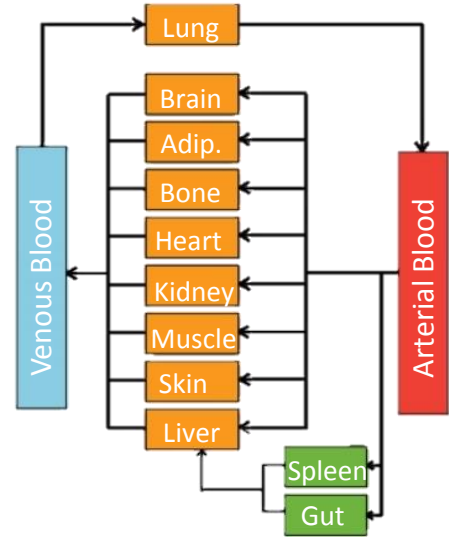
- Mechanical or electrical readouts of cellular functions such as:
 - ***muscle contraction***
 - ***electrical activity*** from neurons and cardiac cells
 - motoneuron → muscle: ***NMJ physiology*** and other combinations
 - barrier integrity (TEER) and active transport for barrier tissues
- Allows ***functional*** analysis of cellular health non-invasively for acute, but more importantly, for ***chronic*** monitoring of human-on-a-chip systems
- ***Reduces substantially***, if not eliminates, the need for measuring ***biomarkers*** in these systems for certain organ mimics. Normally need to measure multiple biomarkers by molecular techniques and put them together ***to extrapolate functional*** activity, with these systems can ***measure directly***.
- Allows ***mechanistic*** determination of toxicity and for target identification.
- Facilitates ***physiological*** determination of drug efficacy and safety

Human-on-a-Chip Systems for Disease Modeling

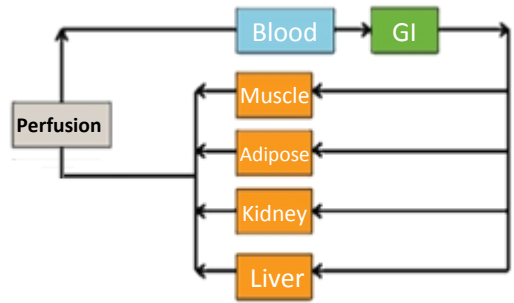
Human Body



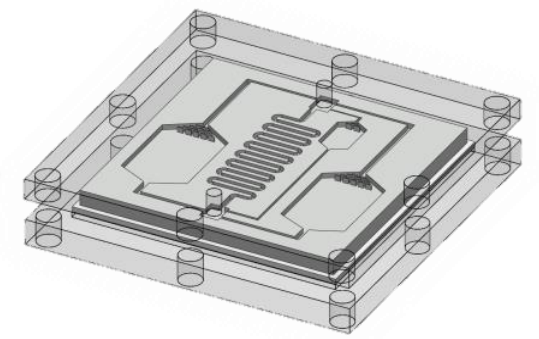
PBPK



Chip PBPK



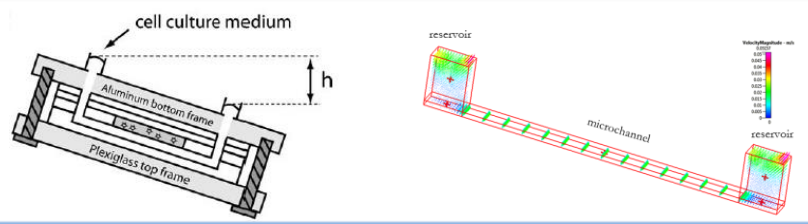
Serum-Free Human-on-a-Chip



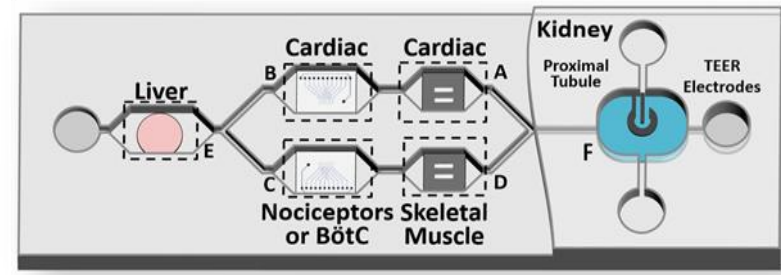
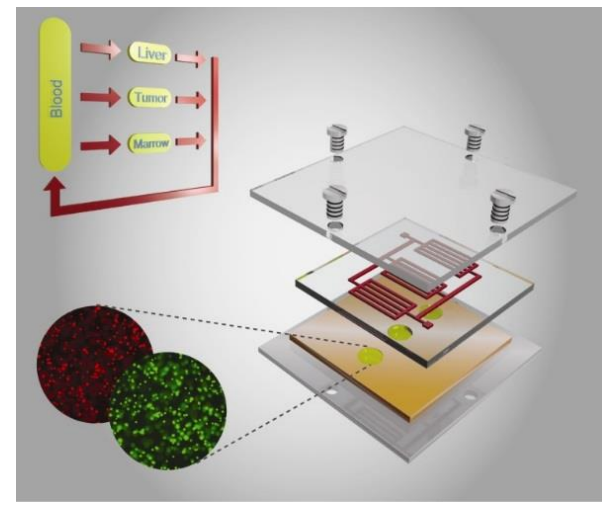
OVER 20 PUBLICATIONS USING THE PUMPLESS SYSTEM

Gravity-induced flow through a microfluidic device on a rocking platform

- Pumpless operation
- Minimizes bubble formation



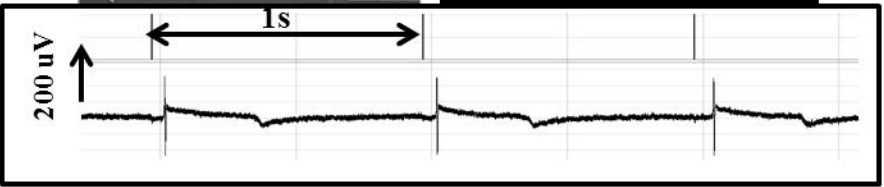
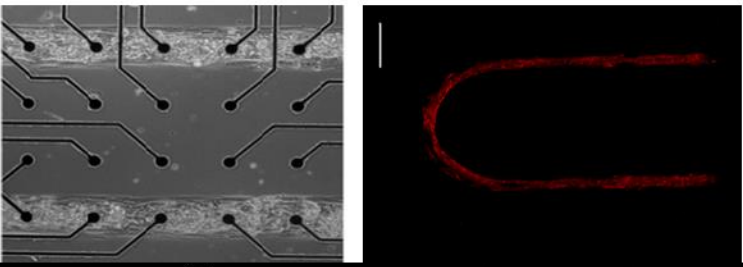
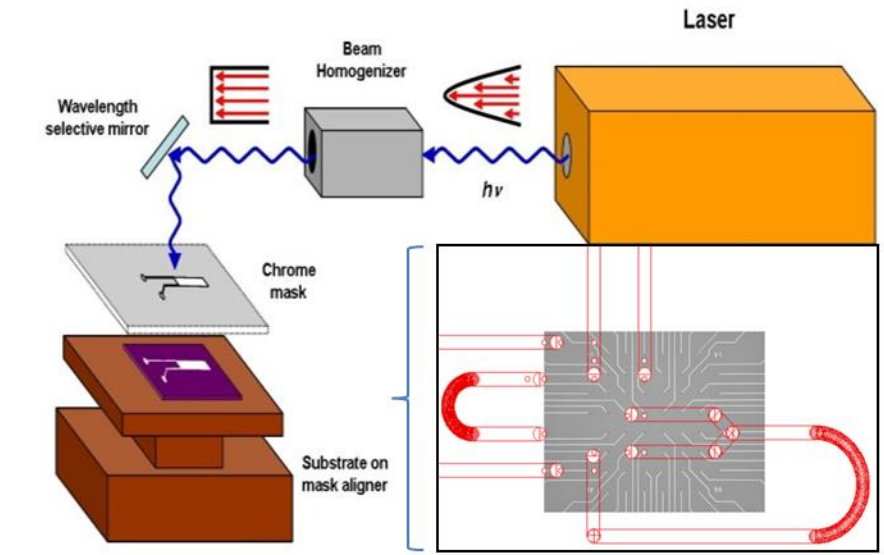
Medium recirculation with gravity-induced flow. Tilting of the device causes liquid to flow between the wells. In a timed manner, the rocking platform changes the angle and medium flows in the opposite direction. [1]



References:

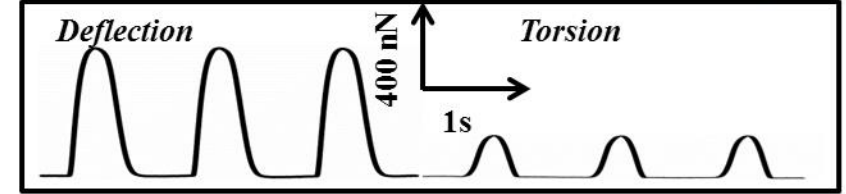
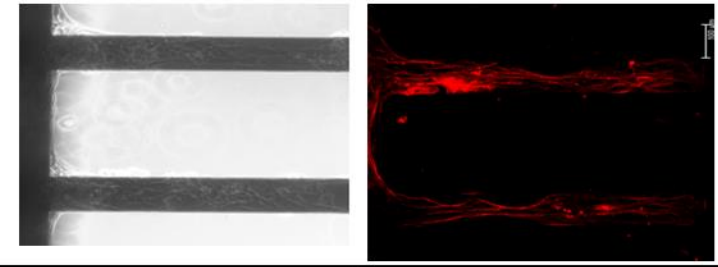
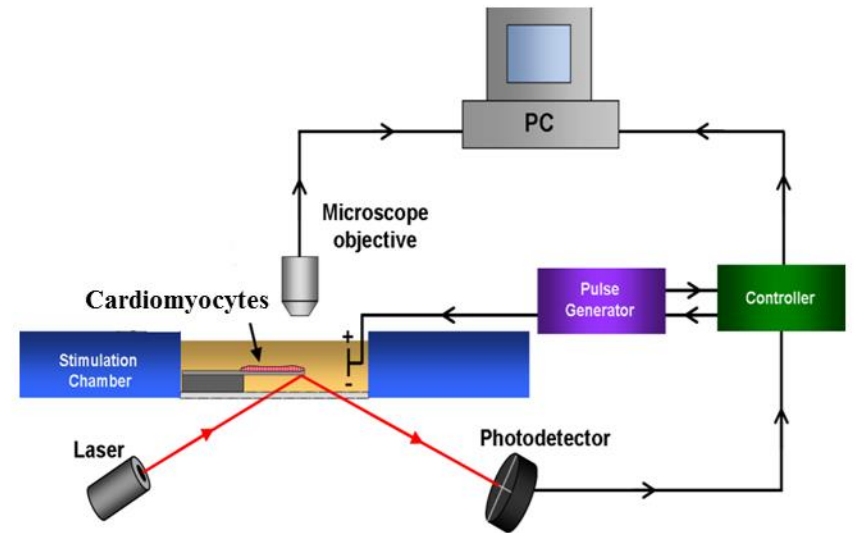
- Oleaga C., et al., *Biomaterials*. 182:176-90 (2018)
- Oleaga C., et al., *Sci Rep*. 6:20030 (2016)
- Chen, H.J., et al., *Nat Biotechnol*, 34:845-851 (2016)
- JH Sung, C Kam, ML Shuler, *Lab on a chip*, 10: 446 (2010)
- Castellanos M, et al., *Proc Natl Acad Sci U S A*. 101(17):6681-6 (2004)
- Sweeney LM, et al., *Toxicol In Vitro*. 9(3):307-16 (1995)

A. Patterned MEA for electrical



Rhythm generation Conduction AP Length

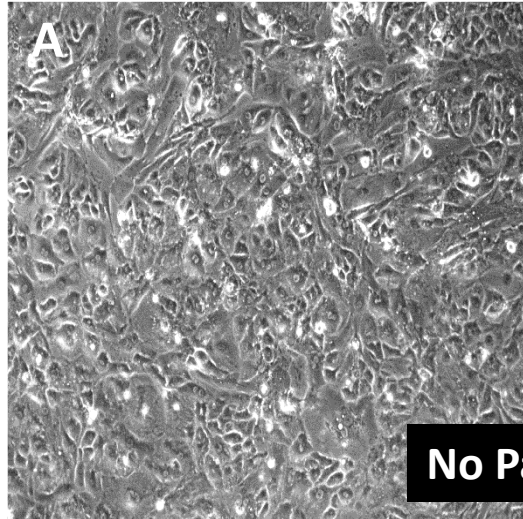
B. Cantilever-based force measurement



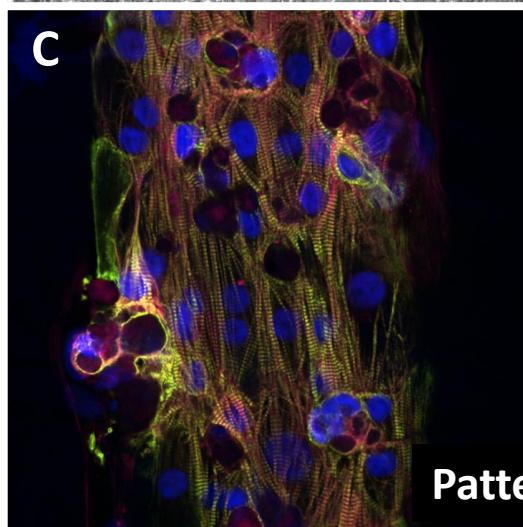
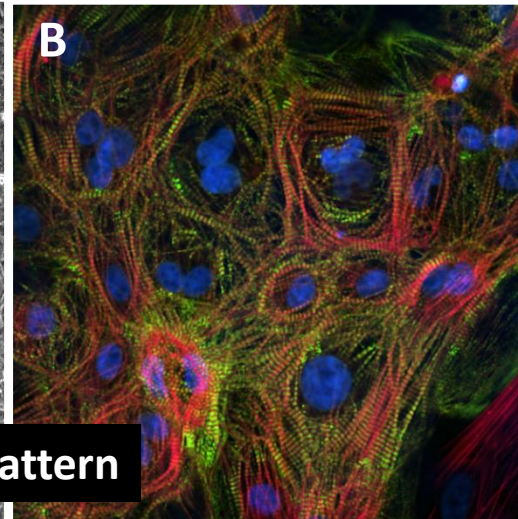
Force

Cardiac output

Morphology and Immunocytochemistry of Patterned and Non-Patterned Cardiomyocytes in serum-free medium

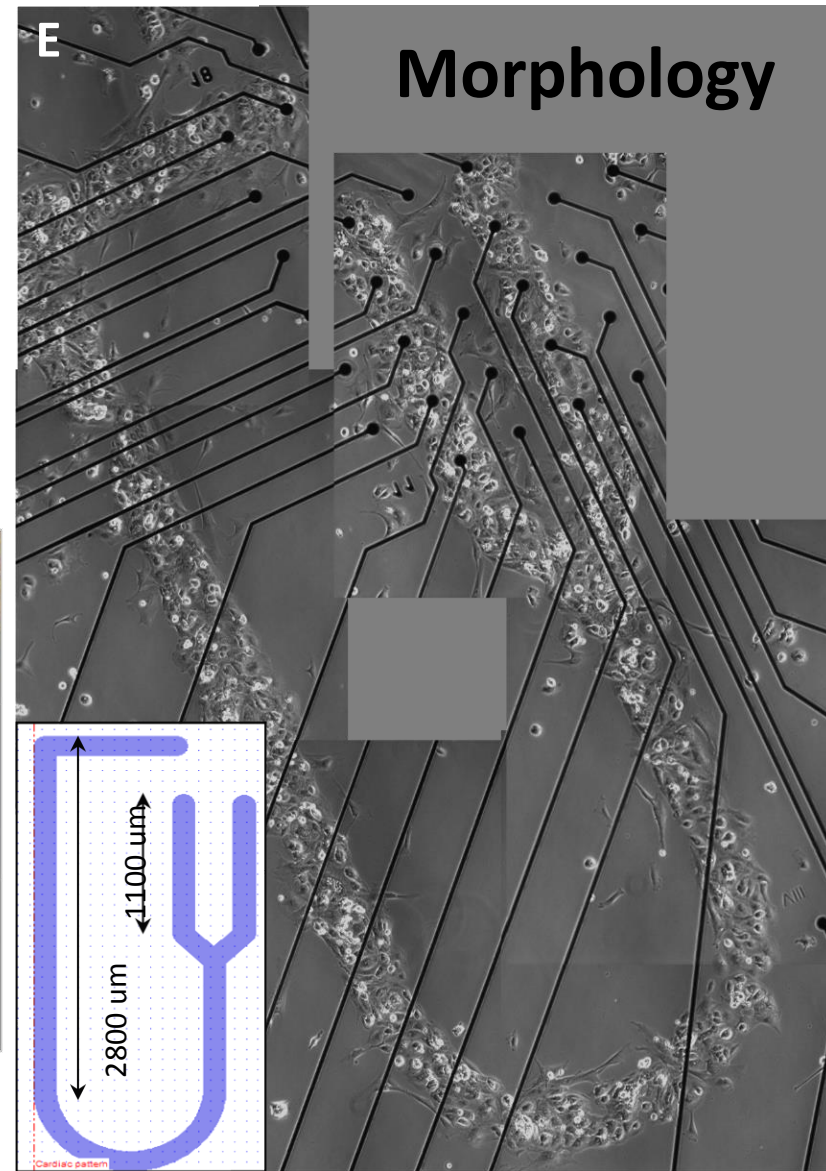
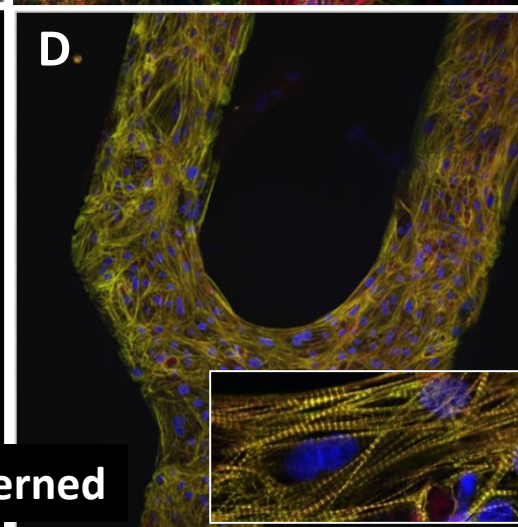


No Pattern

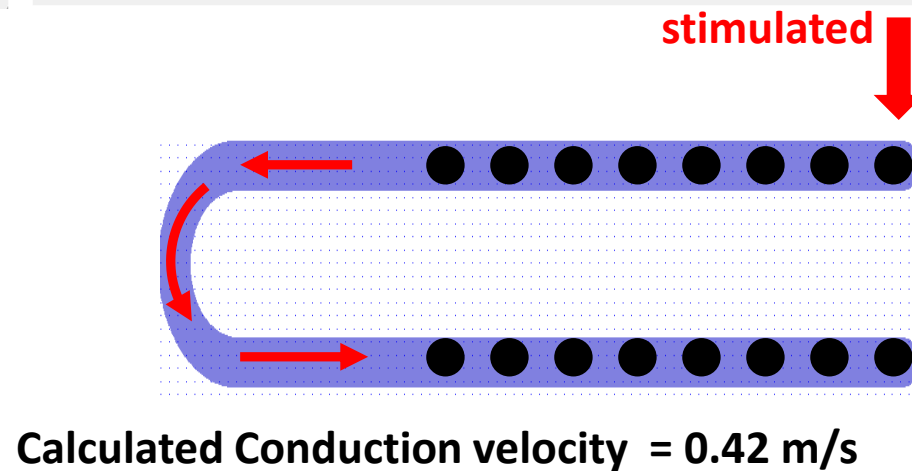
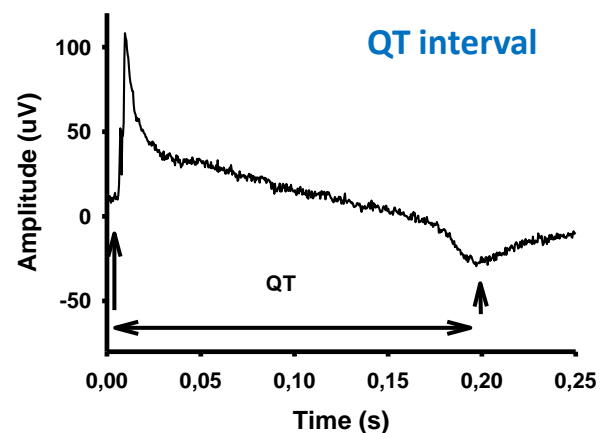
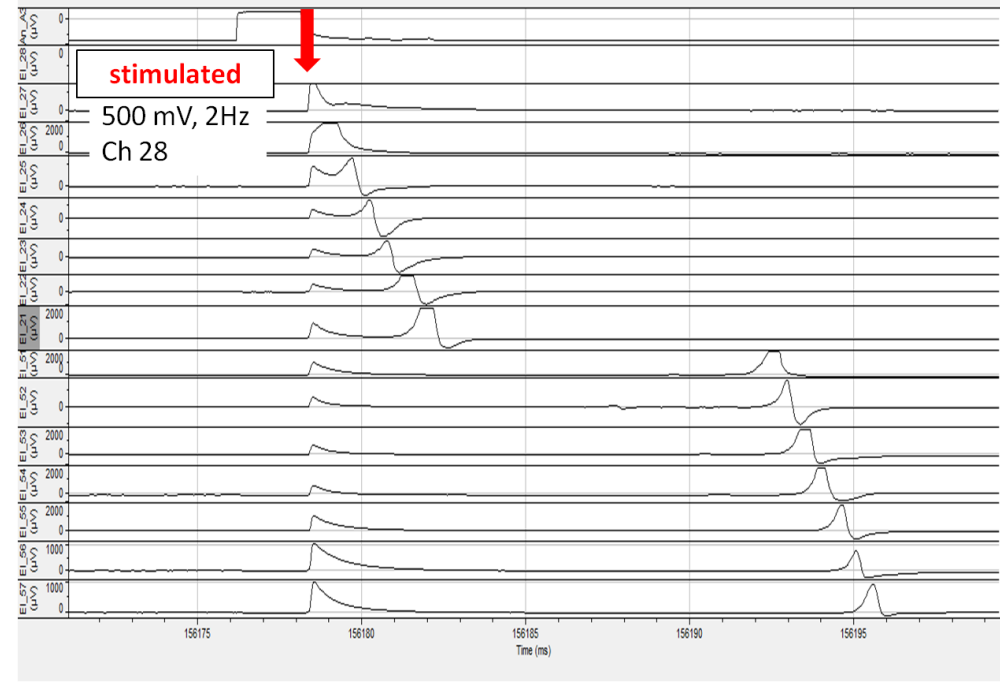
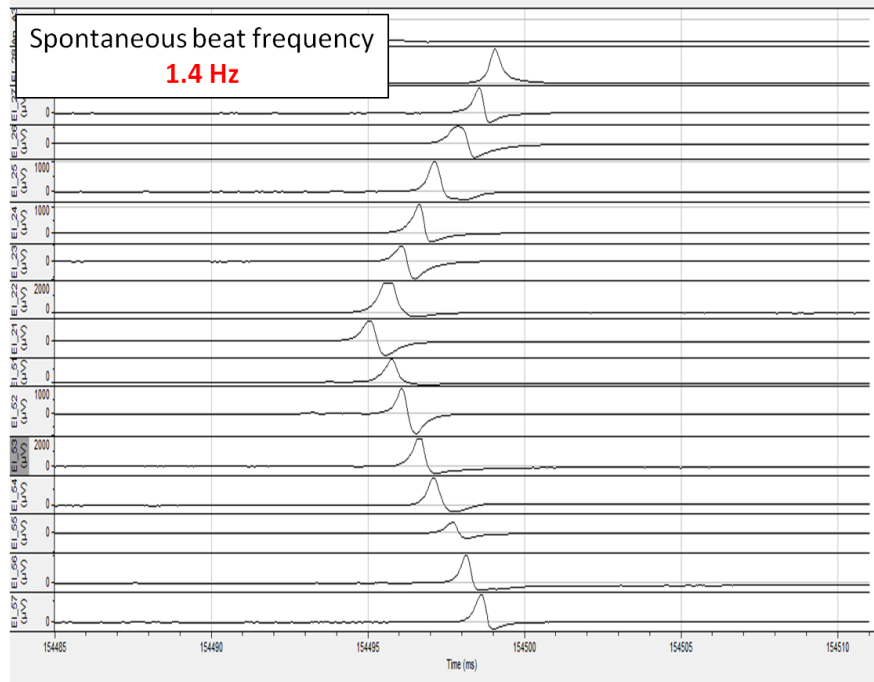


Patterned

Troponin Actin DAPI



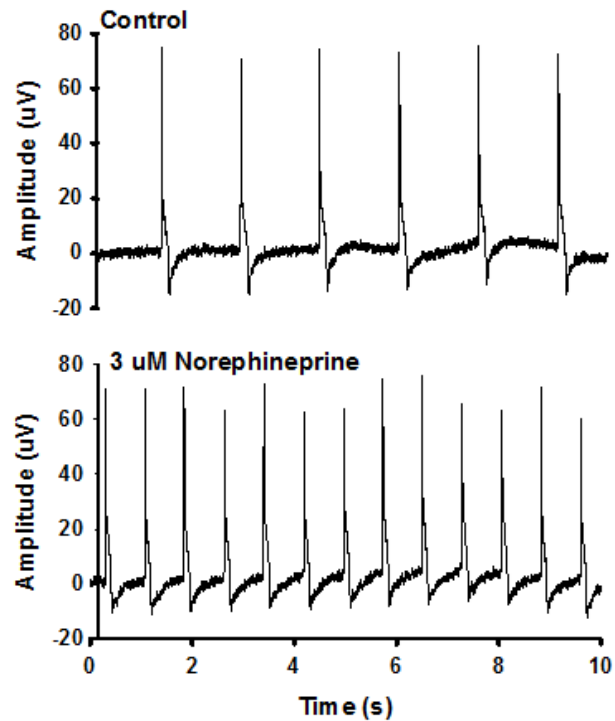
Electrophysiology – cardiomyocytes on MCS MEA Conduction velocity measurement



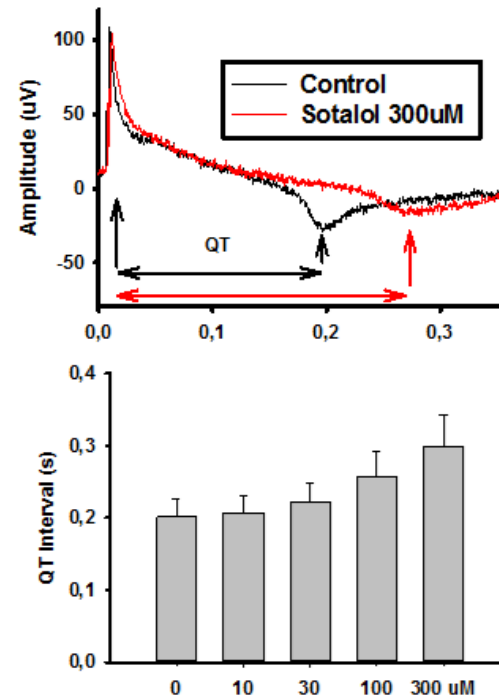
Sample Data Evaluation of Cardiac System

Drugs	Mechanism
Sotalol	<u>Antiarrhythmic Class III</u> : K ⁺ channel blocker Beta-blocker
Verapamil	<u>Antiarrhythmic Class IV</u> : Ca ²⁺ channel blocker
Norepinephrine	α -adrenergic agonist

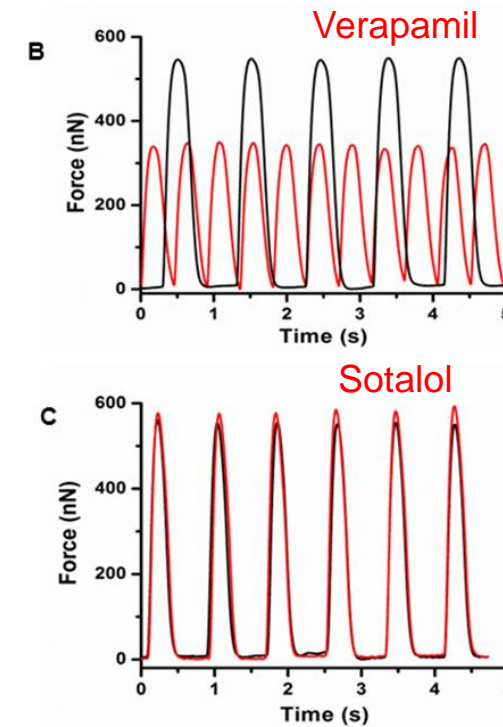
Frequency



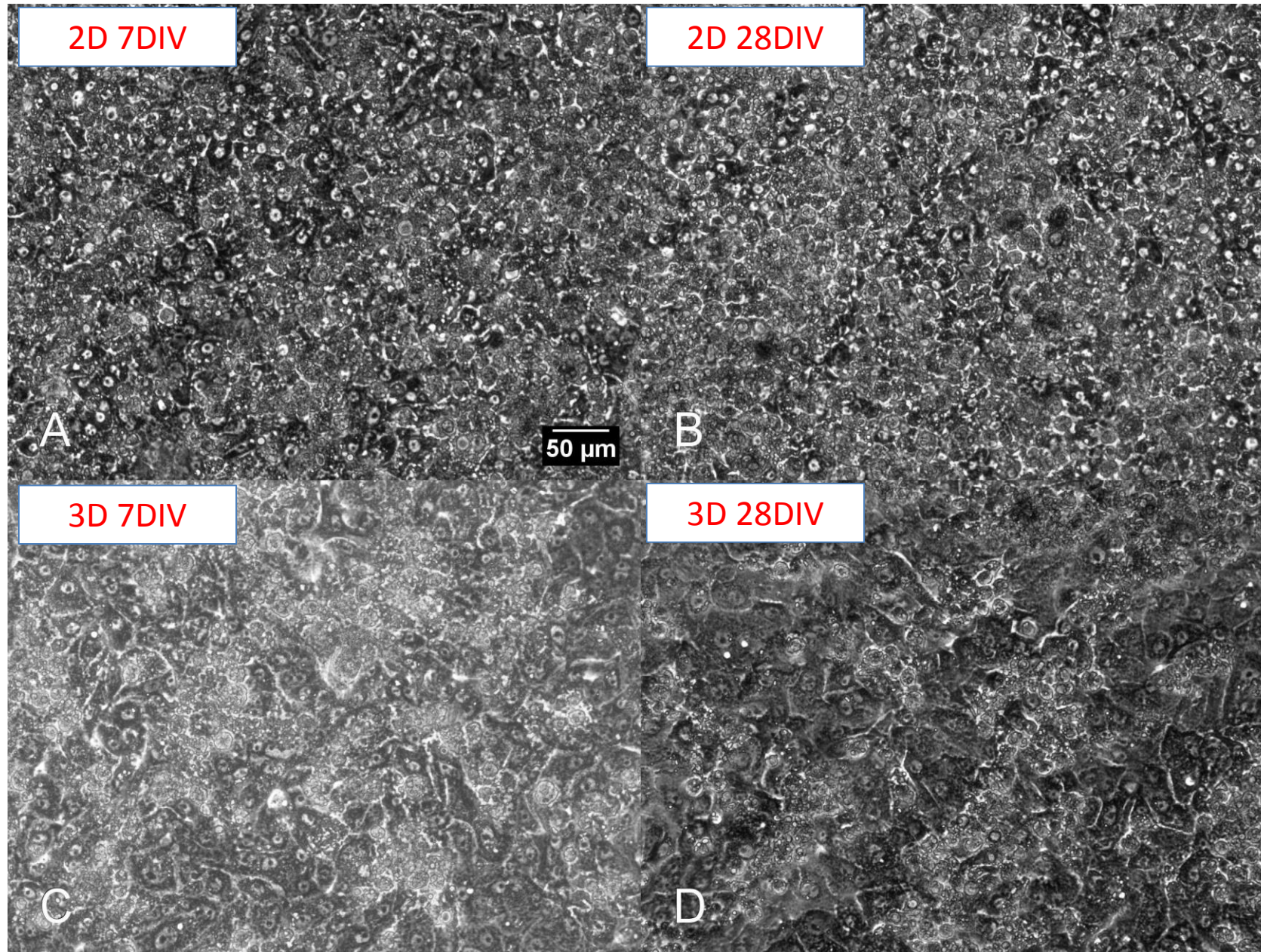
QT interval



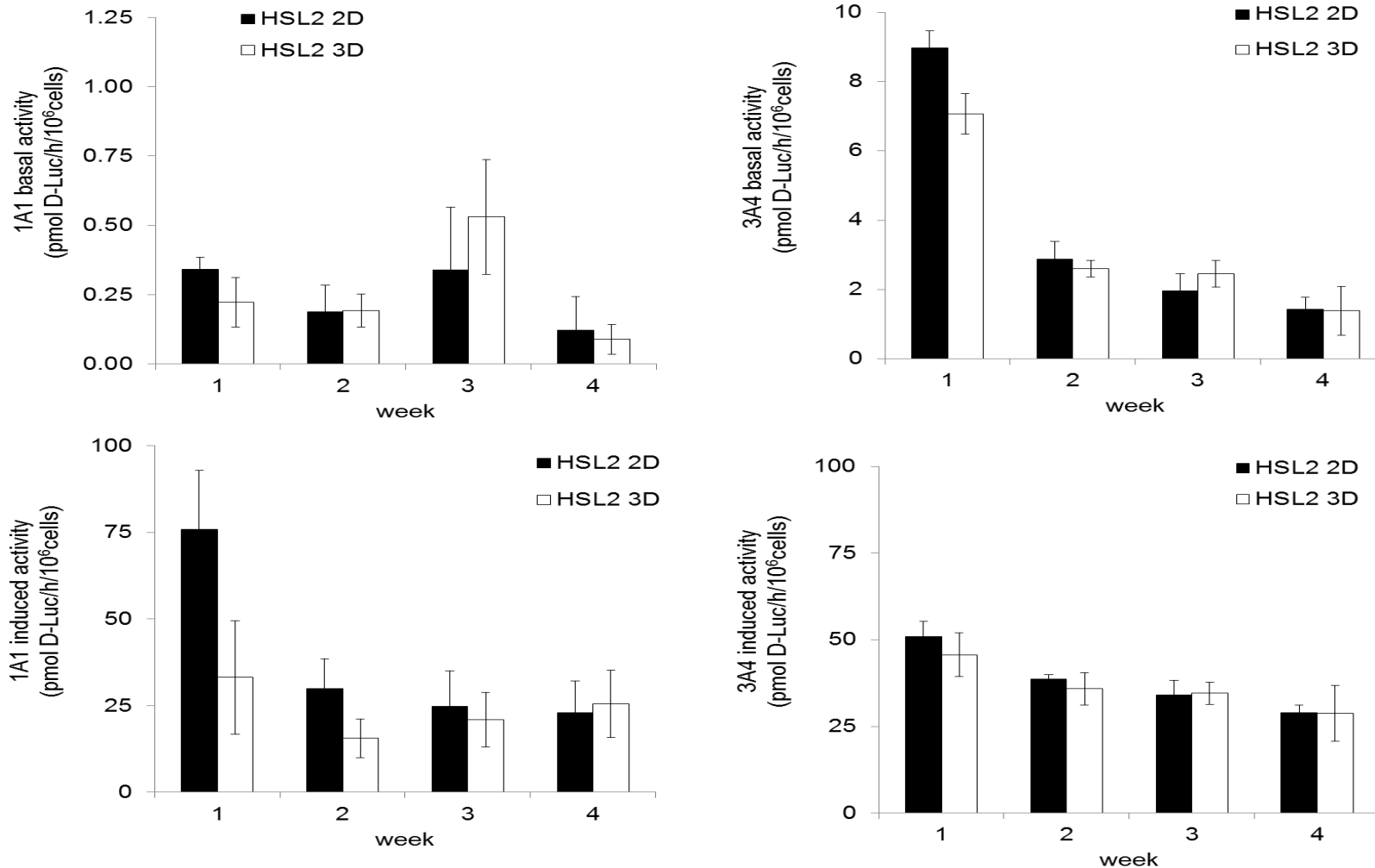
Force



Morphology of Primary Human Hepatocytes in Serum-free Medium at 7 and 28 Days in Culture



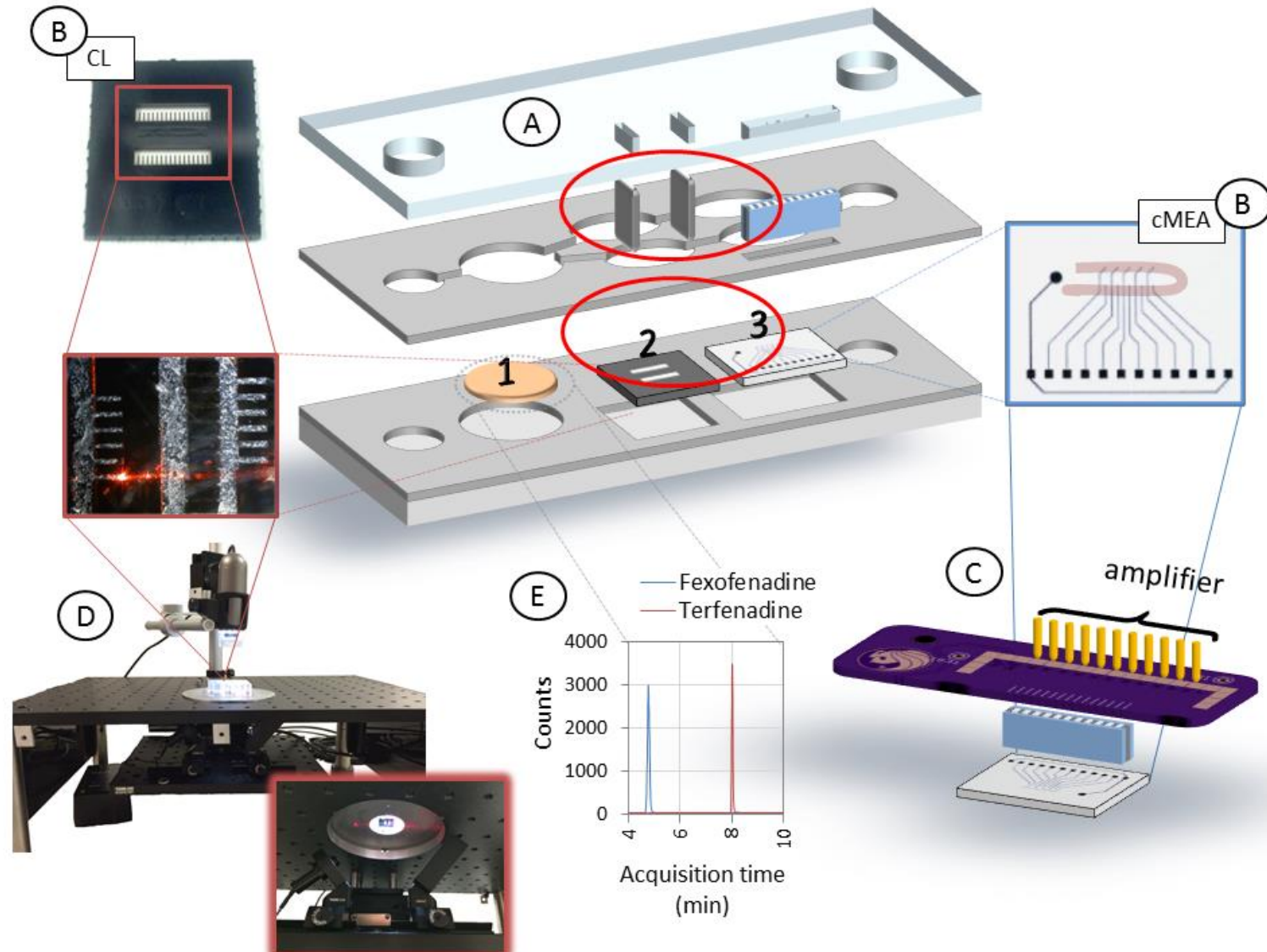
Basal and Induced CYP Activity Levels of 2D and 3D hepatocyte cultures up to 28 days in serum-free medium



Hepatocytes in Serum-free medium at 28 DIV possess reasonable CYP activity levels which are inducible

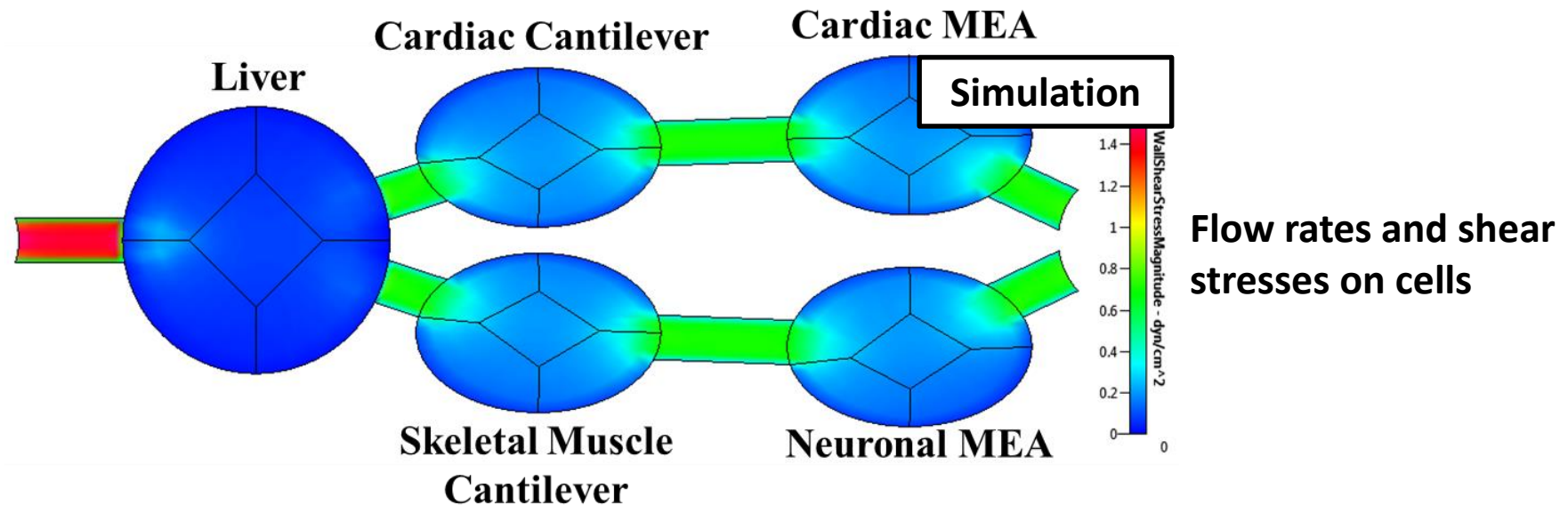
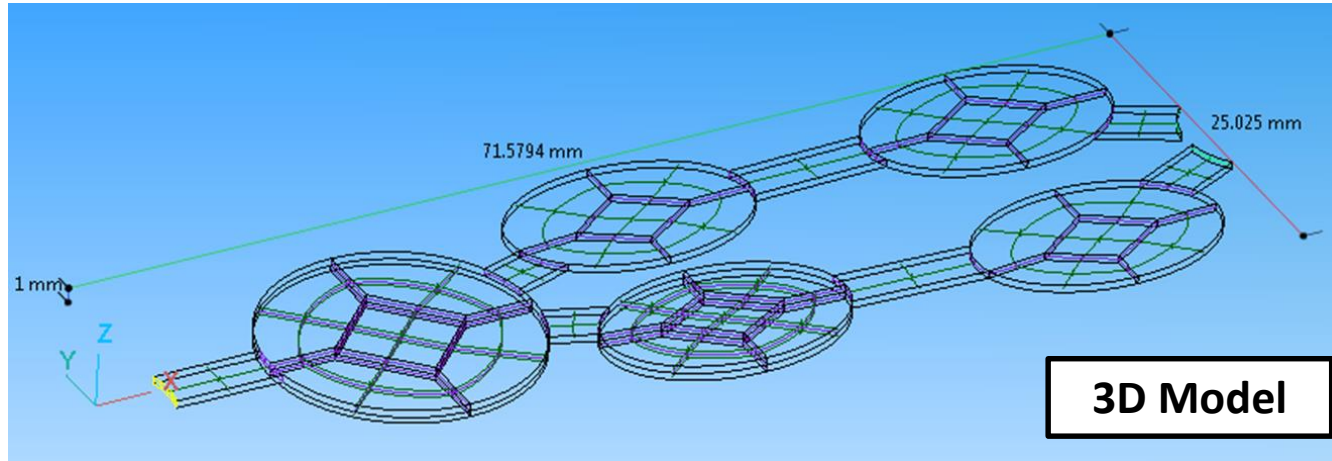
HEART-LIVER

Cardiac and liver co-culture in a pumpless microfluidic system

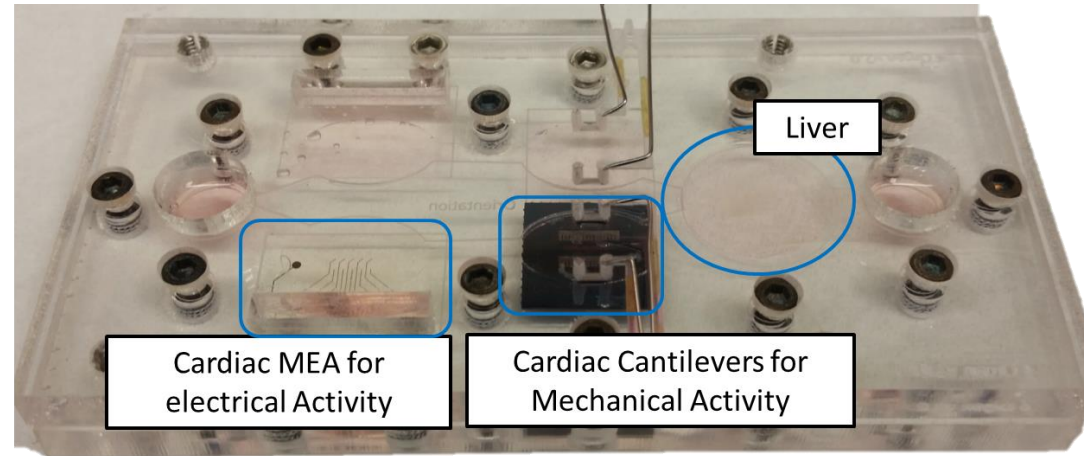


Simulation-Assisted System Design

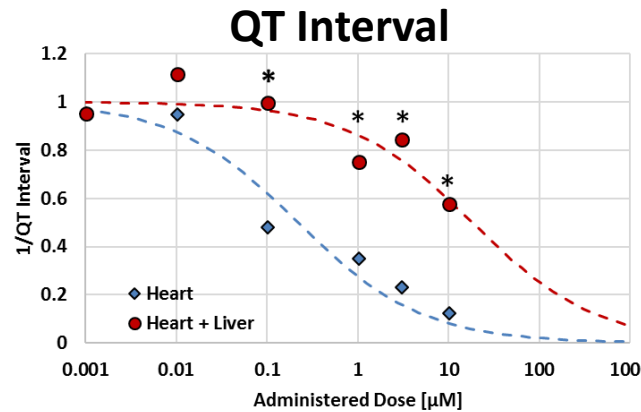
Combination of microfluidic computational fluidic dynamics (CFD) modeling and electrical-like simulation



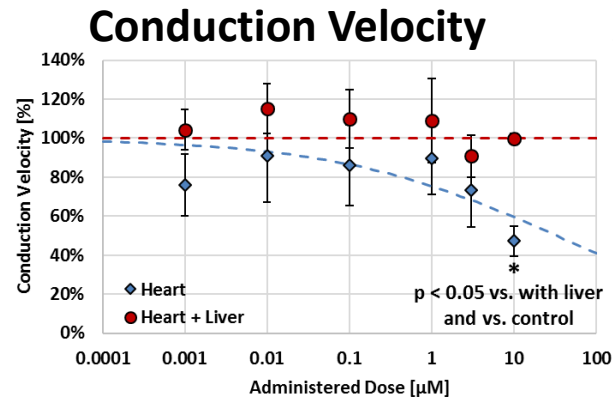
Heart-Liver Systems with Recirculating Serum-Free Medium



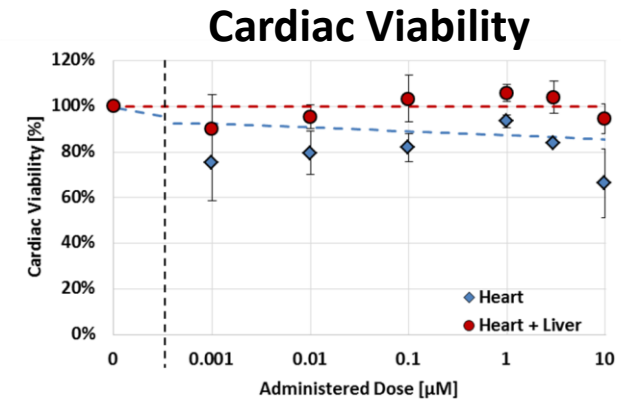
Heart + liver system derived from 4-organ system with similar flow characteristics



Terfenadine Addition Results in Elongation of QT Interval in the Absence of a Liver Component



Terfenadine Addition Reduces Conduction Velocity in the Absence of a Liver Component



Without liver, terfenadine slightly reduces cardiac viability at 10 µM terfenadine

$$IC_{50} = 33 \mu\text{M} \text{ (Heart)}$$

$$IC_{50} = \text{NA} \text{ (Heart + Liver)}$$

$$IC_{50,1} > 10 \mu\text{M} \text{ (Heart)}$$

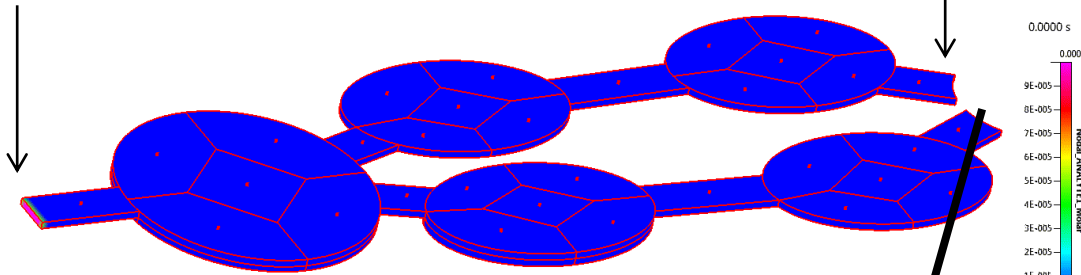
$$IC_{50} > 10 \mu\text{M} \text{ (Heart + Liver)}$$

Lipophilic Compound Concentration in Systems

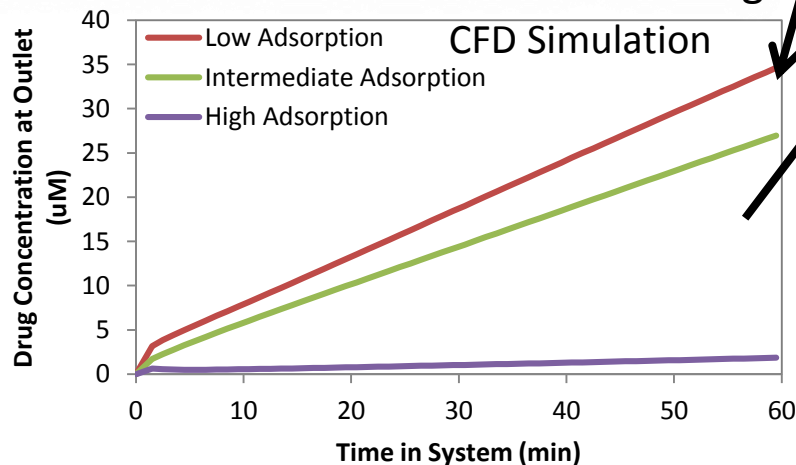
5 min to 24 hours

Compound (330 μM) added to this reservoir for 100 μM final concentration

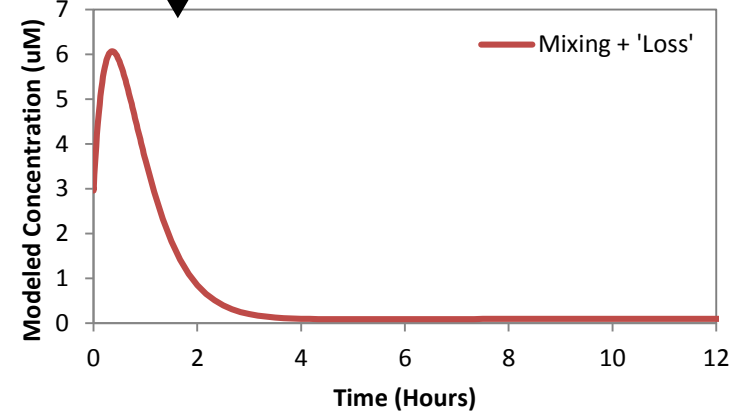
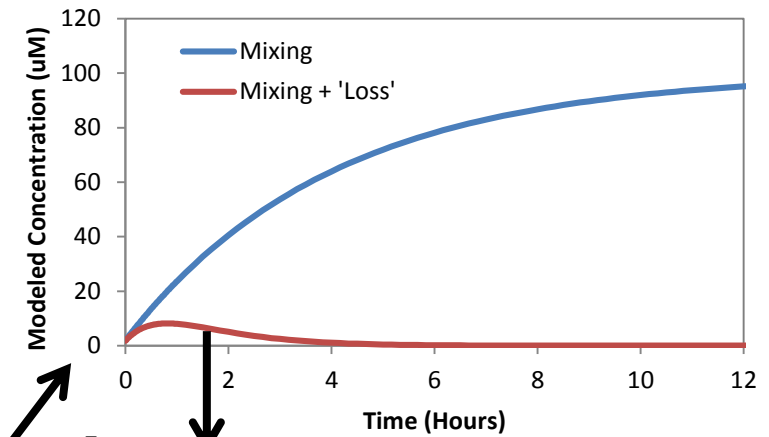
Withdrawal from this reservoir



Simulation of Drug addition to one side with initial perfusion due to volume difference + Rocking



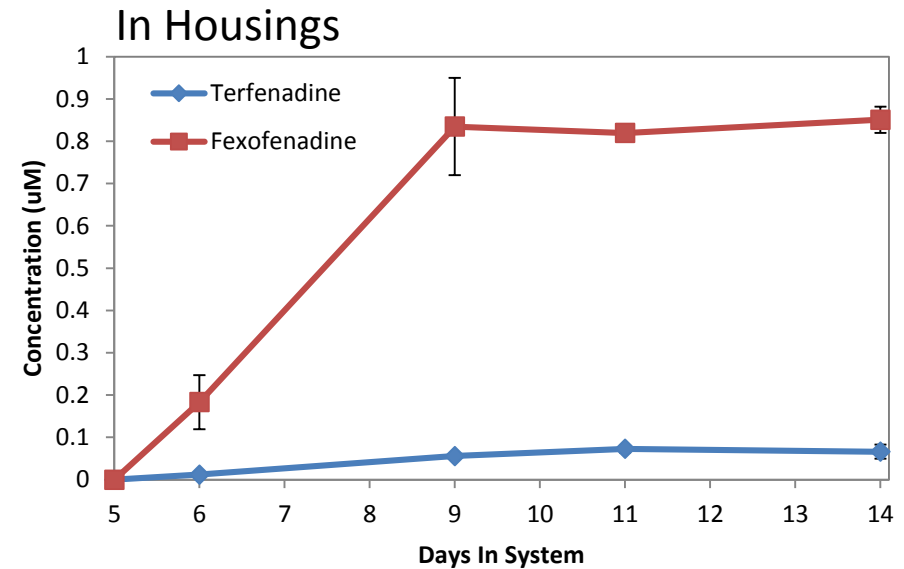
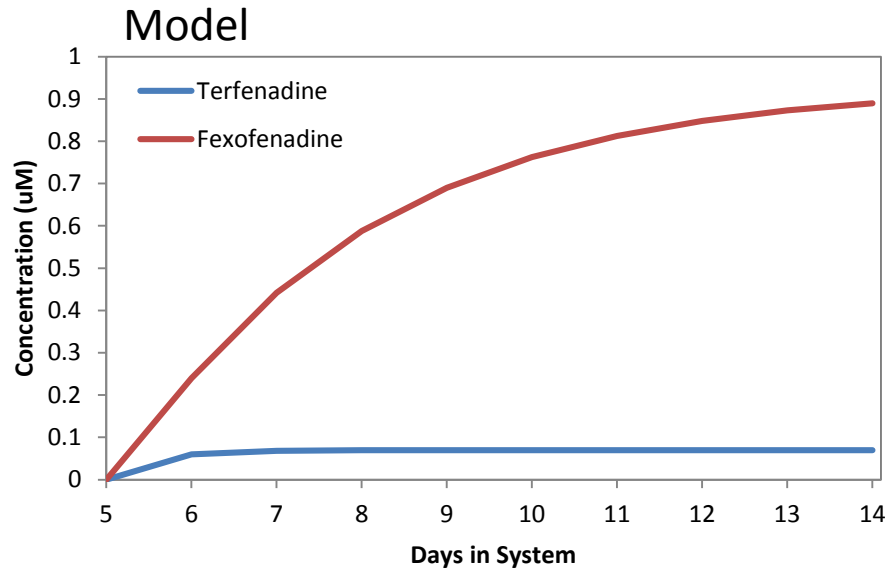
Numerical Simulation



Concentration at reservoir opposite liver dependent on mixing along with adsorption, metabolism, and bioaccumulation ("loss")

Chronic 4 Organ System: HPLC-MS

0.2 μM Daily Addition of Terfenadine



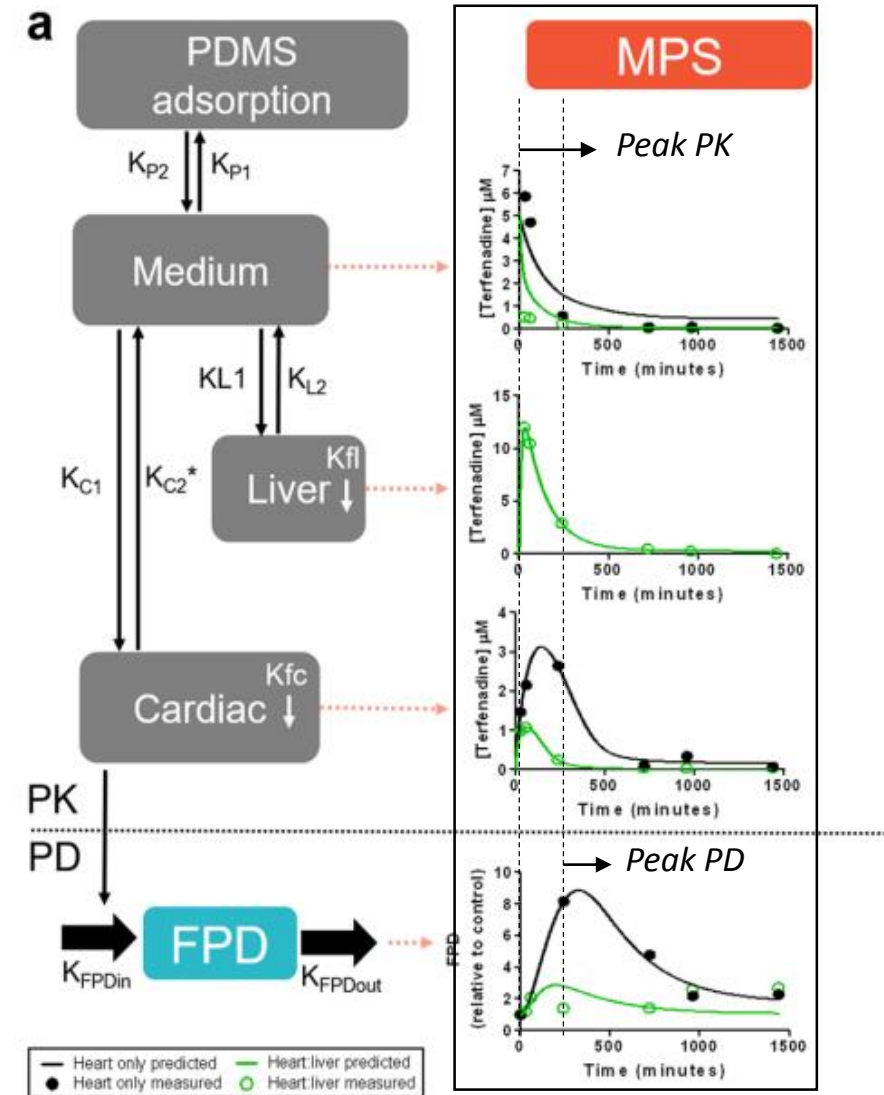
$$f = 0.3, X = 0.8$$

The measured concentrations of terfenadine and fexofenadine in housing systems with chronic addition of drug leveled to a steady state concentration, **as predicted by modeling**

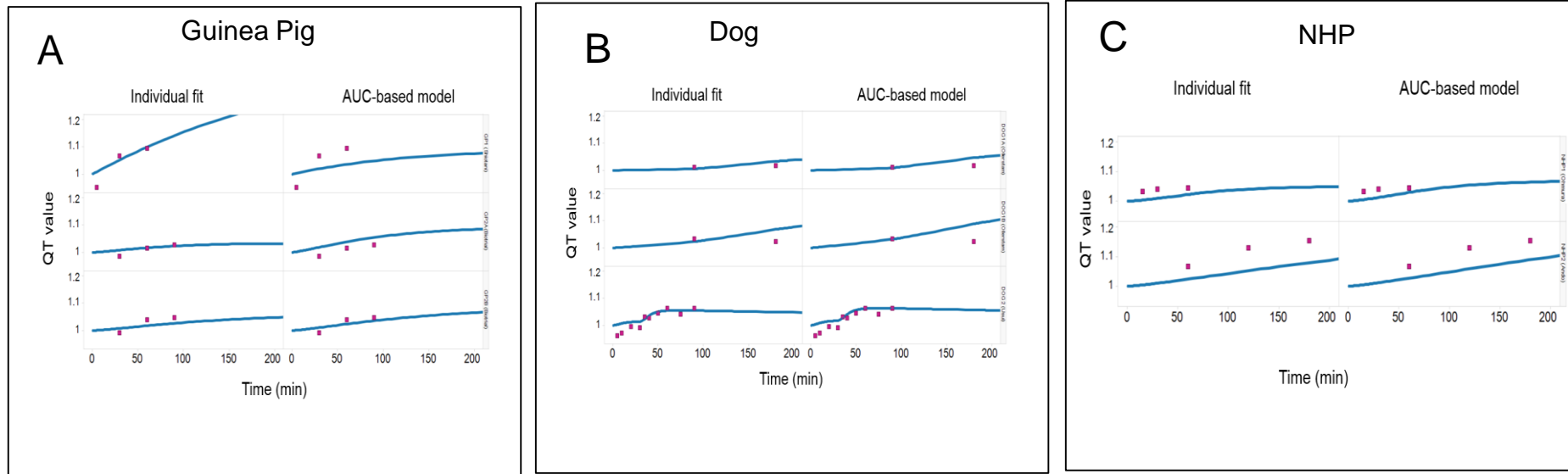
Equilibrium between removal from feeding and addition + metabolism

PK-PD Relationship Approach

- Previous data from Terfenadine (Scientific Reports paper) showed a time between medium concentration and the FPD elongation
 - Similar to monkey data in vivo
- Multi-compartment model incorporating PDMS adsorption, medium, and the tissues was implemented
- A PK model was implemented in that study to obtain the relationship between medium concentration and bioaccumulation in the in vitro systems (K_{C1} , K_{C2})



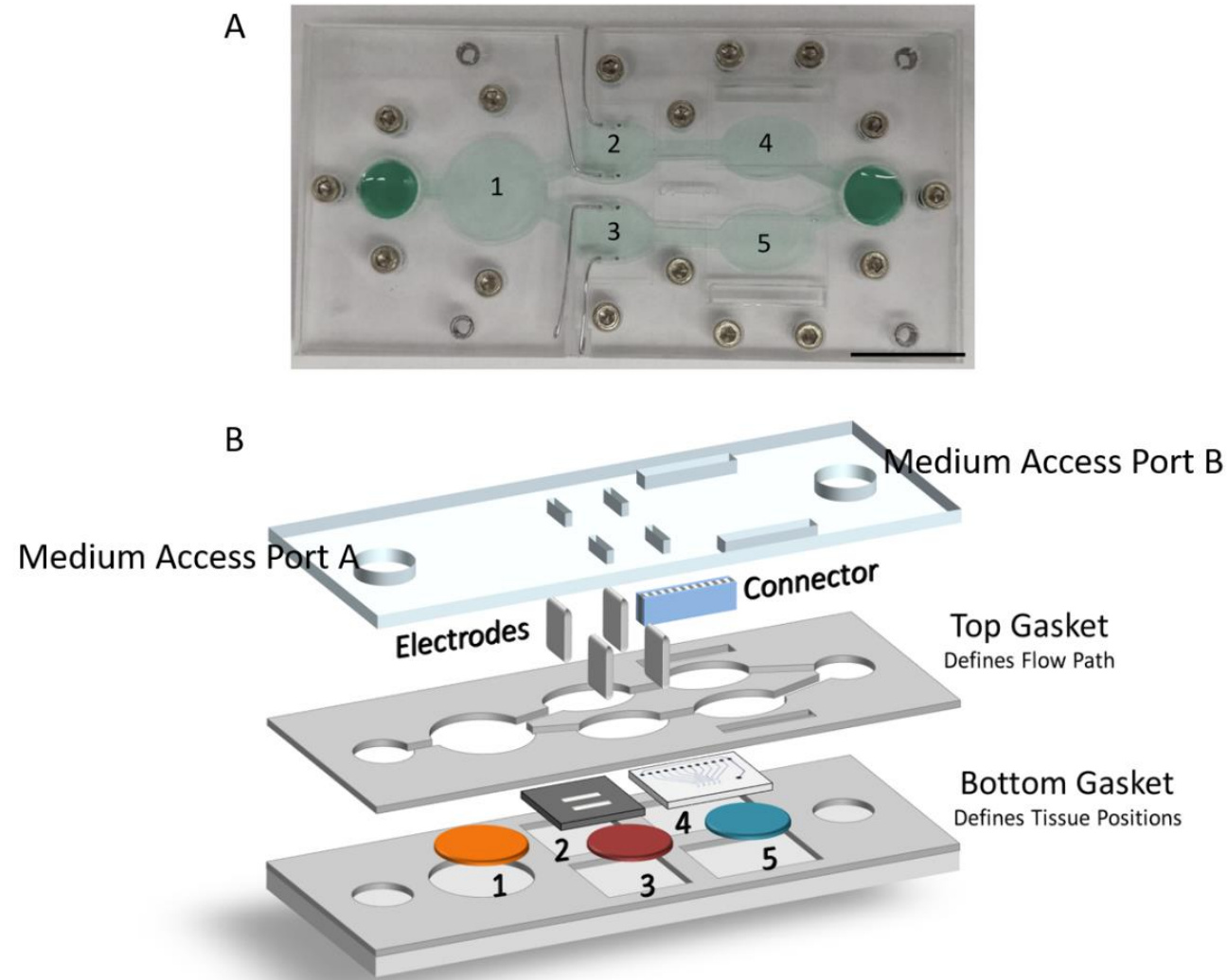
Correlation of In Vitro PKPD Model with In Vivo Animal PKPD Models



Since in vivo animal data has been correlated with clinical data we should be able to correlate our in vitro models with clinical data as well both retrospectively and prospectively

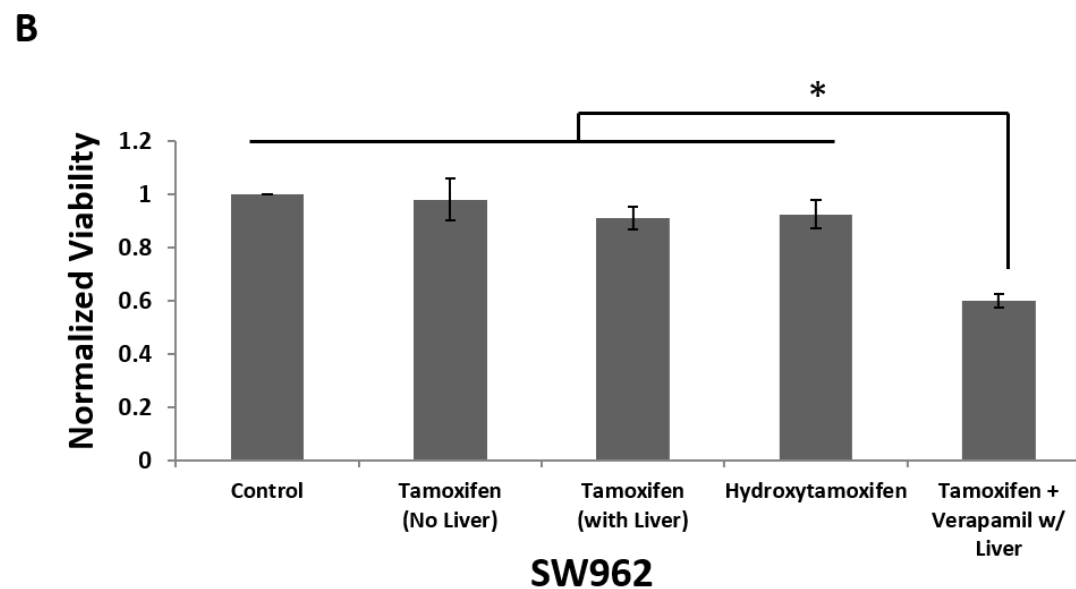
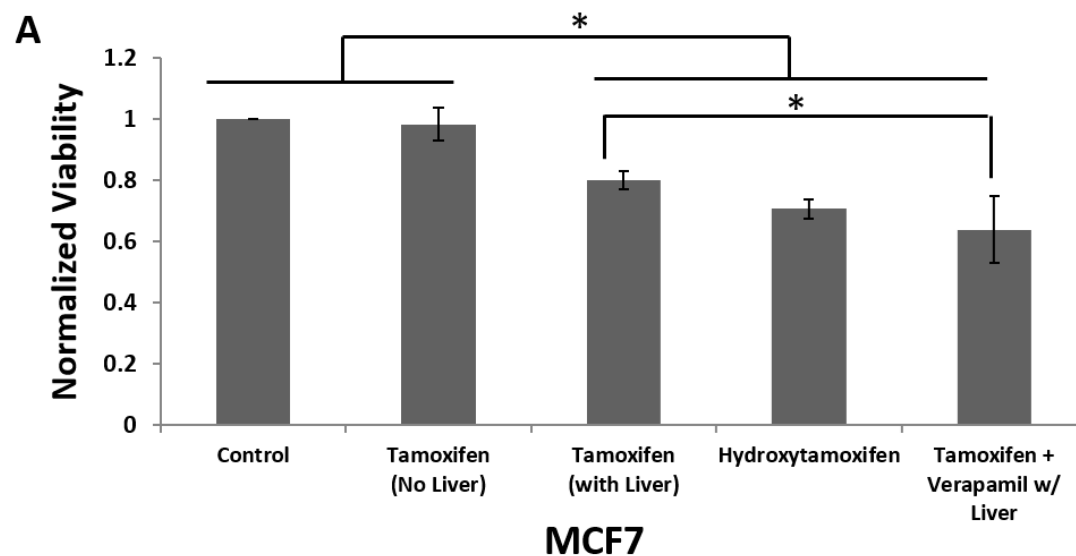


Cancer, Cardiac and Liver System for Efficacy and Tox



Five chamber reconfigurable multi-organ system. Scale bar is 2 cm. B) Schematic representation of the MPS assembly and design used in the system 2 study of tamoxifen. Chamber 1 houses hepatocytes on coverslips Chambers 2 and 4 are cardiac cantilevers and MEAs respectively. Chambers 3 and 5 are for cancer cells SW962 and MCF7. Drugs were applied to Medium Access Port A and initially pass over the liver to mimic aspects of first pass metabolism. Electrodes are embedded for the option of using broadfield stimulation to elicit contraction.

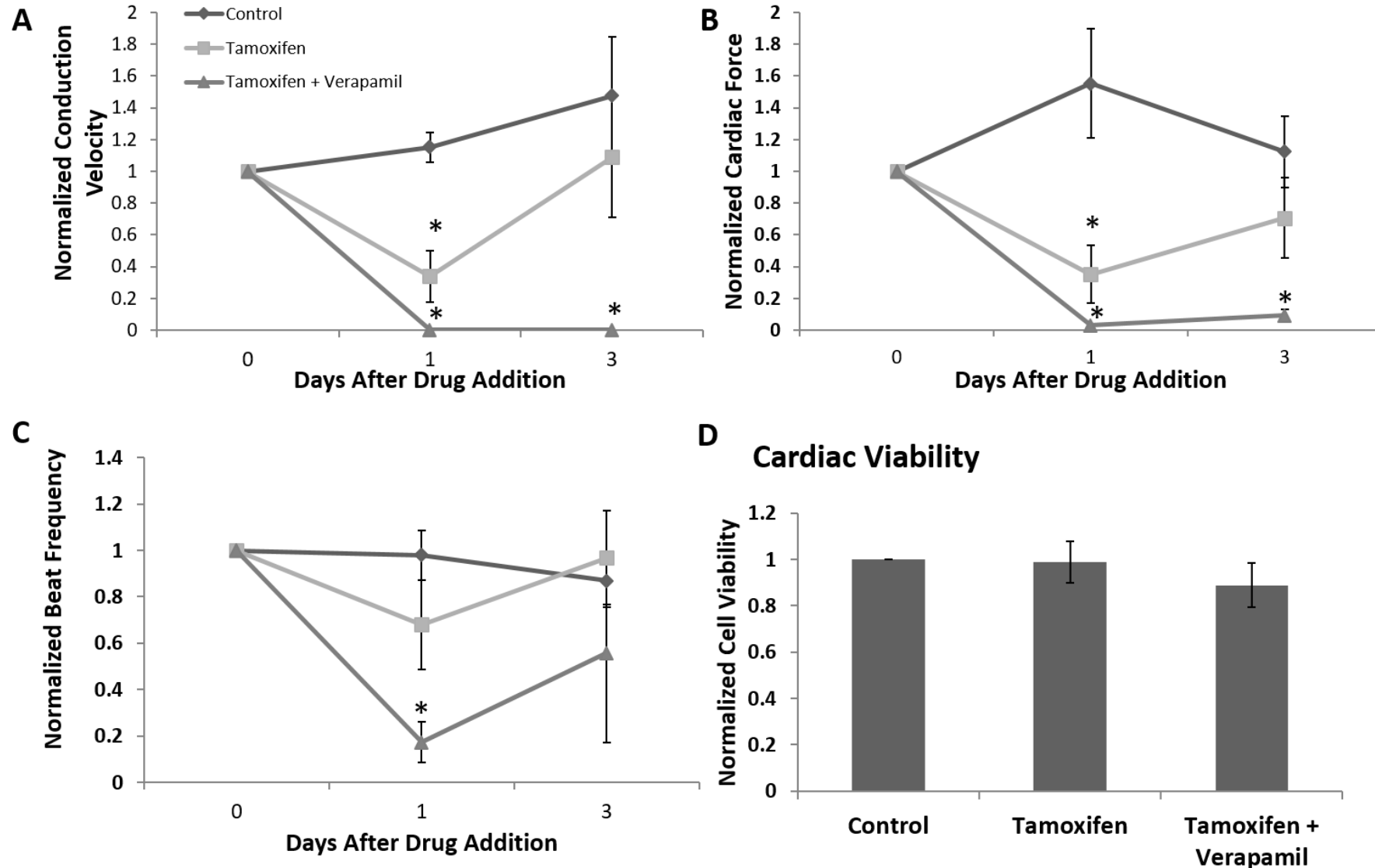
Tamoxifen, with and without metabolism, and the effect on cancer viability



Error bars are represented as SEM. * $p < 0.02$.

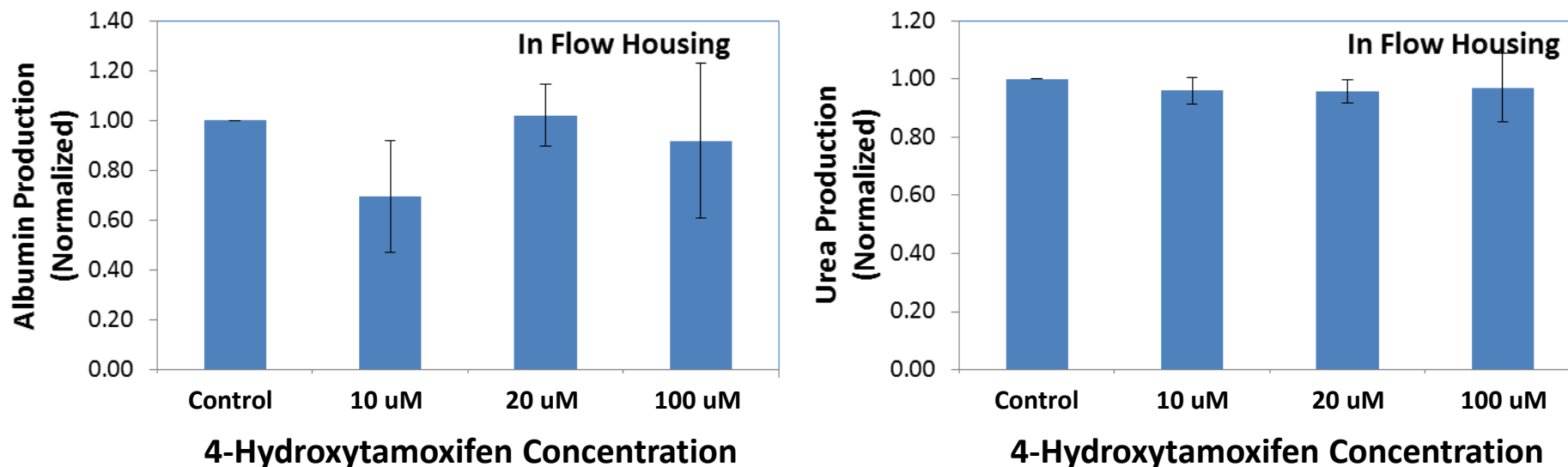
Sentinel Monitoring of Cardiac Function

Cardiac, Cancer, Liver Systems



Error bars are represented as SEM. *p < 0.02

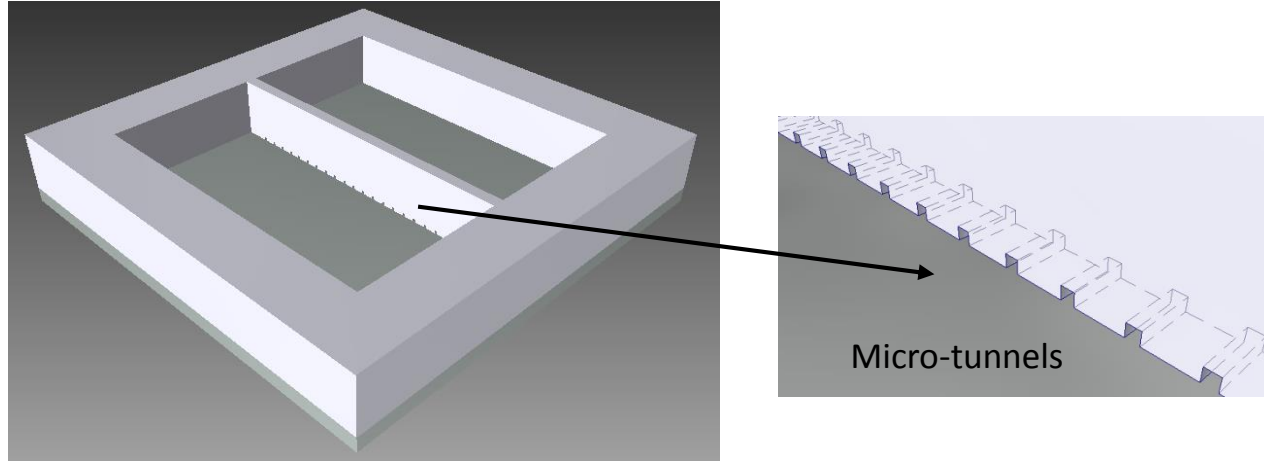
Liver Function in Housings Cancer, Cardiac, Liver System



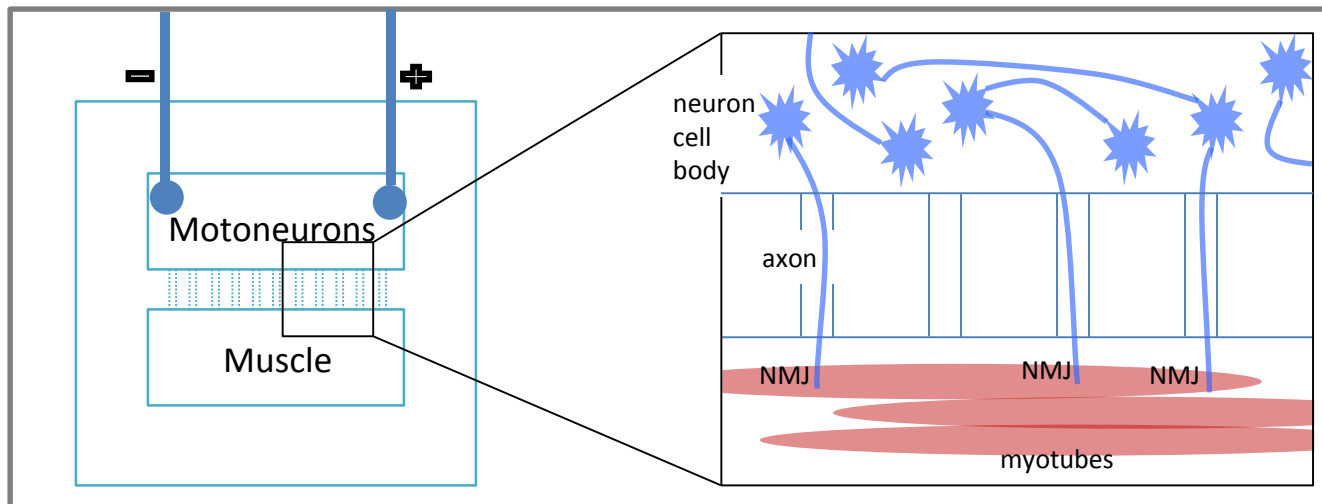
4-Hydroxytamoxifen inside the systems did not affect albumin or urea production after a 24 hour treatment

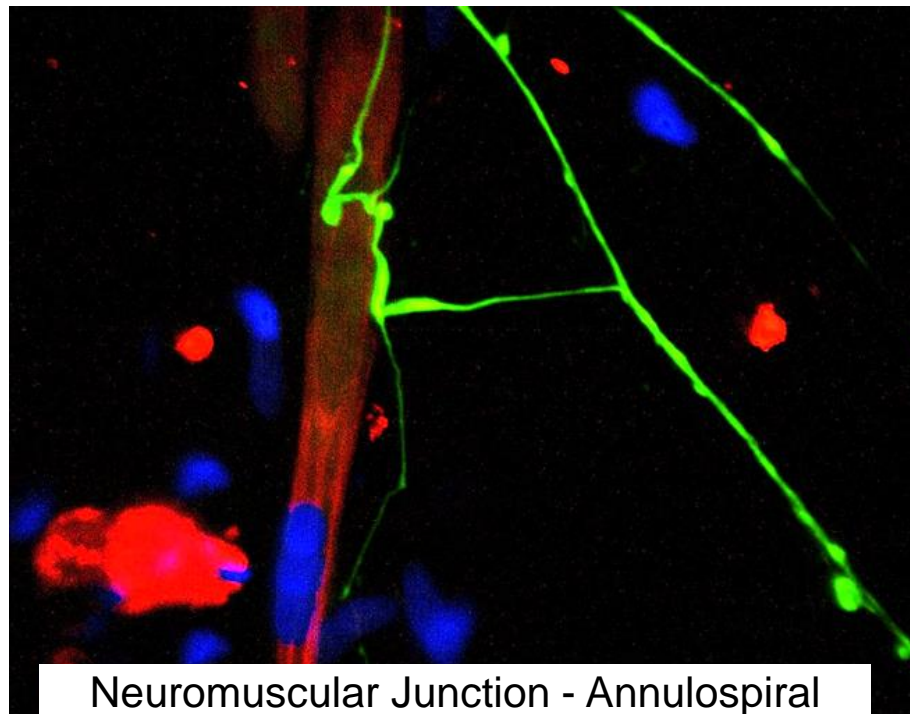
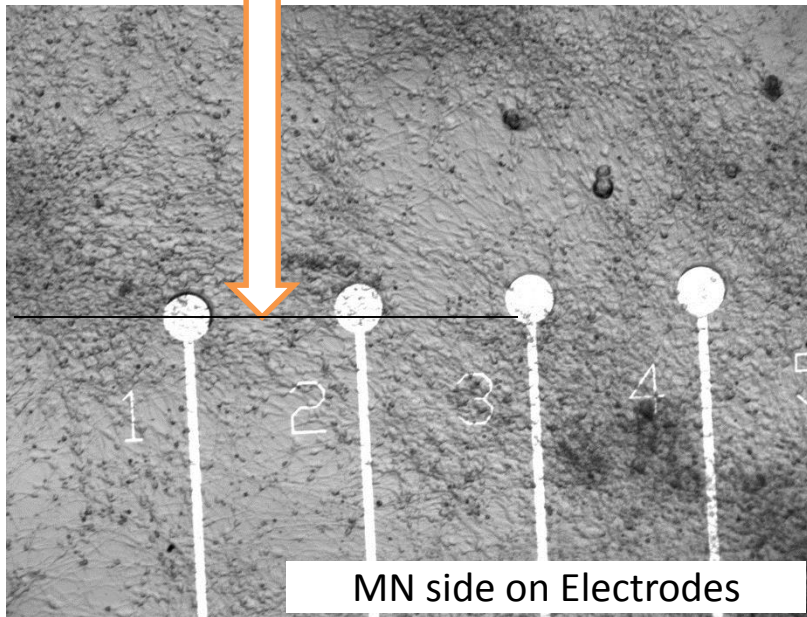
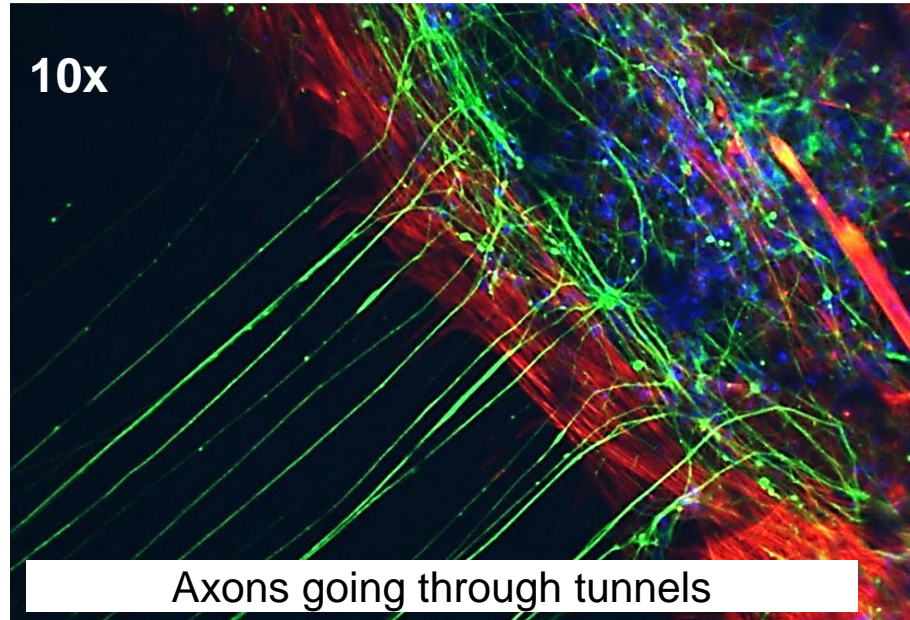
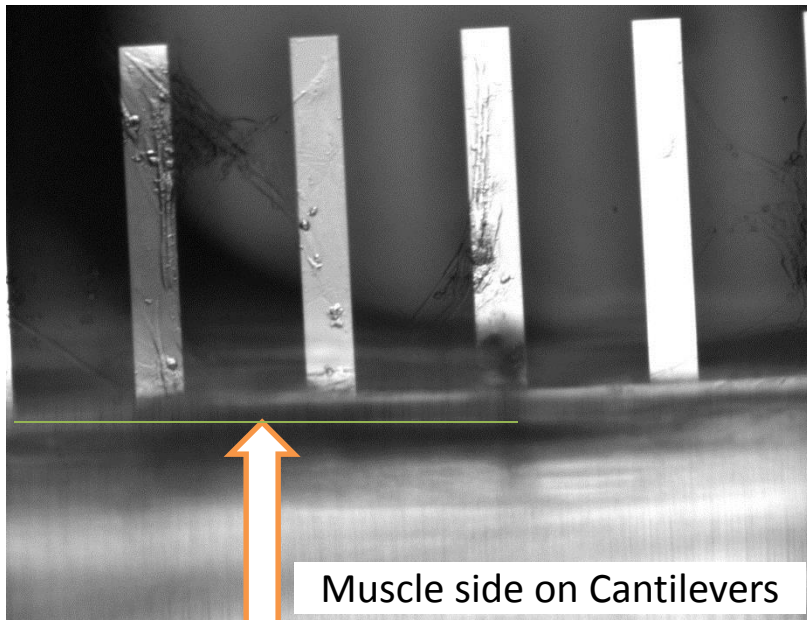


Neuromuscular Junction (NMJ) Platform

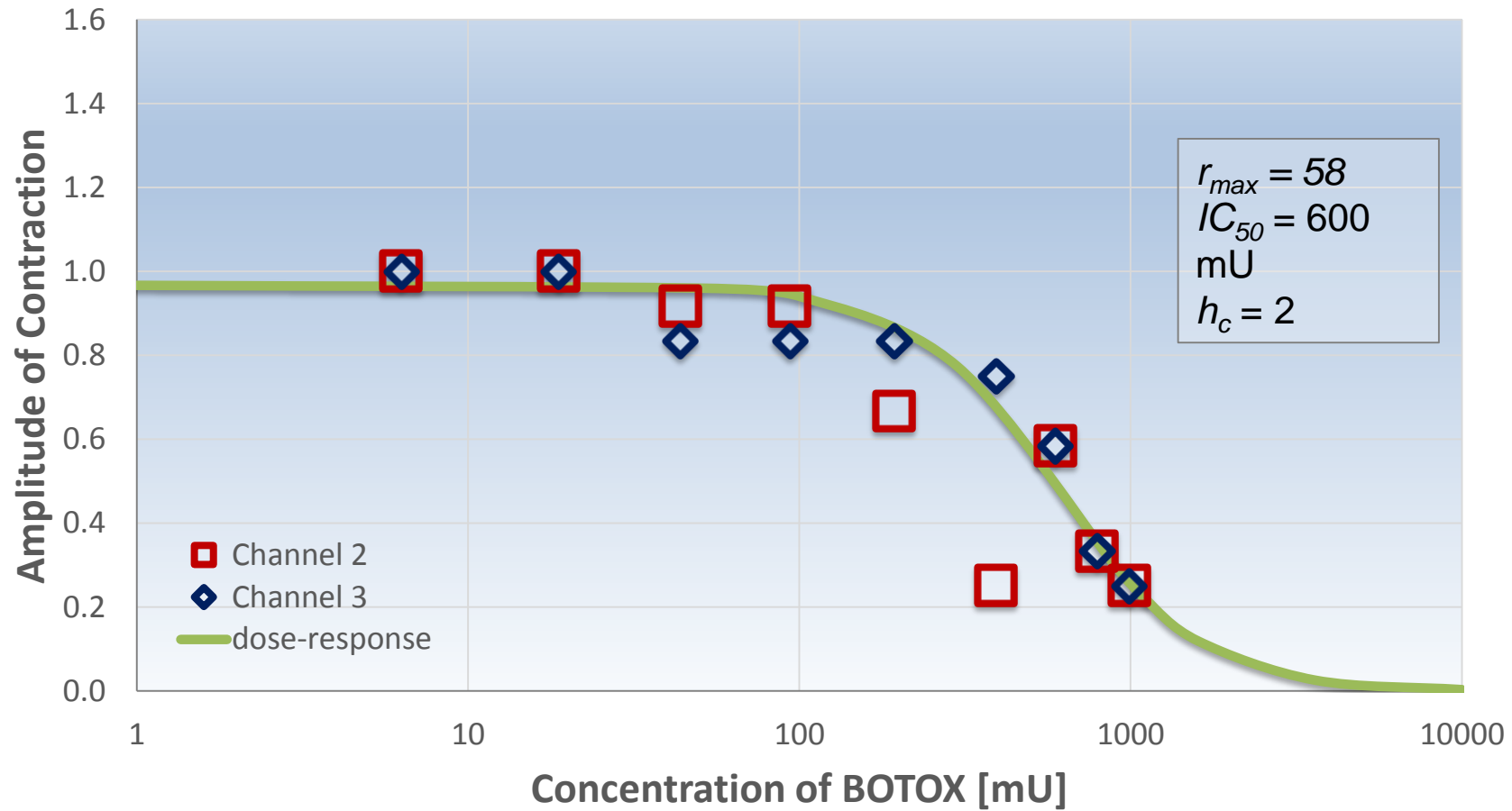


- PDMS molded chambers bonded to glass coverslips
- Two chambers separated by micro-tunnels
- Motoneurons send axons through tunnels and form NMJs
- Electrical stimulation and drugs partitioned by barrier

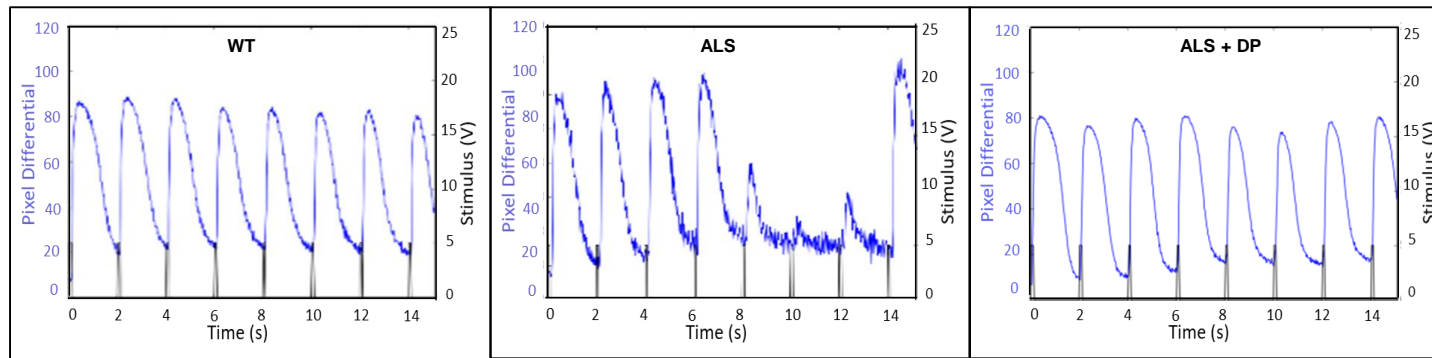
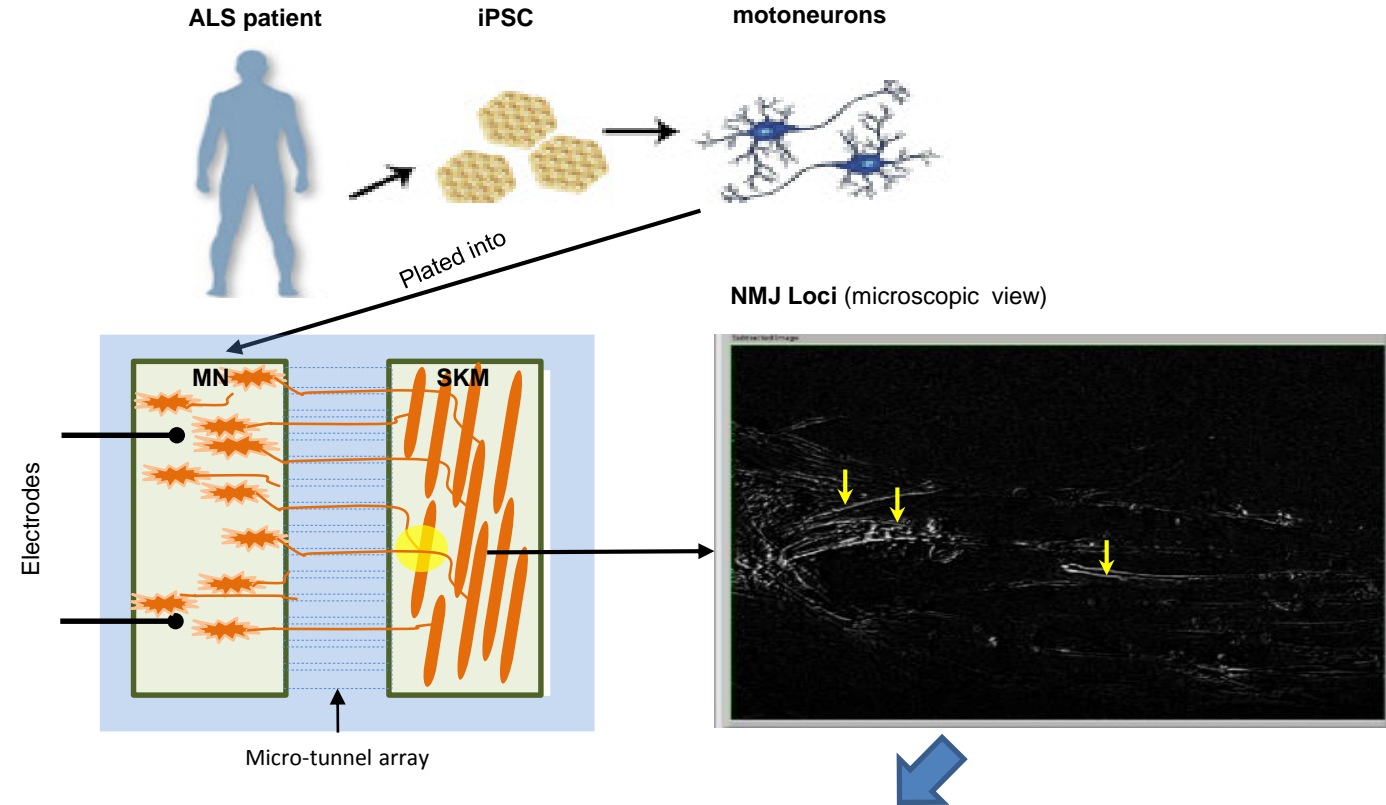




Monophasic Dose-Response for BOTOX at 0.33 Hz



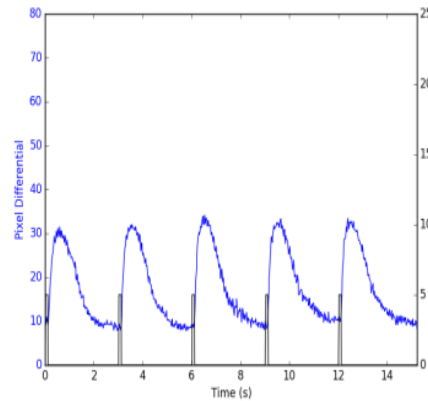
A Human-Based Functional NMJ System for Personalized ALS Modeling and Drug Testing



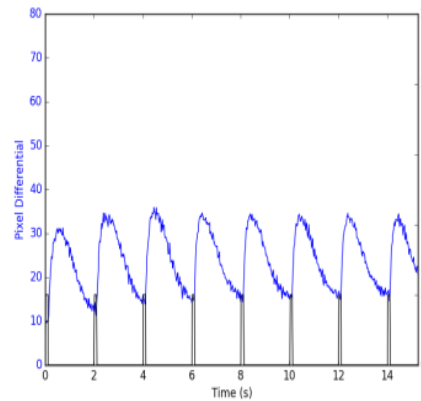
Parameters Analyzed

- Number of functional NMJs/chamber (before and after extensive stimulation)
- NMJ stability (post-NMJ/pre-NMJ)
- NMJ function under different stimulation frequencies (0.33 Hz, 0.5 Hz, 1 Hz, 2 Hz)
--- NMJ fidelity (number of muscle contractions induced by MN stimulation/total number of stimulations)

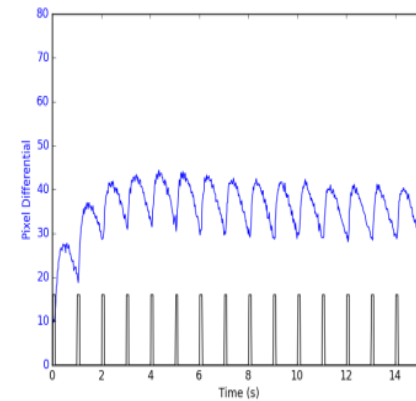
0.33 Hz



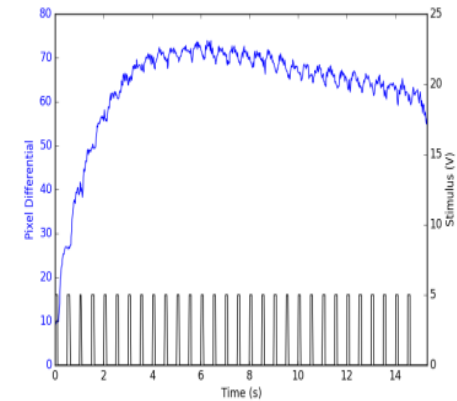
0.5 Hz



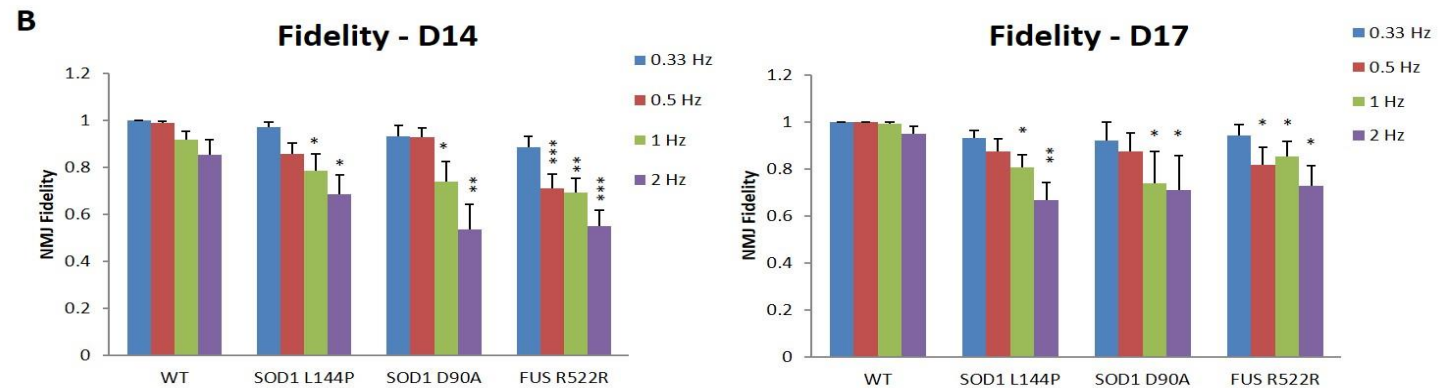
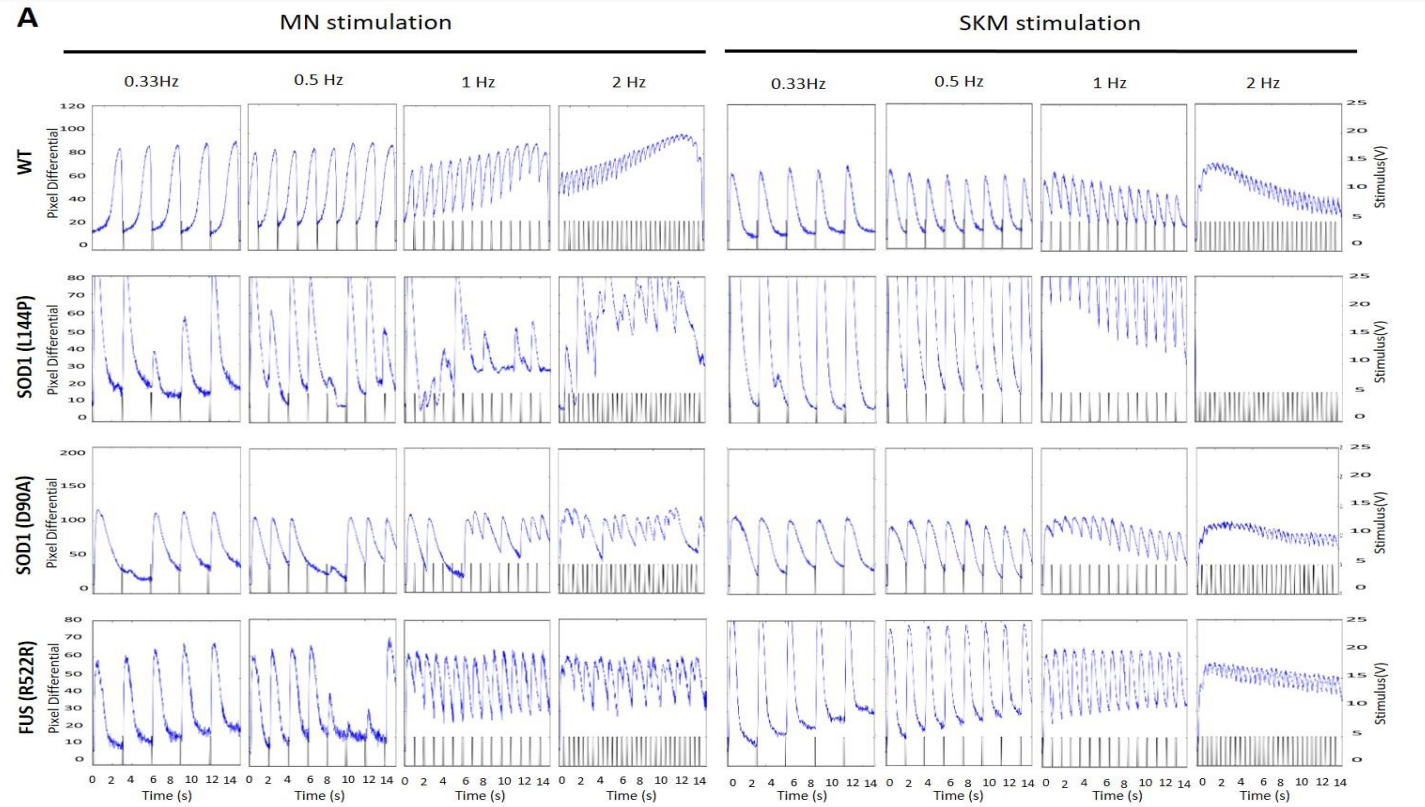
1 Hz



2 Hz

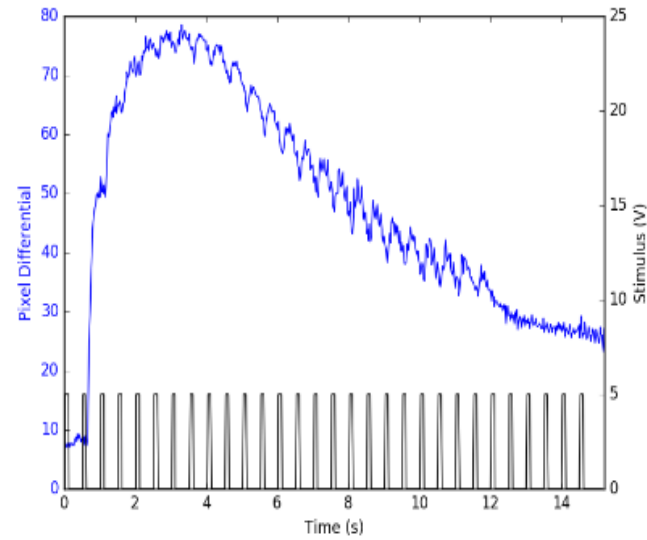


Compromised NMJ fidelity in ALS-NMJs



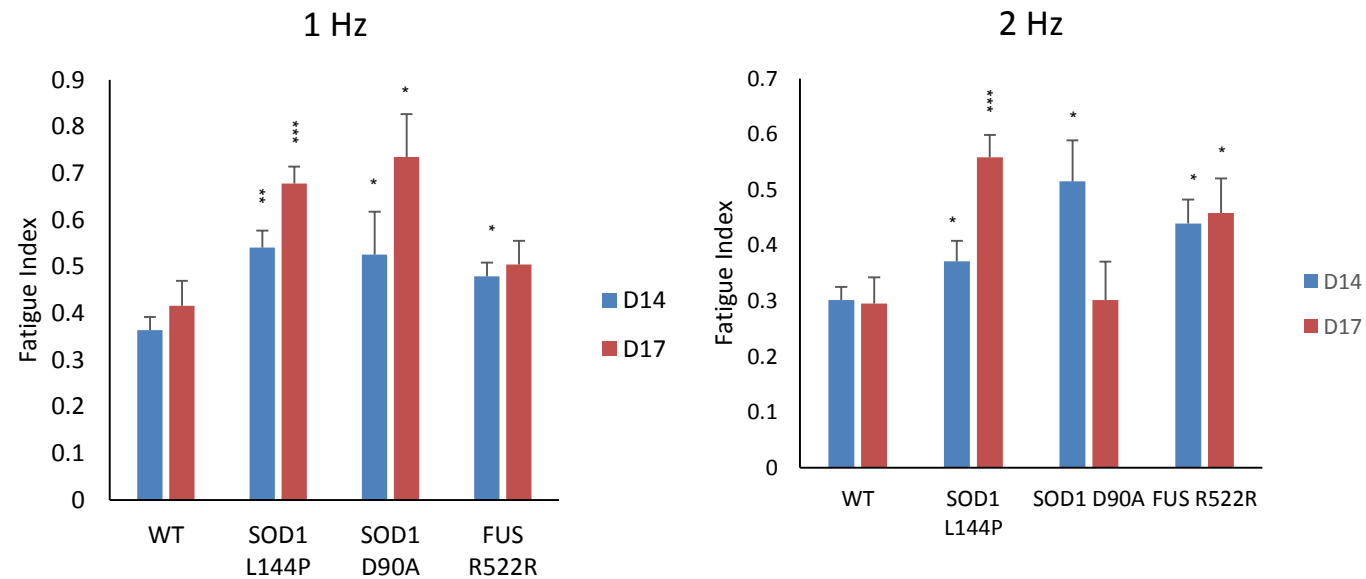
Increased NMJ fatigue index in ALS-NMJs

A

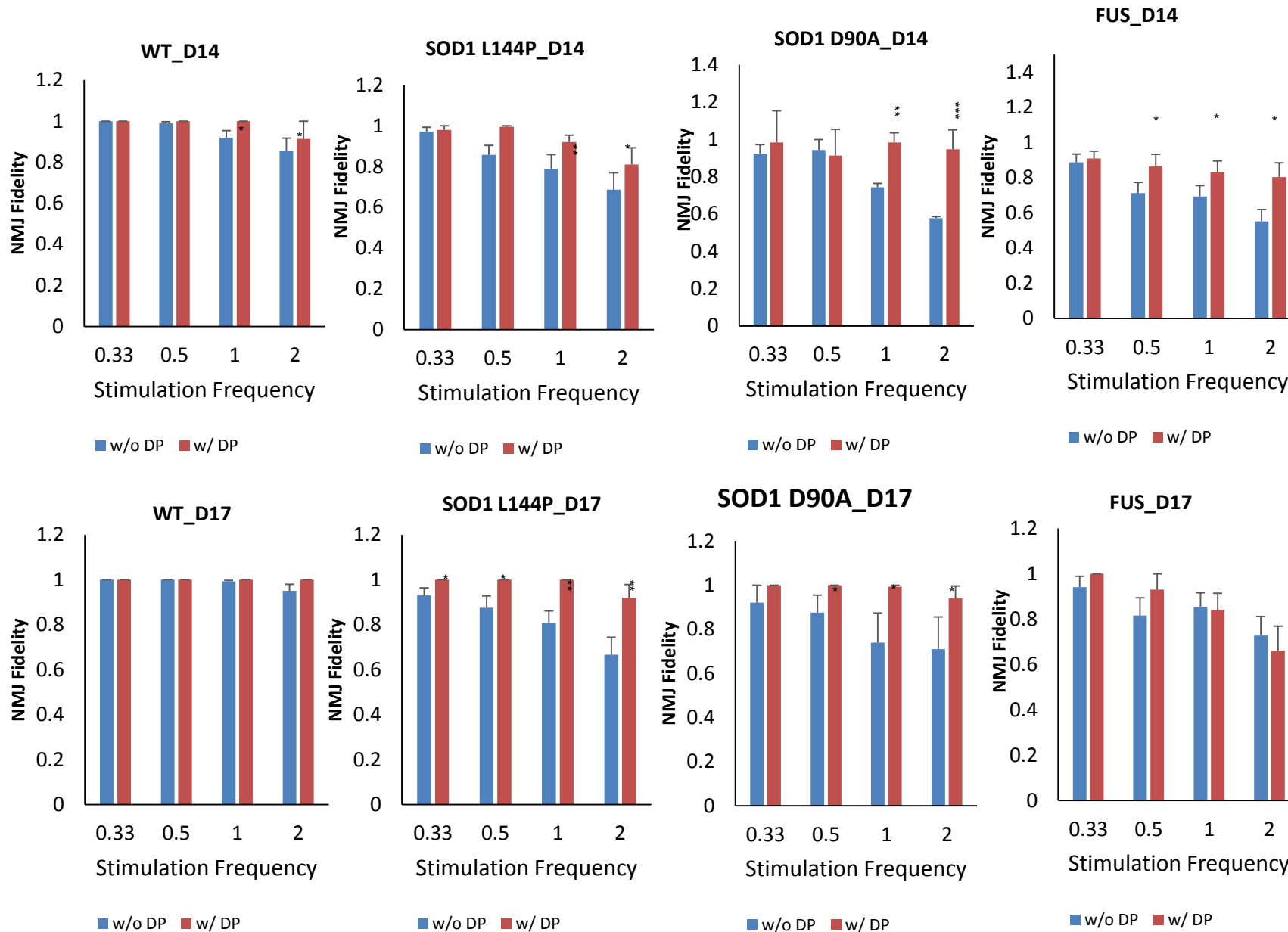


$$\text{Fatigue Index} = 1 - \left[\frac{\text{Area Under Curve}}{\text{Peak Force} \times \text{Time}} \right]$$

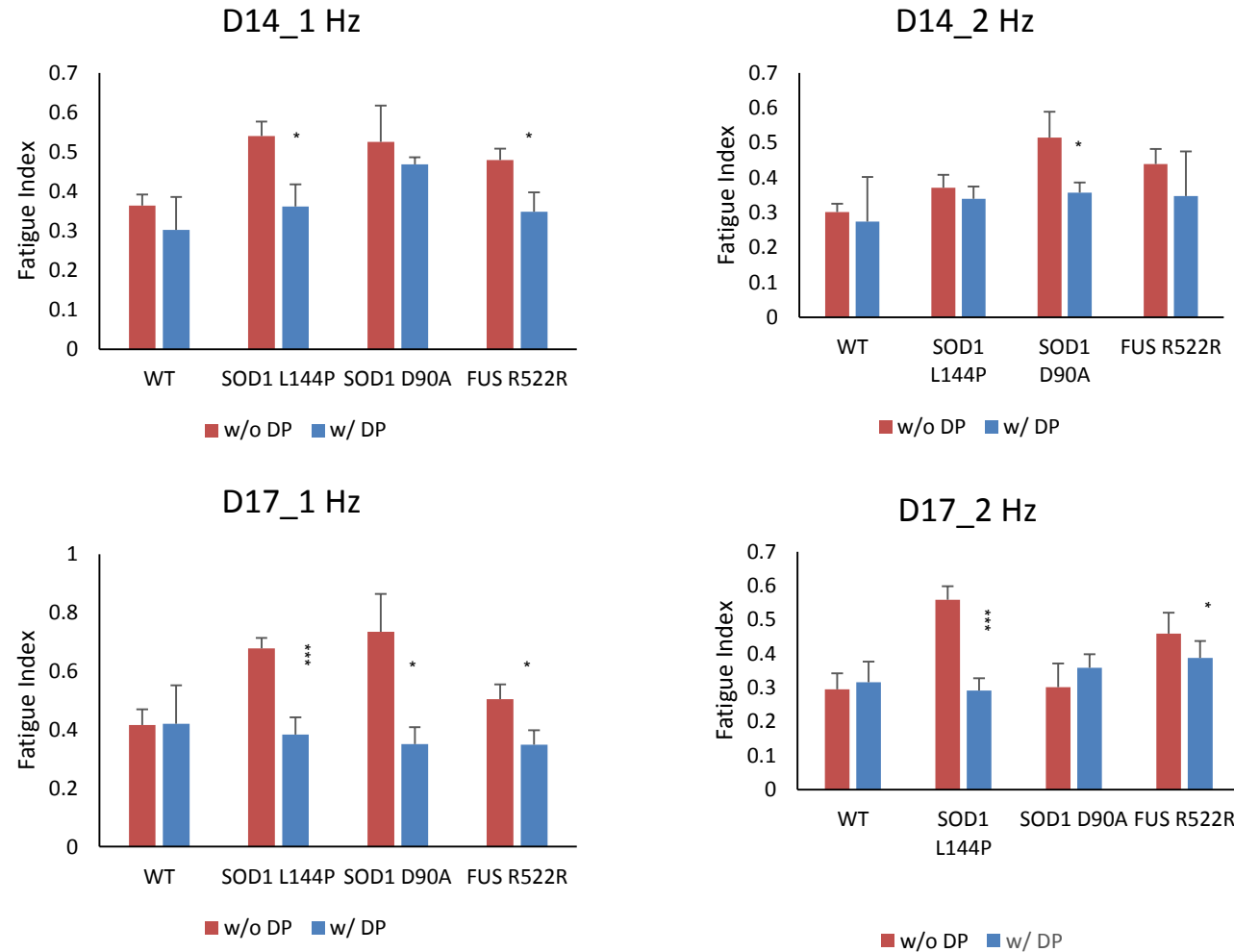
B



Rescue of NMJ fidelity by DP



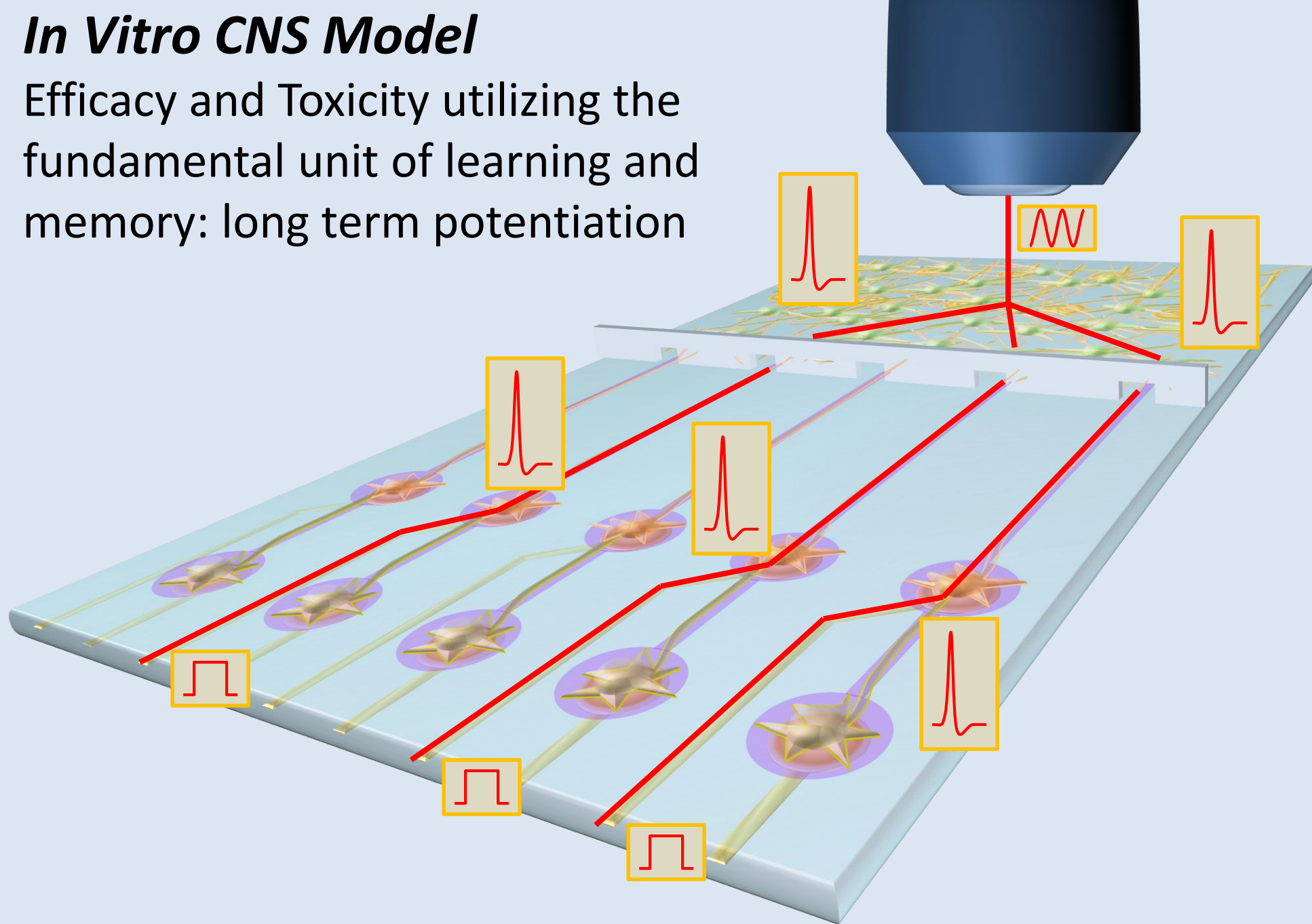
Rescue of NMJ fatigue by DP



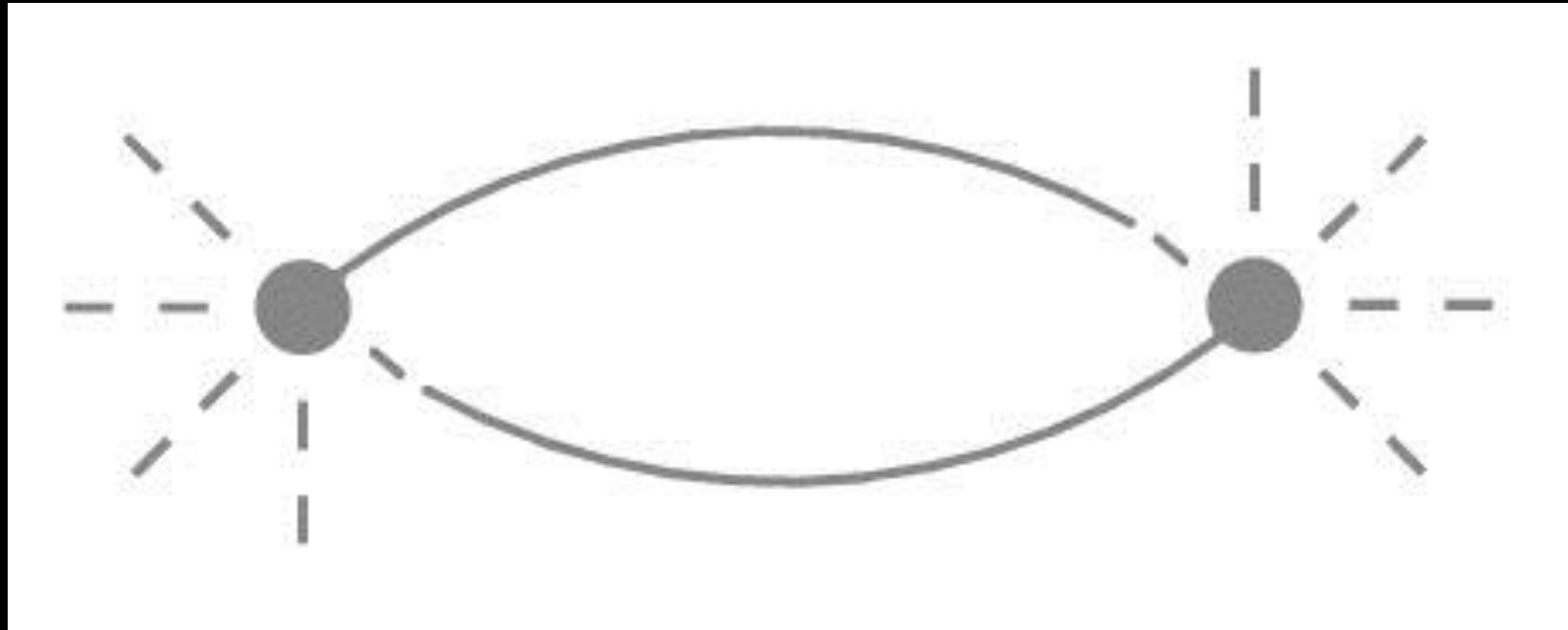
X. Guo, et al., "A human-based functional NMJ system for personalized ALS modeling and drug testing," *Adv. Therapeutics* In Press, Online First: DOI: 10.1002/adtp.202000133, 2020)

In Vitro CNS Model

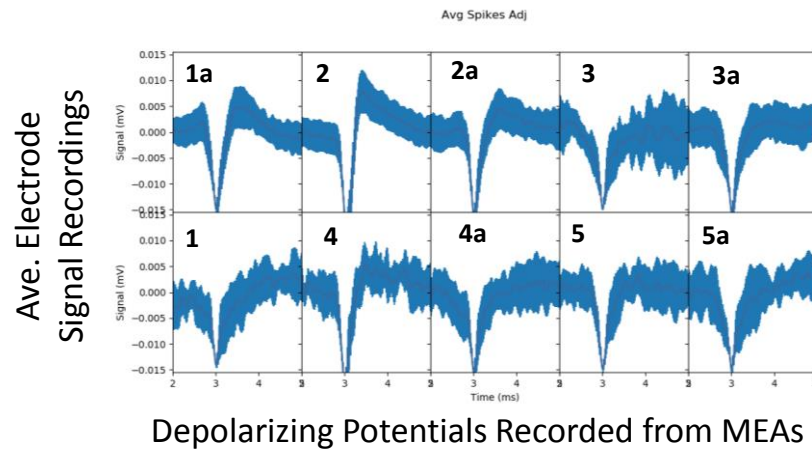
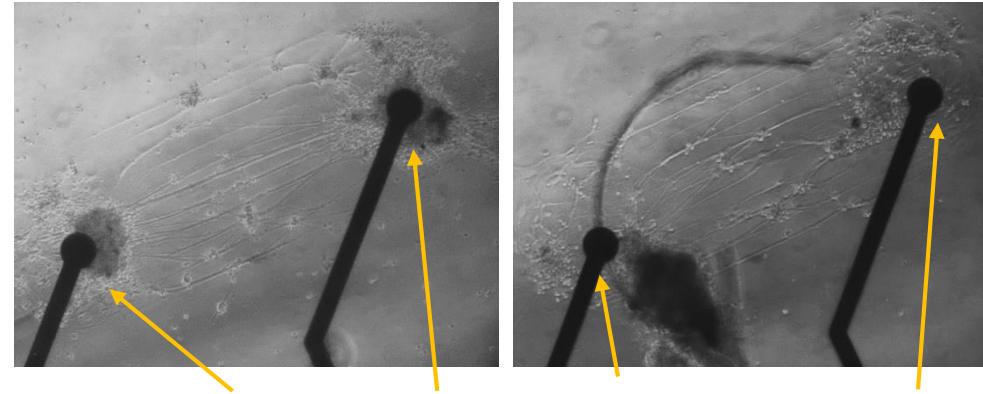
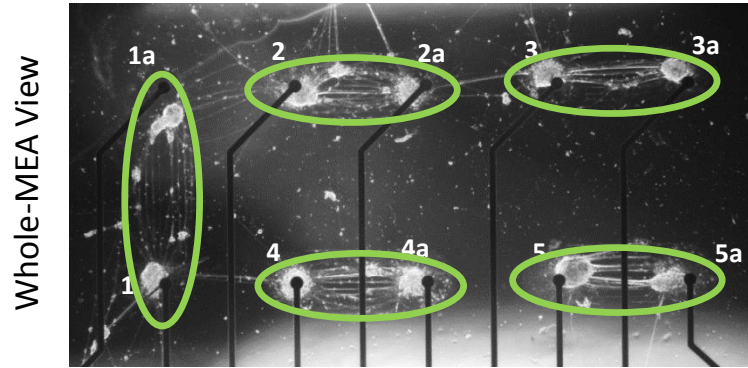
Efficacy and Toxicity utilizing the fundamental unit of learning and memory: long term potentiation



Fundamental unit of long-term potentiation

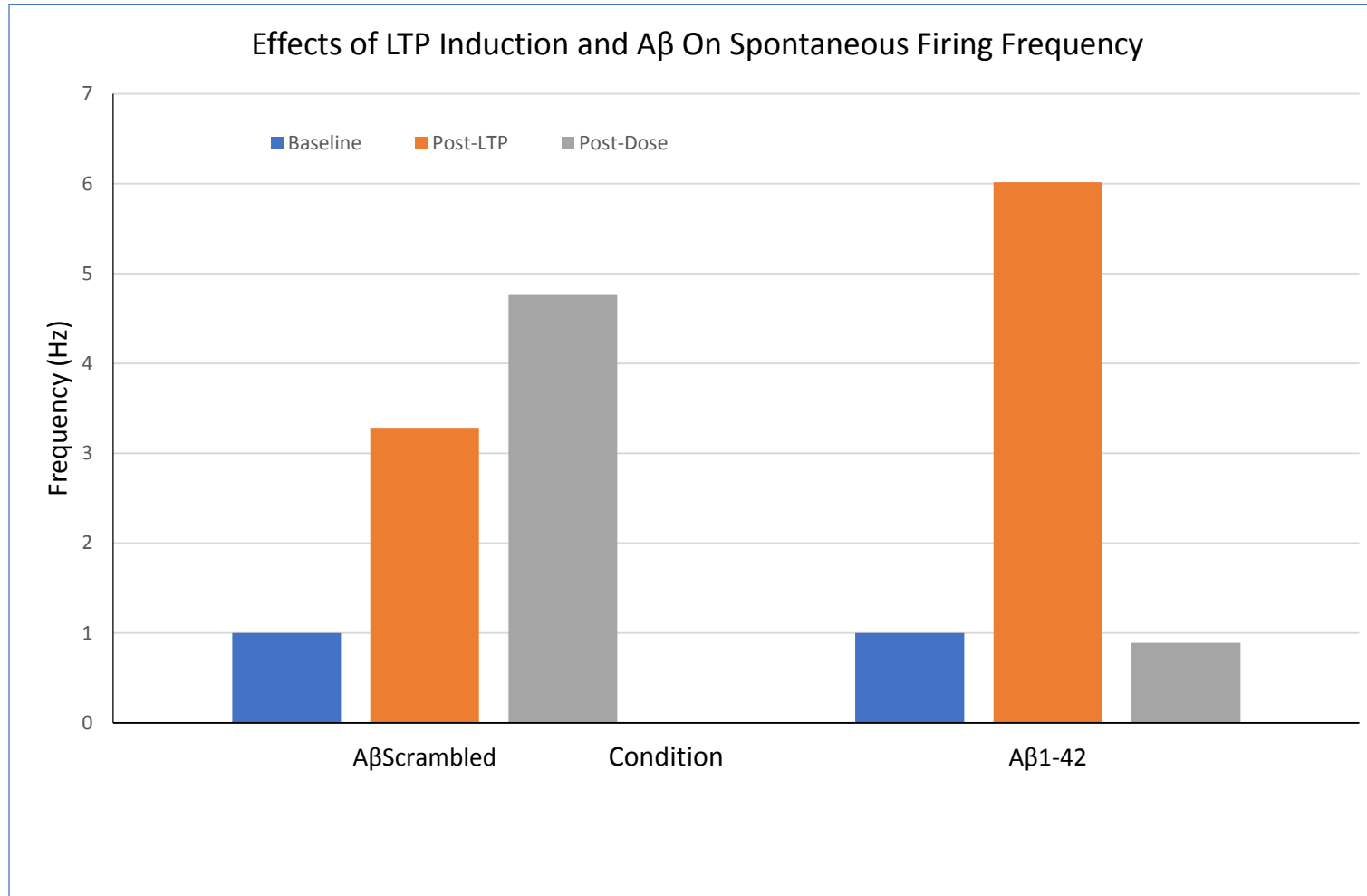


Patterned Neural Networks on MEAs - Long Term Potentiation (LTP)



- High magnification phase images indicating long-term pattern conformity and network formation
- 5 network pairs per MEA
- 45 days *in vitro*
- Spontaneous action potentials recorded on electrodes from paired neural circuits

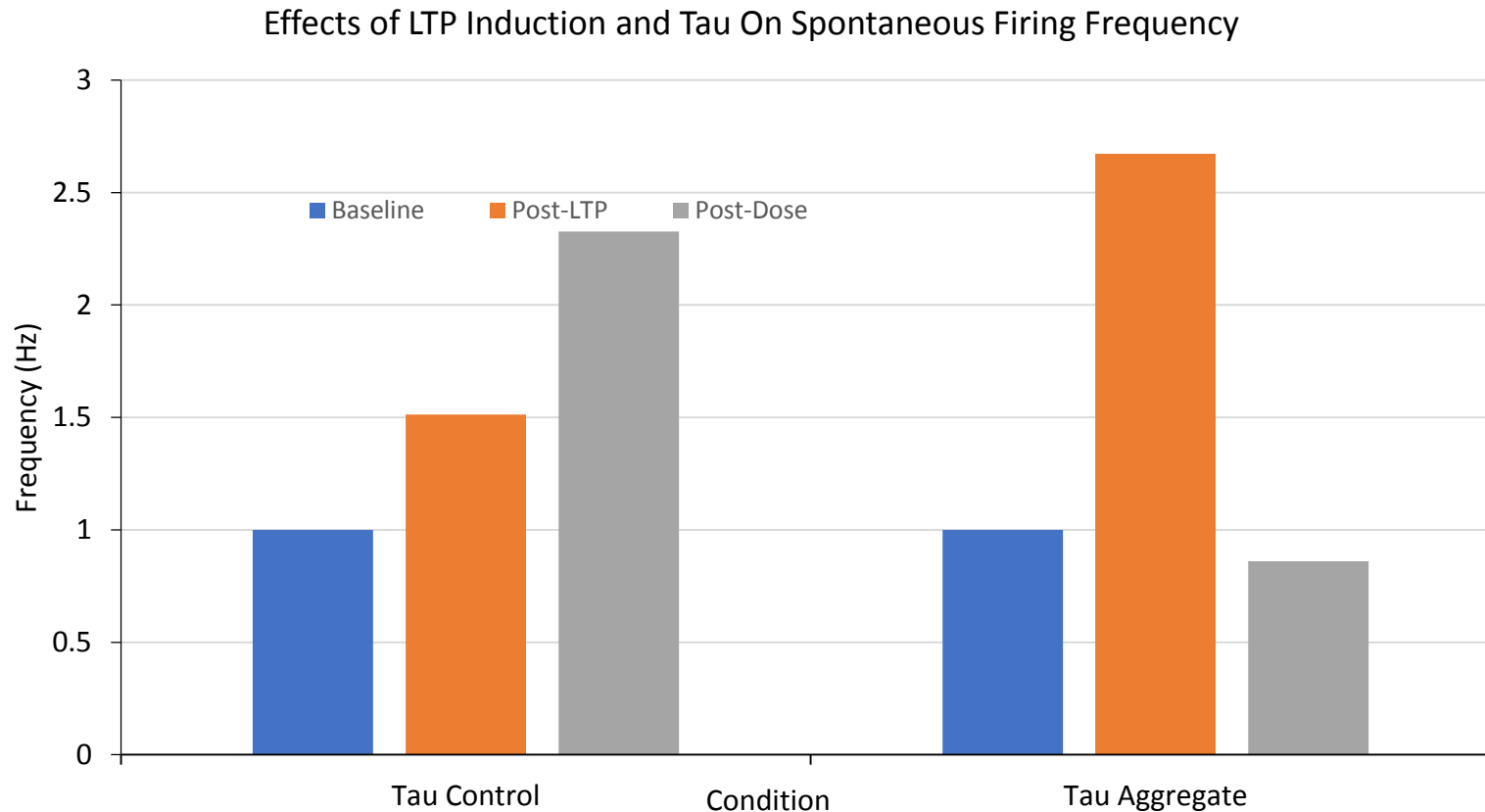
Effects of $A\beta_{1-42}$ on Cortical Neuron Spontaneous Firing Frequency



- LTP can efficiently be induced in cortical neurons grown on MEAs
- Dosing MEAs for one hour with $A\beta_{1-42}$ after LTP induction abolishes the LTP effects compared to $A\beta_{\text{scrambled}}$ treated MEAs

N=4, nested replicates

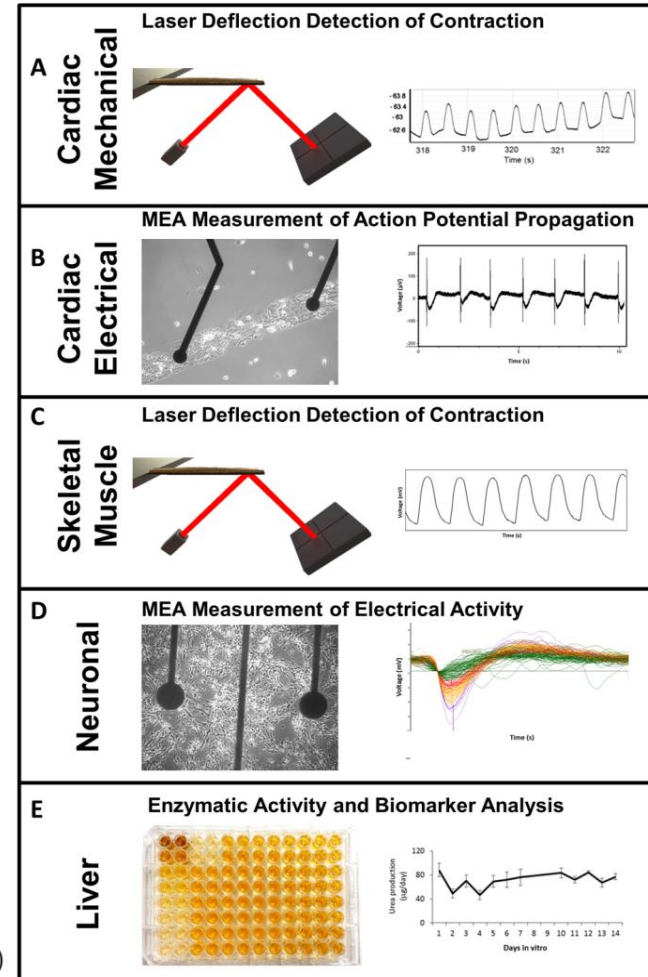
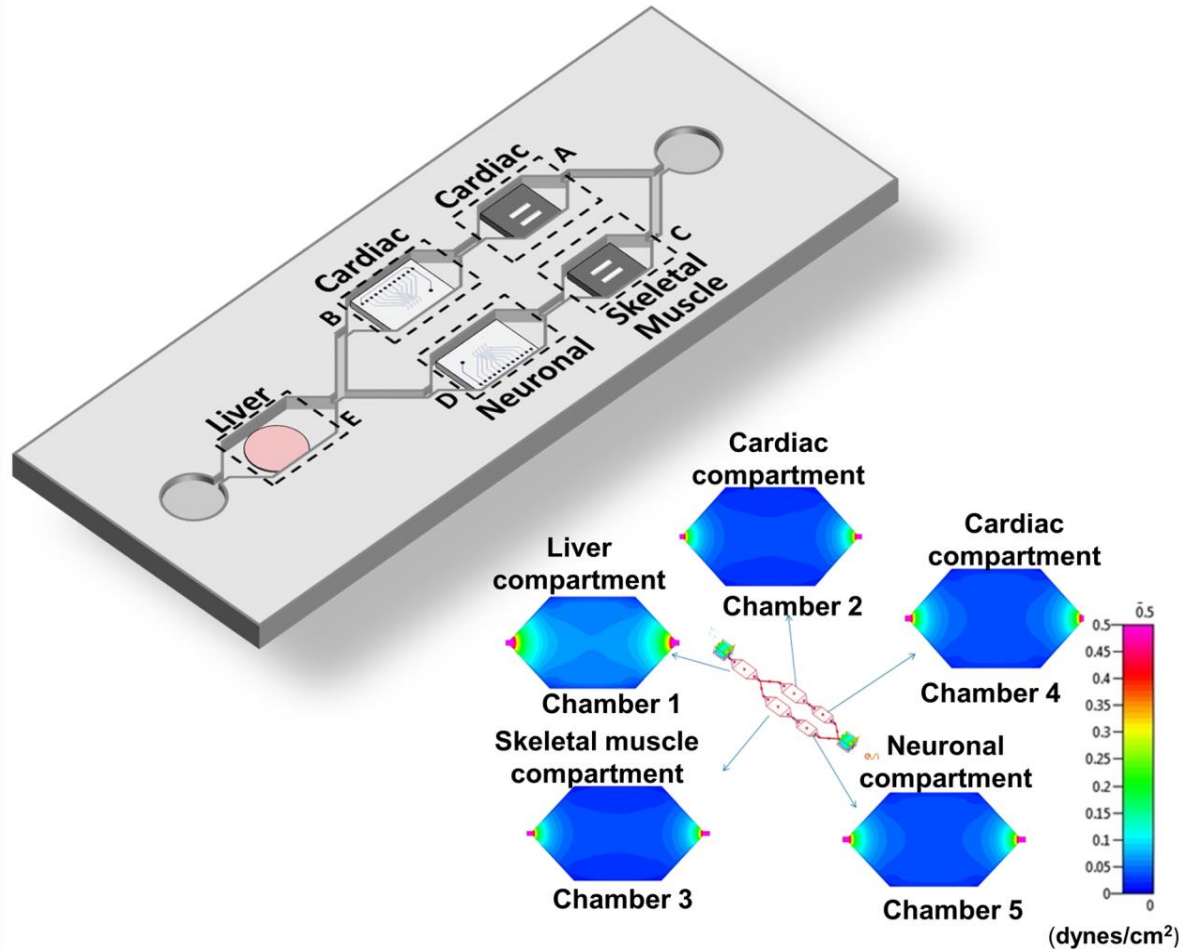
Effects of Tau Aggregate on Cortical Neuron Spontaneous Firing Frequency



- Dosing MEAs for one hour with tau aggregates after LTP induction abolishes the LTP effects compared to tau buffer control MEAs

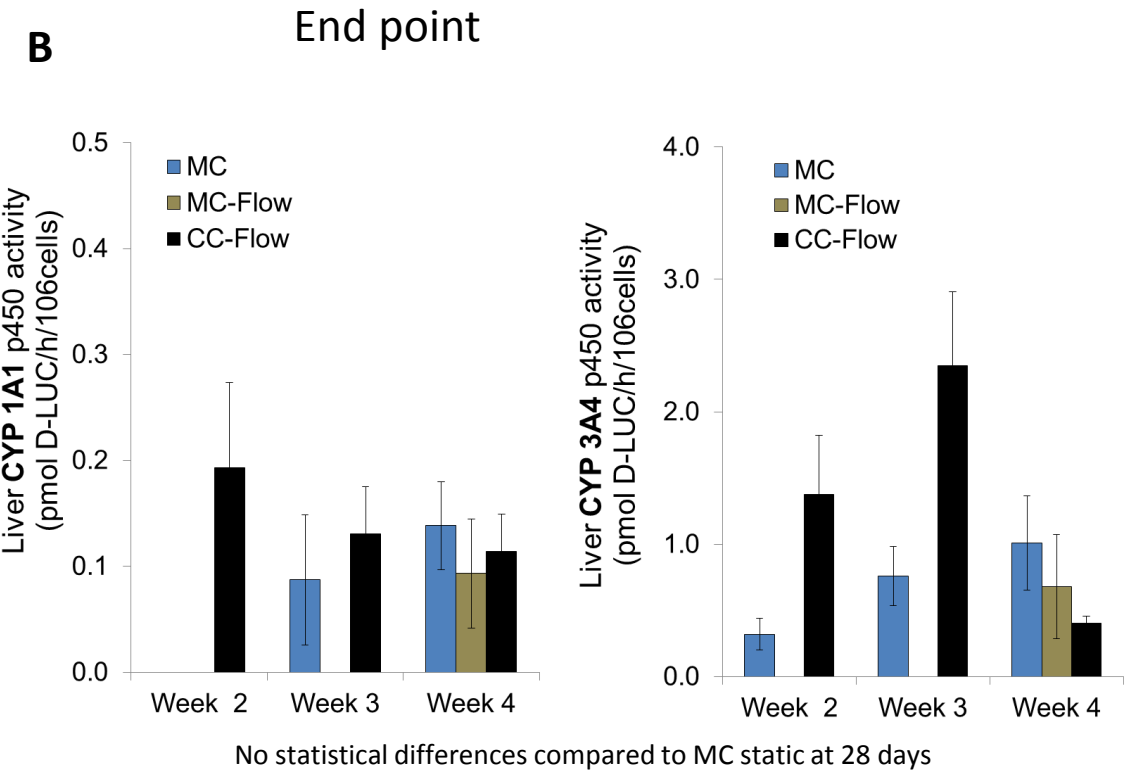
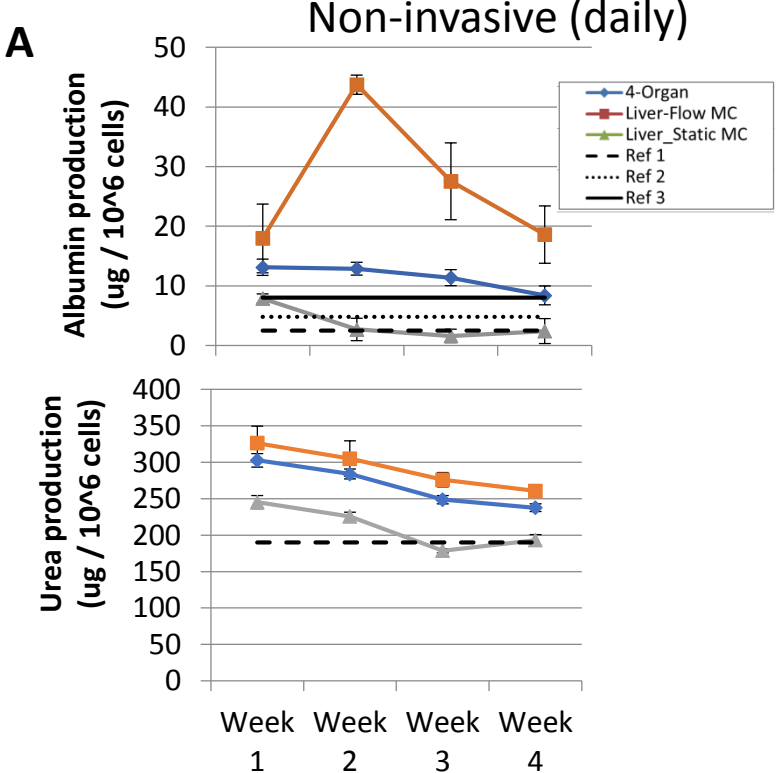
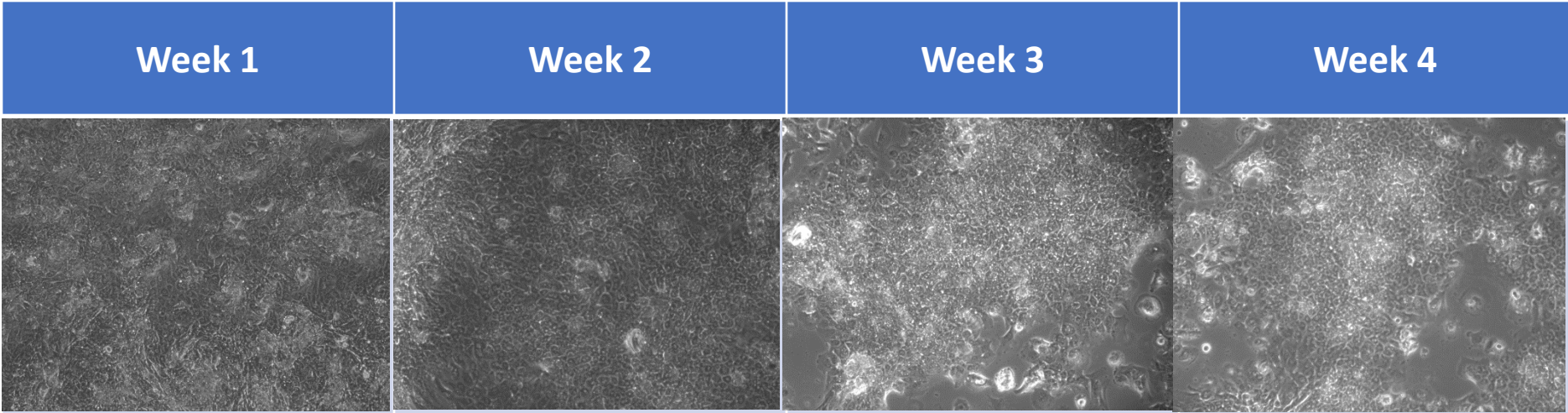
N=4, nested replicates

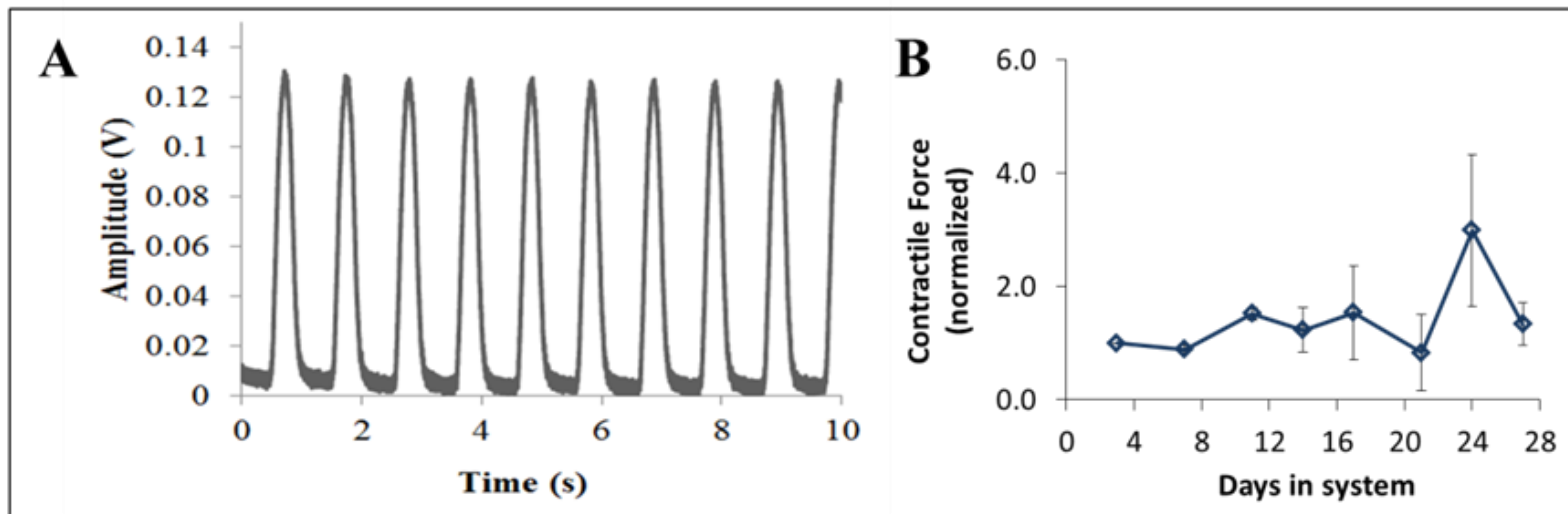
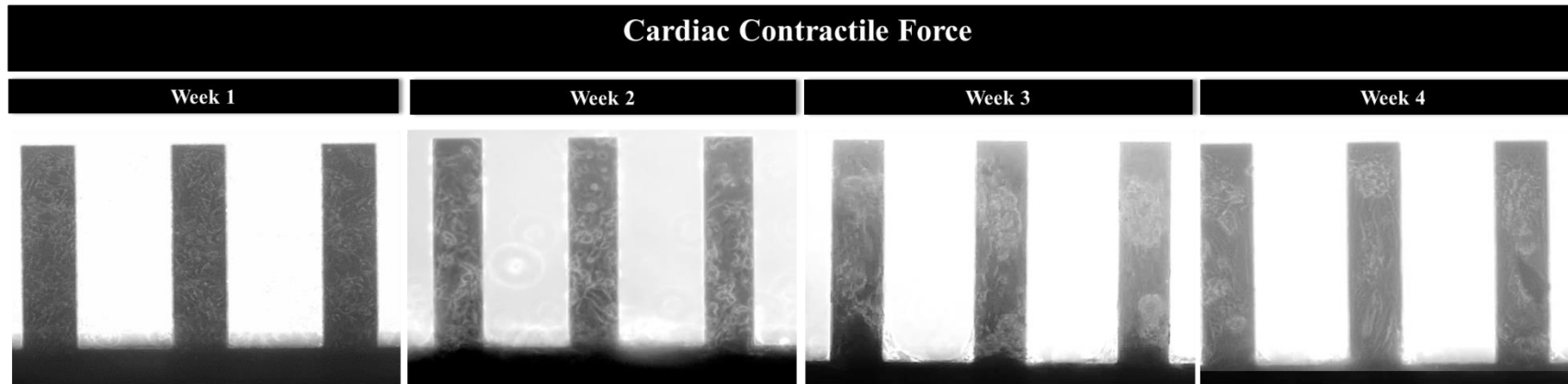
Functional Measurements in 4-Organ Systems



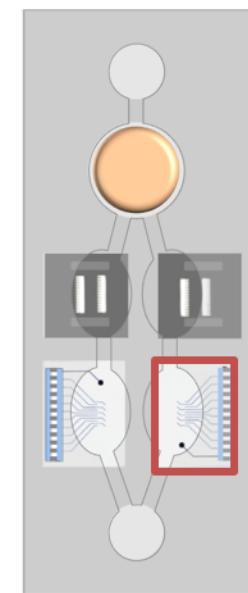
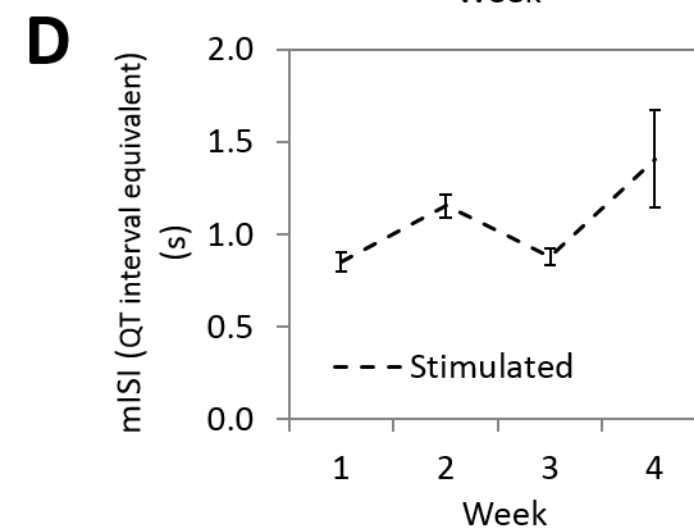
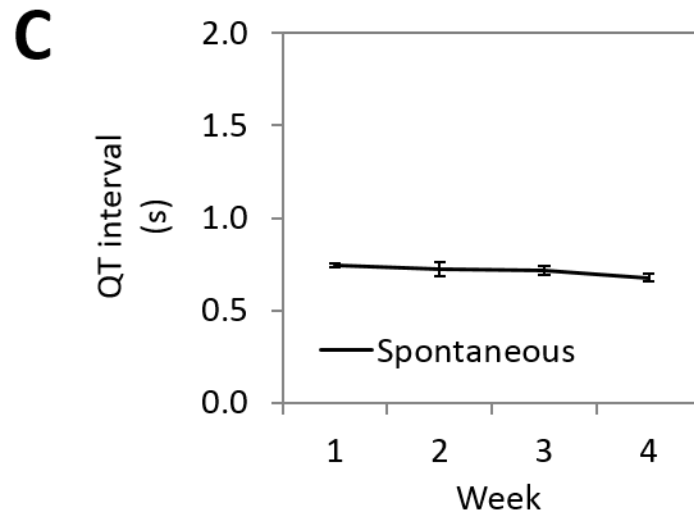
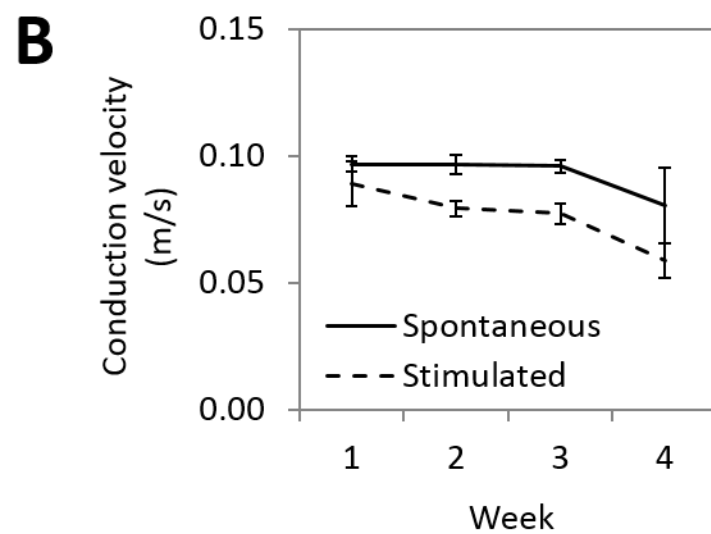
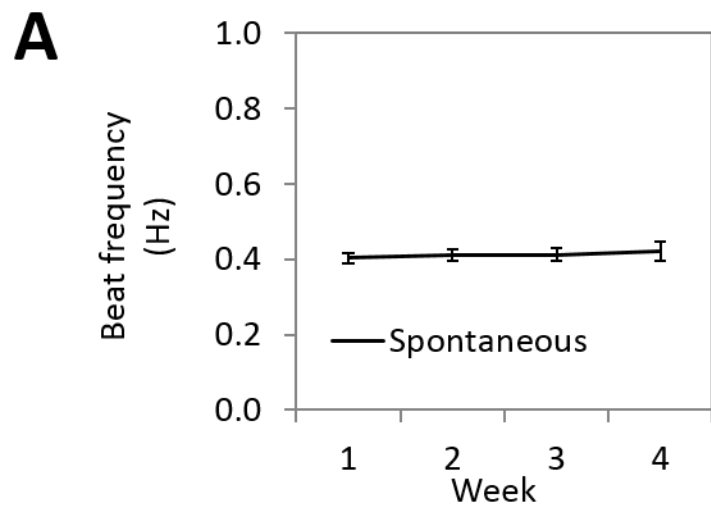
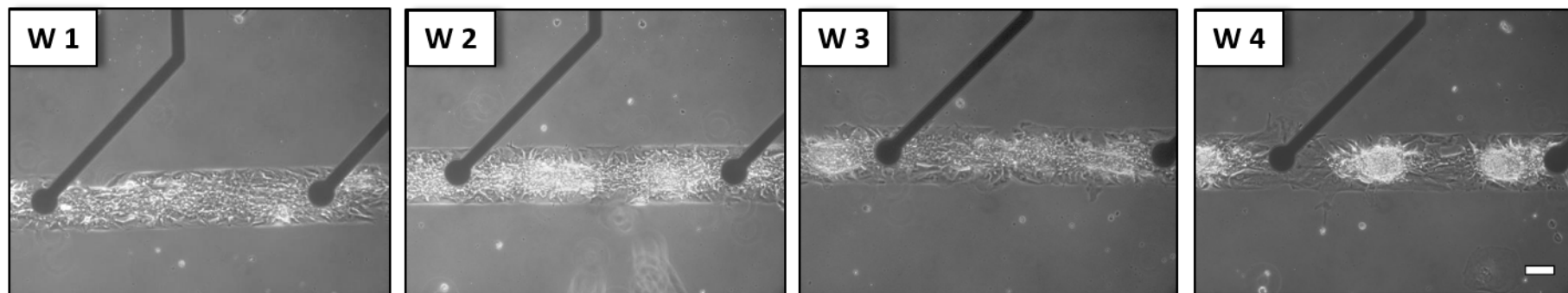
Oleaga et al. 2016. *Nature Scientific Reports* "Multi-Organ toxicity demonstration in a functional human *in vitro* system composed of four organs"
 Oleaga, et al. 2019. *Advanced Functional Materials* "Long-Term Electrical and Mechanical Function Monitoring of a Human-on-a-Chip System"

Liver Module



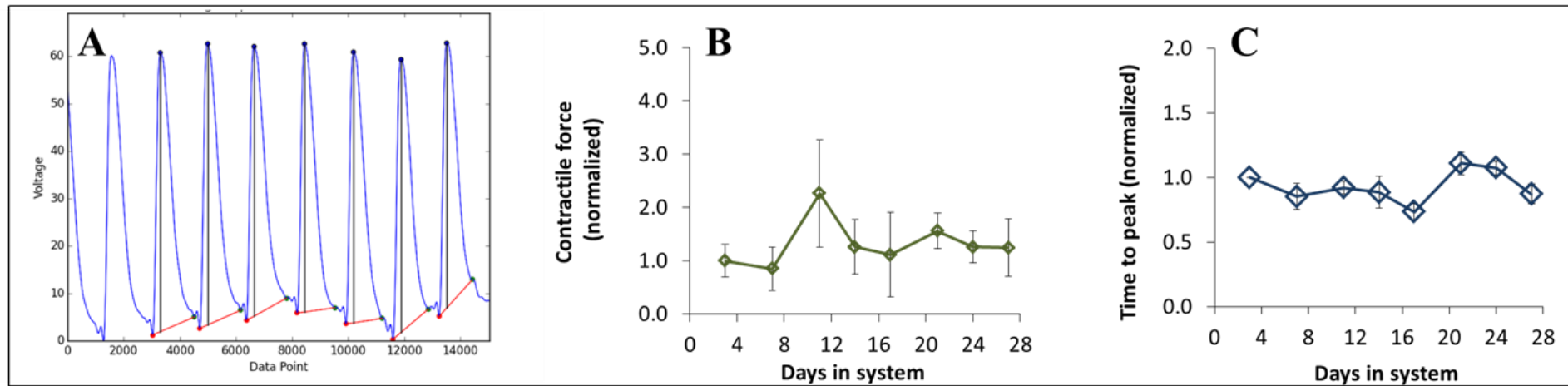
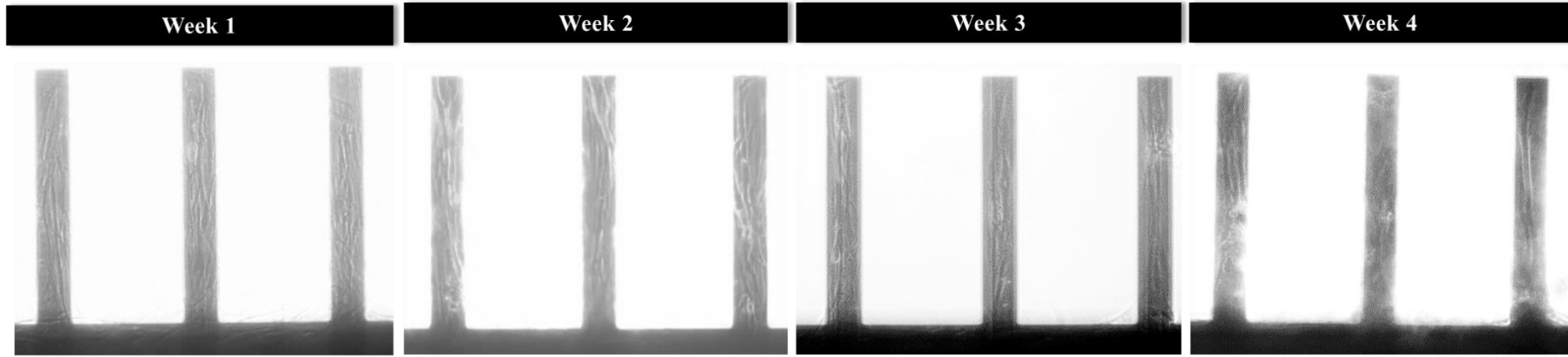


The cardiac module maintained its contractile properties during the 28 days. (A) Example of spontaneous contractile activity output and (B) stable contractile activity indicates stable force generation for cardiomyocytes throughout the 28 day period.

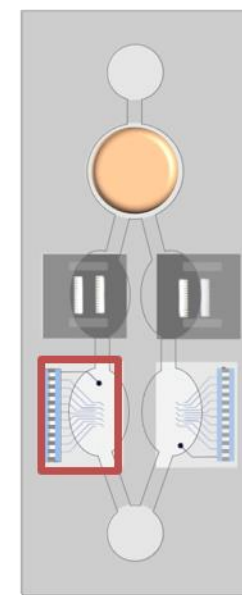
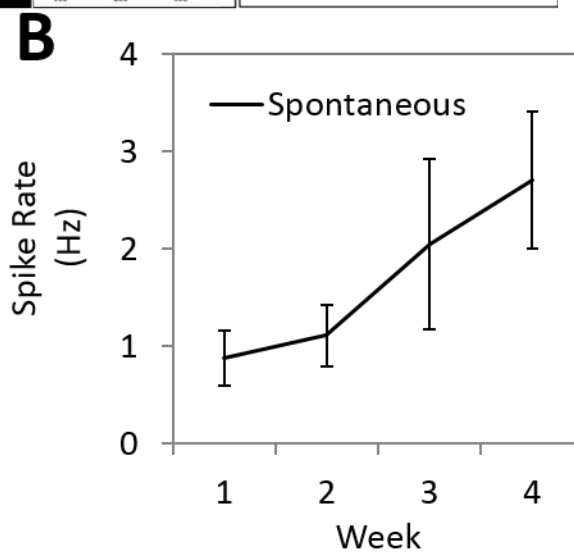
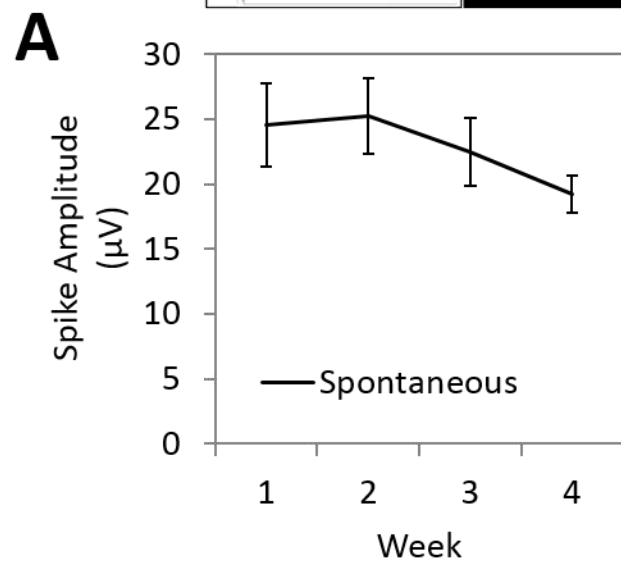
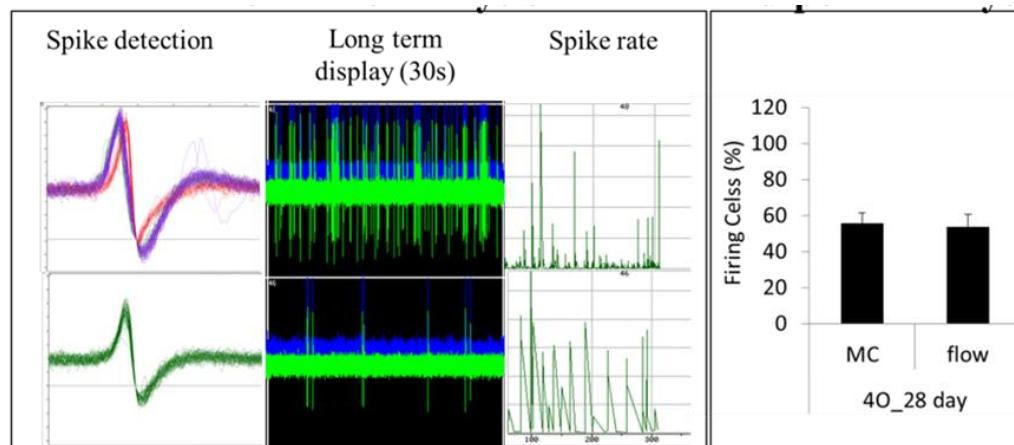
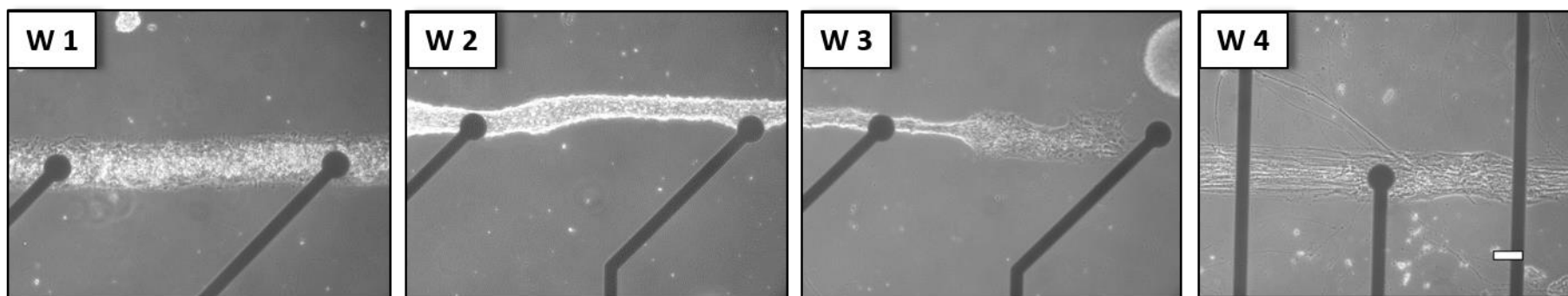


CARDIOMYOCYTES

Muscle Contractile Force

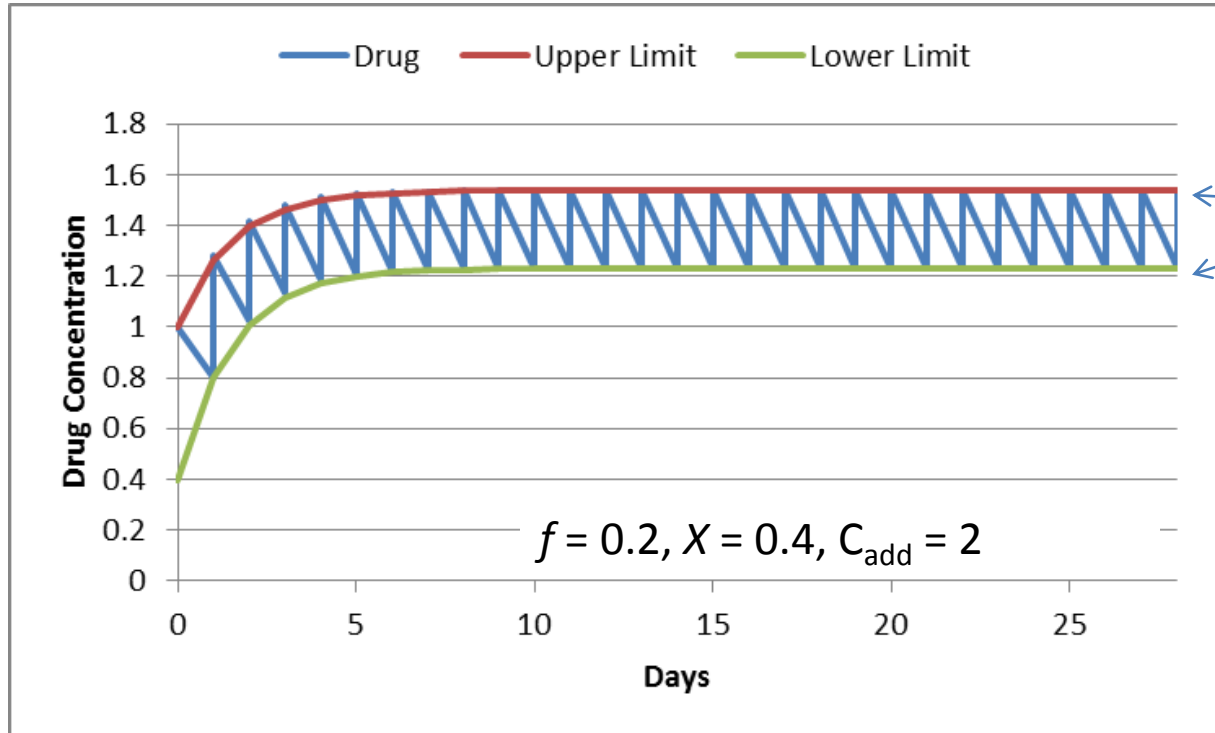


The muscle module maintained its morphological characteristics for the entire 28 days under flow. (A) Example of muscle contractile recordings, (B) stable contractile force and (C) time to peak indicates stable function of the myotubes throughout the 28 day period.



MOTONEURONS

Iterative Data: Drug Concentration



Match
Equations

Steady state concentration of drug
After medium change

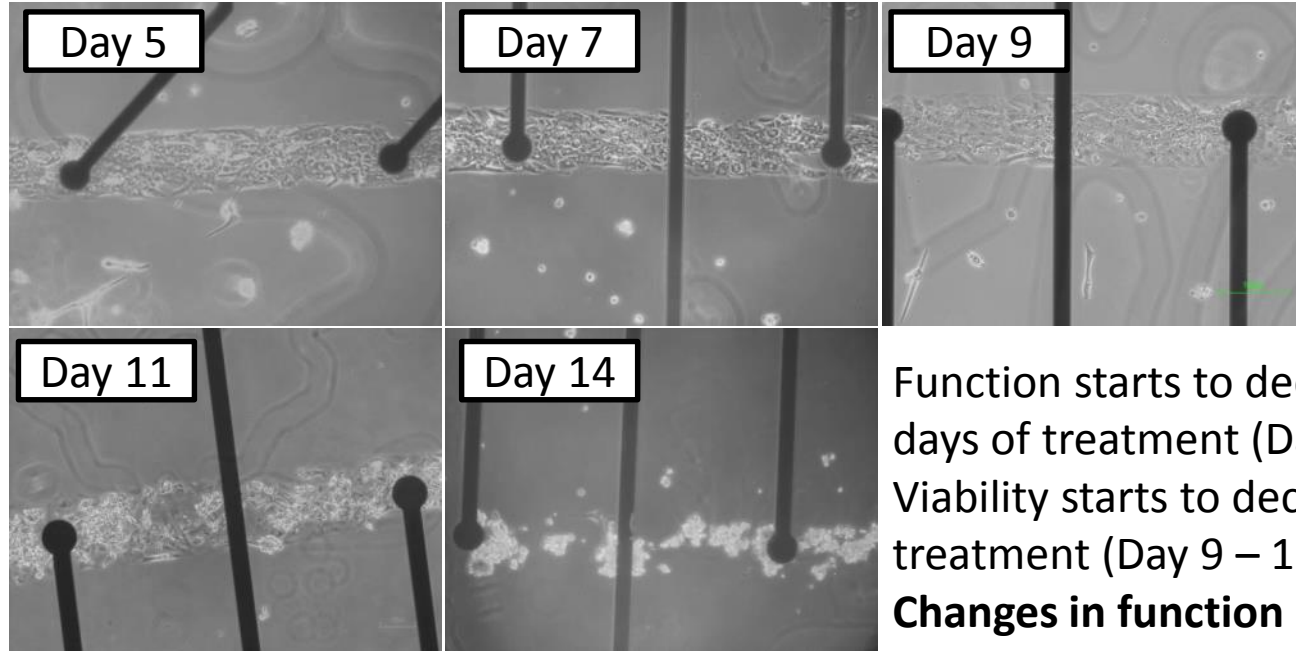
$$C_{drug,ss,I} = \frac{C_{add}X}{1 - (1 - f)(1 - X)}$$

Right before medium change

$$C_{drug,ss,F} = \frac{C_{add}X(1 - f)}{1 - (1 - f)(1 - X)}$$

Upper and Lower limit follow “Carburization” like curve – exponential
with time constant of
 $t_c = \pi(1-f)(1-X)$

Chronic Low-Dose Doxorubicin

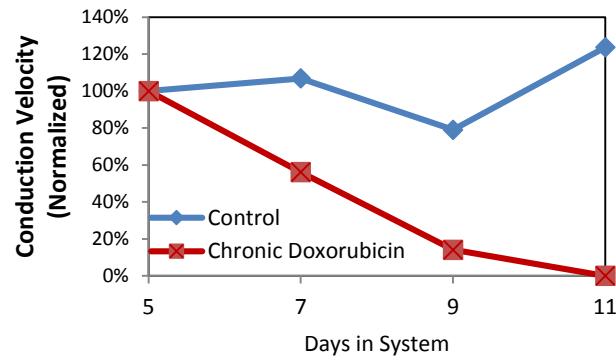


0.5 μ M Doxorubicin repeated dose started at day 5 and continues to day 14

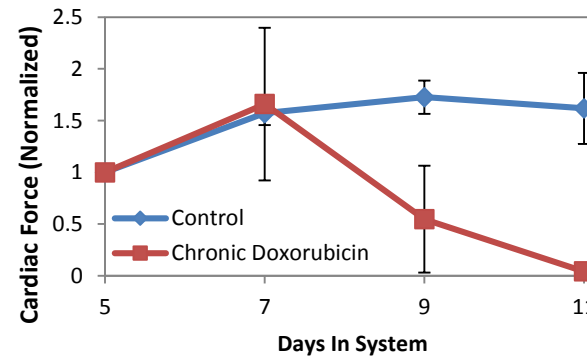
Function starts to decrease between 2 and 4 days of treatment (Day 5 – 7)

Viability starts to decrease around 4 to 6 days of treatment (Day 9 – 11)

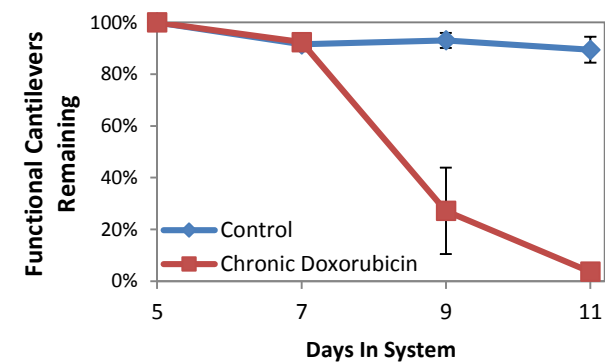
Changes in function precede changes in viability



Steady decrease in Conduction velocity

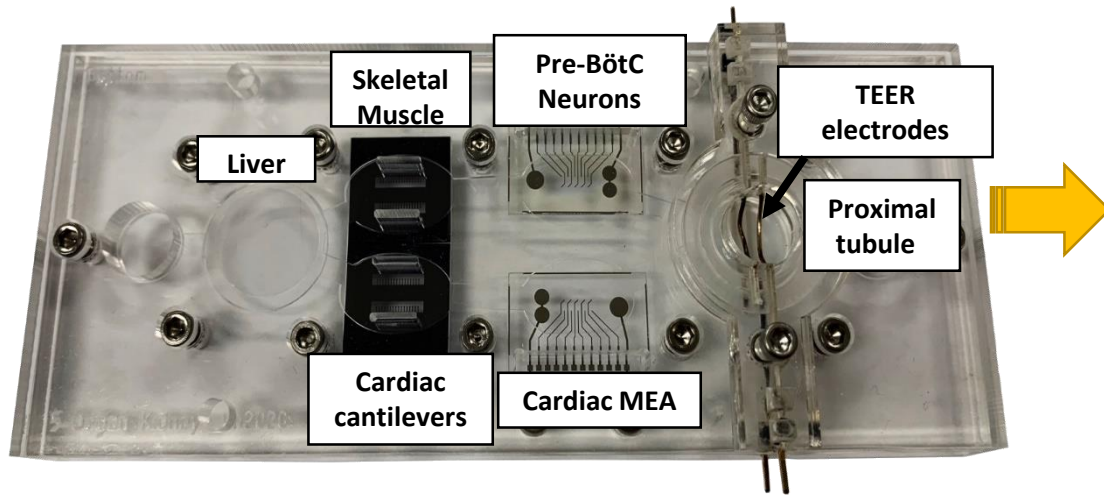


Weakening of contractile force



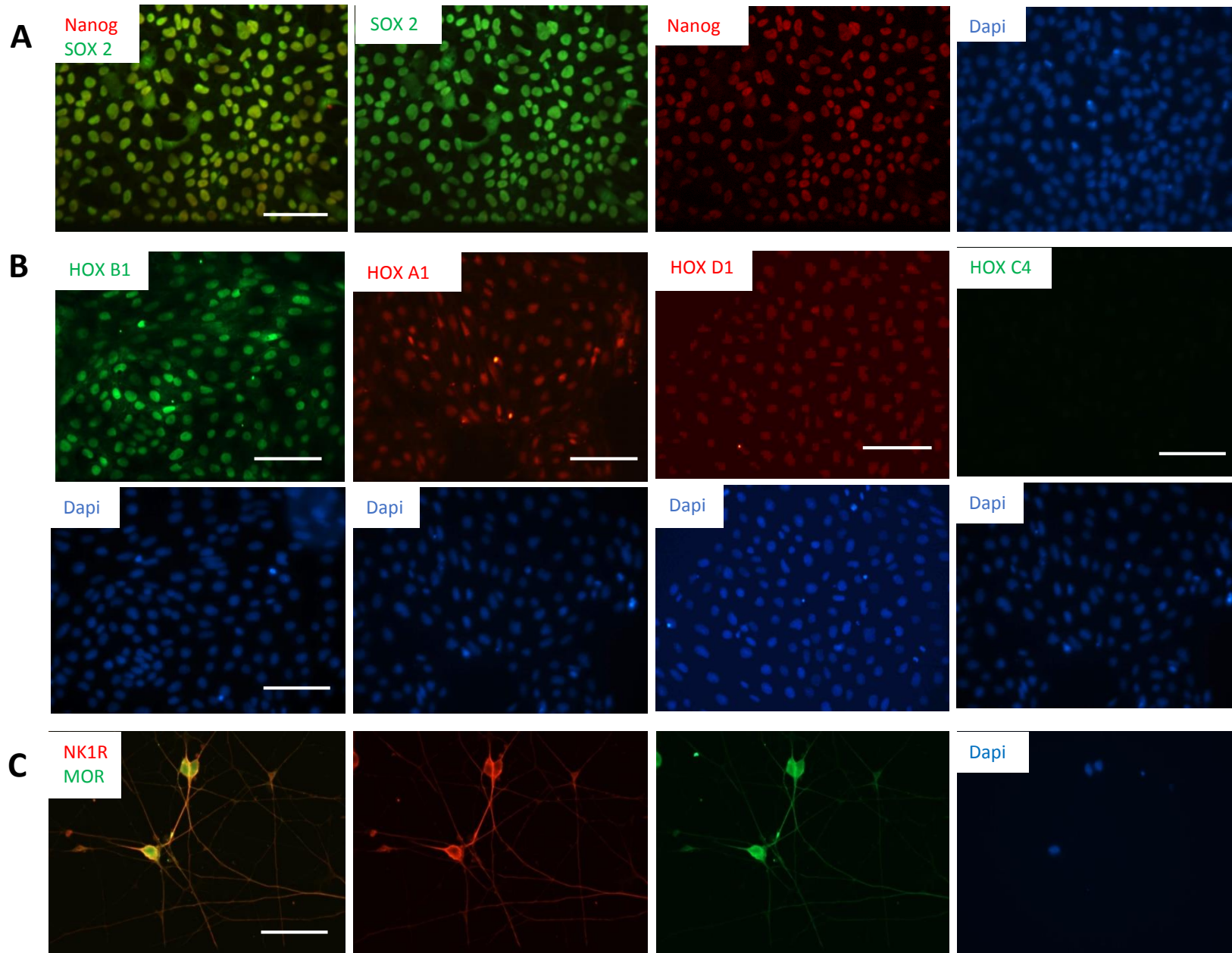
Steady loss of contractile functionality

Develop an opioid overdose (OD) model using a multi-organ human-on-a-chip system



- Evaluate the acute and chronic effects of OD and OD treatments such as naloxone
- Evaluate treatment efficacy and toxicity for cardiac, liver, skeletal muscle, and kidney
- Evaluate opioid OD and OD treatments in the presence of recirculating monocytes
- Evaluate opioid OD and OD treatments in the presence of disease comorbidities including cardiomyopathy and acute infection

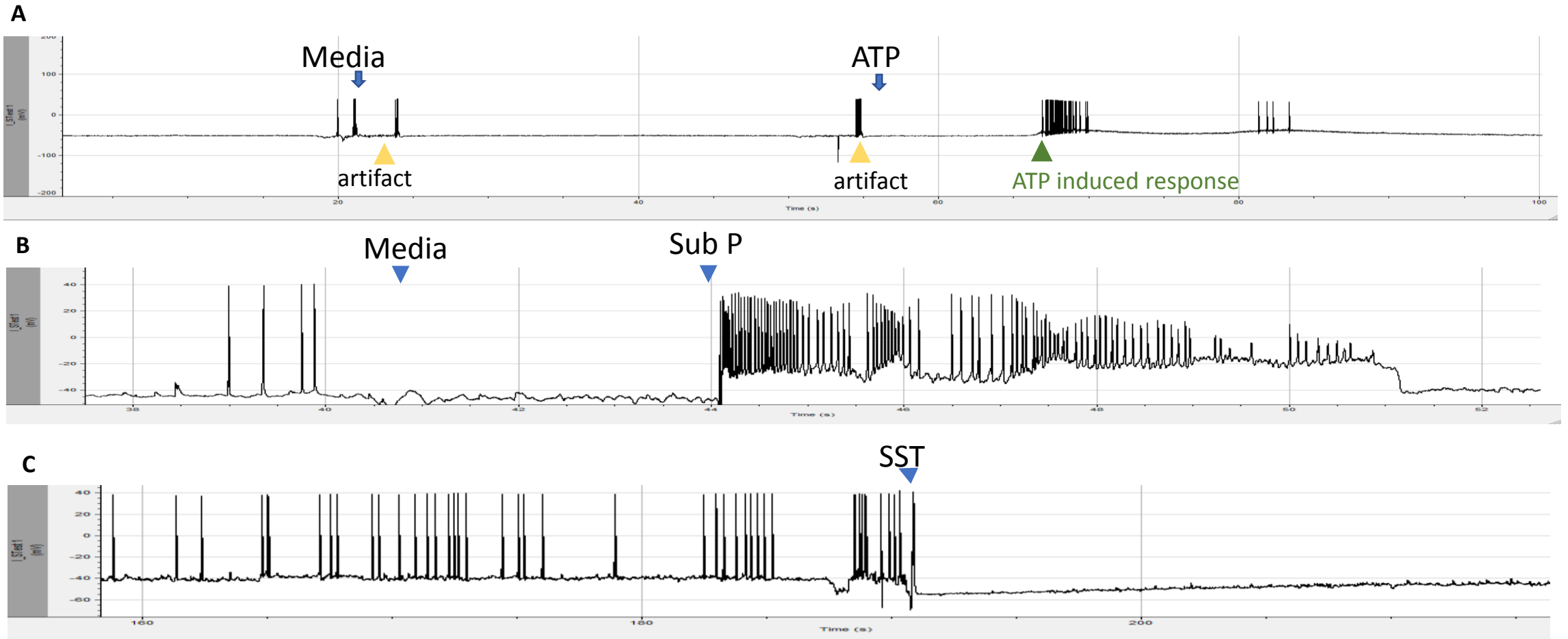
Expression of stage markers correspondent to Pre-BotC differentiation



Differentiation of pre-BotC neurons from hiPSC characterized by immunocytochemistry. A) HiPSCs stained positive to pluripotent markers Nanog and SOX2. Scale bar: 100 μ m. **B)** Cells at early stage of differentiation expressed the set of rhombomeric genes correspondent to the derivative region for preBotC complex during development: positive to HoxA1, HoxB1 and HoxD1 but negative to HoxC1. Scale bar: 100 μ m. **C)** Differentiated neurons plated at low density were stained positive for the typical preBotC markers NK1R and MOR. Scale bar: 50 μ m.

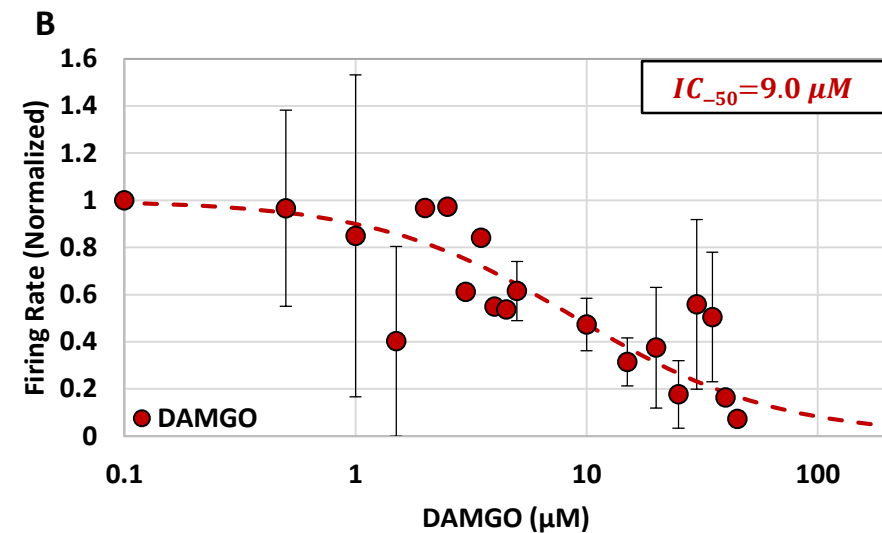
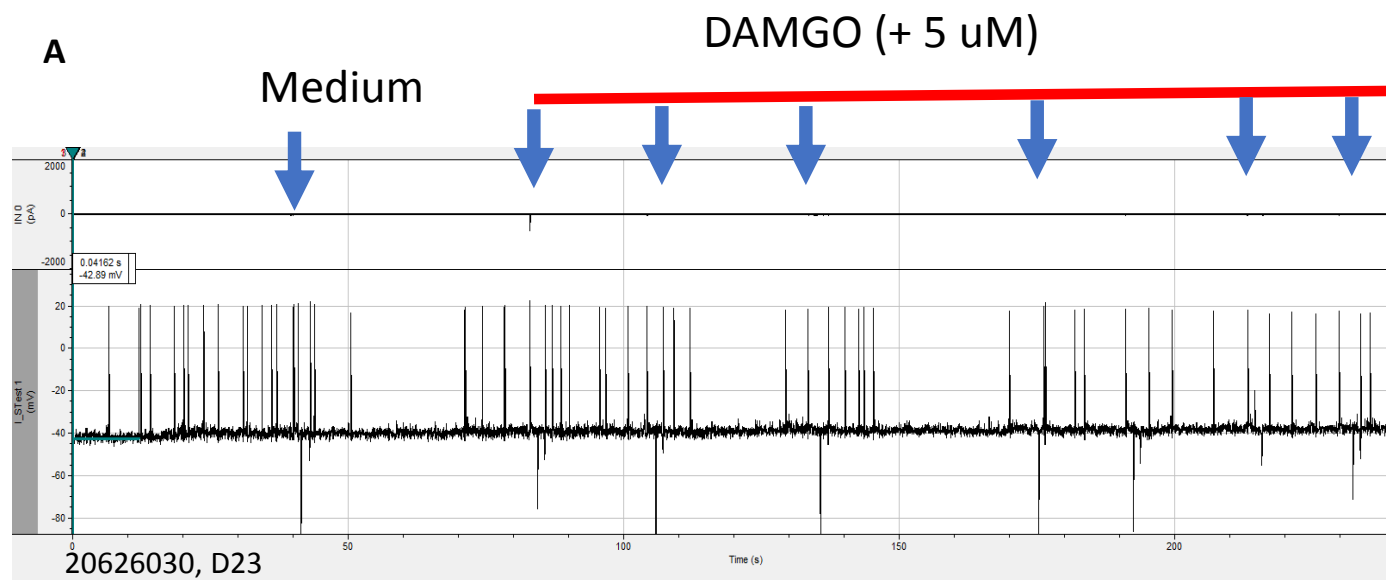
→ **Successfully differentiated Pre-BotC neurons from human iPSC**

Patch clamp recordings from iPSC-Pre-Botc neurons: ATP, Substance P (Sub P) and Somastatin (SST)



Patch clamp analysis of iPSC-pre-BotC neurons. A) Under gapfree condition, dosing of ATP (100 μ M) induced depolarization and burst of action potential. **B)** Treatment with Substance P (Sub P) increases iPSC-Pre-BotC neuronal activity. **C)** Treatment with Somatostatin (SST) inhibits iPSC-Pre-BotC neuronal activity

iPSC-PreBotc neurons demonstrated reduction of neuroactivity in response to DAMGO

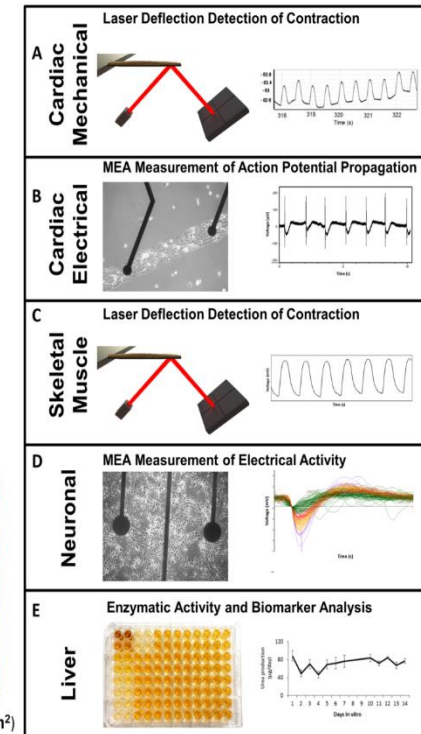
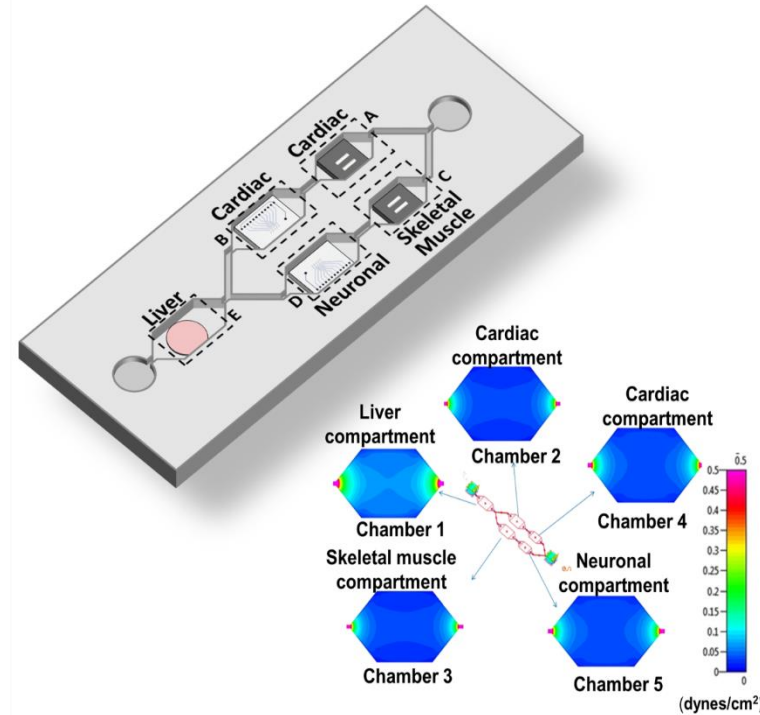
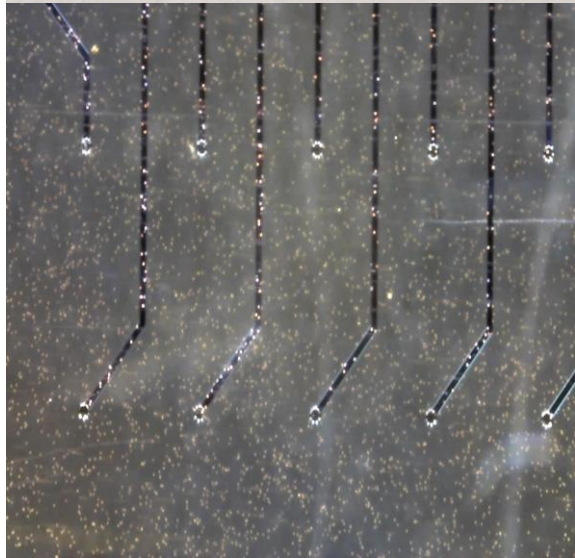
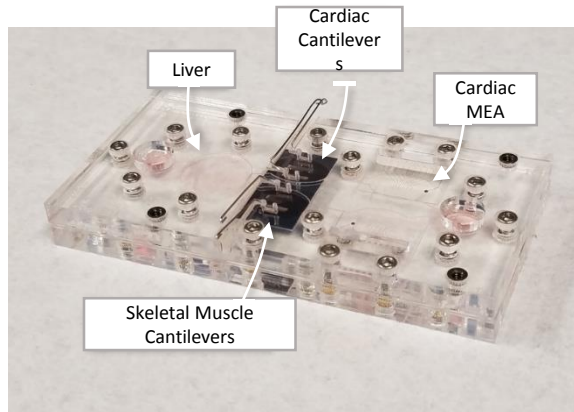


iPSC-pre-BotC neuronal response to DAMGO. A) Patch clamp analysis showed decrease iPSC-Pre-BotC neuronal activity after DAMGO treatment **B)** DAMGO dose-response curve for iPSC-Pre-BotC neurons

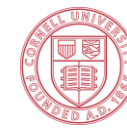
DAMGO's effect:

- Decrease Pre-BotC neuronal activity

Our Multi-Organ MPS Device Supports Recirculating Immune System Cells

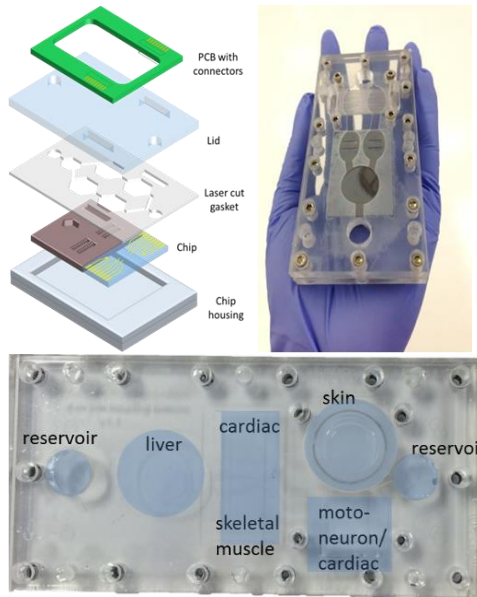


Barrier Tissue Organ Systems

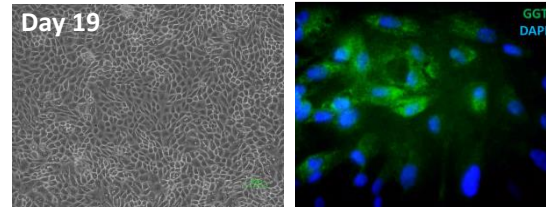


Cornell University

Skin in 4-Organ System

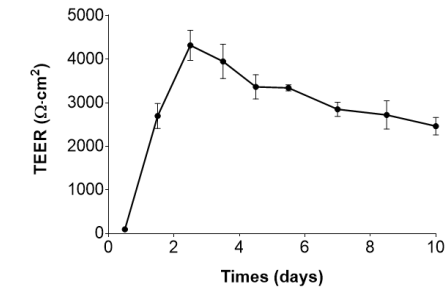
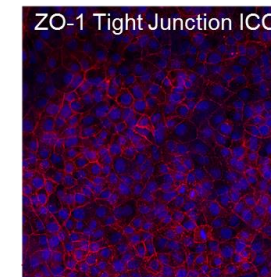
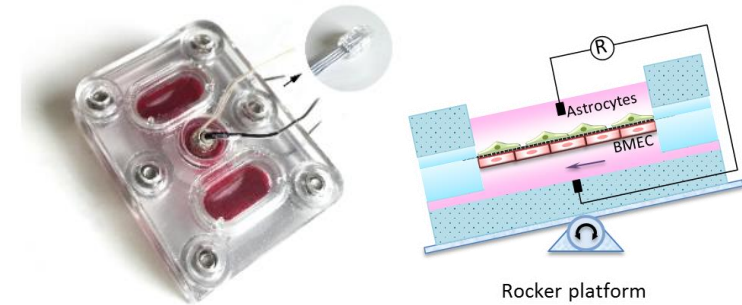


Proximal Tubule System



- Human proximal tubule cells grown on membranes under continuous flow maintain conformal monolayer
- Cells stain for kidney cell marker **Gamma-glutamyl transpeptidase (GGT)**

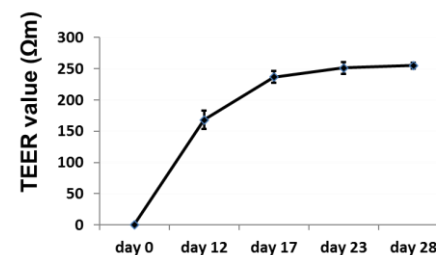
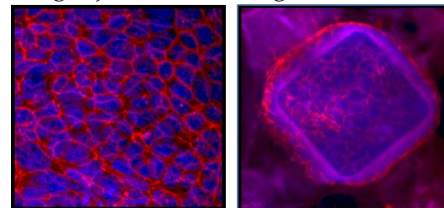
Human Blood-Brain Barrier System



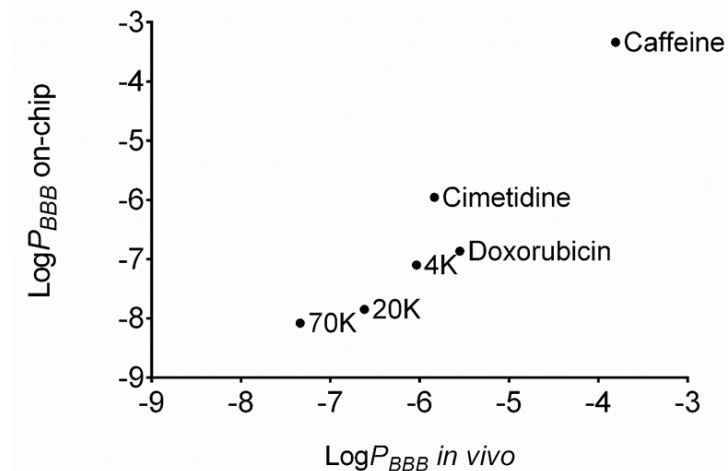
Gastrointestinal Tract Barrier System

Primary Human Colon Epithelial Cells, by knock-in of telomerase reverse transcriptase (TERT), co-cultured with myofibroblasts and 5 nM GSK-3β inhibitor

Tight junction staining in 2D and 3D



Compound Permeability Comparison



What COULD efficacy mean in terms of regulatory evaluations?

- Allow pre-clinical results to steer and/or limit clinical trial construction
- Reduce the number of people necessary for clinical trials, especially for Phase III, by creating human variants to represent uncommon genome profiles
- Allow in vitro clinical trials for rare diseases
- Better evaluations for children
- Better evaluation for aged individuals
- The ultimate precision medicine → individualized disease chips for each human

